Thermal Actuation and Fluidic Characterization of a Fluorescence-Based Multiplexed Detection System

by

Hany Mohamed Arafa

A Dissertation Presented in Partial Fulfillment
of the Requirements for the Degree
Master of Science

Approved August 2018 by the
Graduate Supervisory Committee:

Jennifer Blain Christen, Chair
Michael Goryll
Barbara Smith

ARIZONA STATE UNIVERSITY

August 2018

ABSTRACT

This work describes efforts made toward the development of a compact, quantitative fluorescence-based multiplexed detection platform for point-of-care diagnostics. This includes the development of a microfluidic delivery and actuation system for multistep detection assays. Early detection of infectious diseases requires high sensitivity dependent on the precise actuation of fluids.

Methods of fluid actuation were explored to allow delayed delivery of fluidic reagents in multistep detection lateral flow assays (LFAs). Certain hydrophobic materials such as wax were successfully implemented in the LFA with the use of precision dispensed valves. Sublimating materials such as naphthalene were also characterized along with the implementation of a heating system for precision printing of the valves.

Various techniques of blood fractionation were also investigated and this work demonstrates successful blood fractionation in an LFA. The fluid flow of reagents was also characterized and validated with the use of mathematical models and multiphysics modeling software. Lastly intuitive, user-friendly mobile and desktop applications were developed to interface the underlying Arduino software. The work advances the development of a system which successfully integrates all components of fluid separation and delivery along with highly sensitive detection and a user-friendly interface; the system will ultimately provide clinically significant diagnostics in a of point-of-care device.

ACKNOWLEDGMENTS

The journey through my short (but hectic) graduate career at ASU has been an incessant fluctuation of ups and downs. As this phase of my life comes to an end, I have reached the conclusion that I would be nowhere near where I am had it not been for a number of significant individuals in my life.

I would like to thank my advisor Dr. Jennifer Blain Christen for welcoming me into her laboratory as a fledgling high school student and for providing me with mentorship and guidance through my seven years at Arizona State. She went above and beyond in supporting me through these years and it has been my pleasure to work under her guidance. I would also like to thank the multitude of past and present graduate students in her lab especially David, Sahil, Paul, Ian, Meilin, and Uwa for putting up with more than I ever asked for in advice and guidance in research and in life.

I would also like to thank Dr. Michael Goryll for graciously helping me through the graduate school application process and for giving me advice when I needed it the most. I would also like to thank him for graciously agreeing to serve on my committee. I would also like to thank Dr. Barbara Smith for her helping me understand paper microfluidics and for graciously agreeing to serve on my committee.

I would also like to thank my friends for setting me straight and graciously listening to all of my experimental stuggles.

Most importantly, I would like to thank my parents, Mohamed and Heba, for being there for me at my best and even more so at my worst. If not for my parent's endless love and care, I wouldn't be the person I am today (even though I am admittedly a work in progress). I would like to thank my father Mohamed for opening up my eyes to the expansive world of science and engineering and sparking my interest in research. I would like to thank my mother Heba for her unwavering patience with

me during all 22 years of my existence. Last but definitely not least, I would like to thank my brother Omar for being an inspiration and a constant source of motivation for me in all areas of life.

I am eternally in all of your debts.

TABLE OF CONTENTS

Page

LIST OF TABLES vi

LIST OF FIGURES vii

CHAPTER

1 INTRODUCTION 1

1.1 The Emergence of Lateral Flow Assays 1

1.2 Blood as an Diagnostic Tool 4

1.3 Development of a Fluorescence-based Lateral Flow Platform for Detection of Biomarkers in Whole Blood 5

1.4 Characterization of Capillary Driven Fluid Flow 8

1.5 Characterization of Fluid Flow through Porous Media 11

1.6 Review of Blood Fractionation Methods 12

1.6.0.1 Membrane Filtration 14

1.6.0.2 Capillary and Hydrodynamic Separations 18

1.7 Experimental Overview 19

2 BLOOD FRACTIONATION AND ASSAY IMPLEMENTATION 20

2.1 Testing of Filtration Membranes 21

2.1.1 Plasma Yield Experimental Setup 22

2.1.2 Evaporation and Fluid Retention Experiments 28

2.2 Implementation in the Lateral Flow Assay 32

3 VALVE ACTUATION AND FLUIDIC CONTROL 41

3.1 Introduction 41

3.2 Design and Validation of PID Controller 41

3.3 Wax Valves 46

CHAPTER Page

3.3.1 Autofluorescence of Wax 47

3.3.2 Characterization of Fluidic Flow with a Hydrophobic Wax Treatment 52

3.4 Sublimating Valves 57

3.4.1 Flow Characterization of Sublimating Valves 58

3.4.2 Compatibility of Naphthalene 62

4 MODELING OF FLUID FLOW IN A POROUS MEDIUM 67

4.1 Mathematical Modeling 67

4.1.1 Governing Equations and Assumptions 67

4.1.2 Mathematical Model Development 70

4.2 COMSOL Modelling 70

5 DEVELOPMENT OF A SOFTWARE TO INTERFACE THE DATA ACQUISITION PROGRAM FOR THE LATERAL FLOW PLATFORM 72

5.1 Computer Interface Development 72

5.2 iOS Application Development 74

6 CONCLUSIONS & FUTURE WORK 79

REFERENCES 81

APPENDIX

A CODE FOR PROGRAMS 85

B PROTOCOLS FOR ASSAYS 121

C IRB DOCUMENTATION FOR BLOOD COLLECTION 126

BIOGRAPHICAL SKETCH 144

LIST OF TABLES

Table Page

1. A Comparison of Various Commercial Membranes Marketed for the Filtration of RBCs. 15
2. The 2^3 Factorial Design for the Set of Wax Experiments to Test the Effect of Autofluorescence. 47
3. The 2^3 Factorial Run Chart for the Set of Wax Experiments to Test the Effects of Autofluorescence Which Includes the Interactions between Each of the Factors. 48

LIST OF FIGURES

Figure Page

1. Various Types of Paper Based Microfluidic Devices Which Are Described in the Section and the Various Types of Functionalizations that Can Be Applied to the Surface. 3
2. A Sample Nanoparticle Based Immunoassay and Schematic (`**P**osthuma-Trumpie2009). 6
3. A Schematic of the Excitation and Emission Sources of the Setup. Part (a) Shows the Green Emission LED, (B) Shows the Housing of the Emission and Excitation Filters, and (C) Shows the Orange Excitation Photodiode along with the Charge Integration Amplifier Circuit (`**7**797711). 8
4. A Relation of the Output Voltage of the Charge Integration Circuit Which Is Directly Related to the Intensity of the Fluorescent Signal (`**7**797711). . . . 9
5. Contact Angle for Both Non-Wetting and Wetting Fluids (`**y**uan2013contact). 10
6. Various Methods of Blood Fractionation of Small Samples. 13
7. An SEM Image of the Vivid Plasma Separation Membrane. The Asymmetric Nature of the Polysulfone Membrane Can Be Clearly Seen in This Cross Section.*Courtesy of Pall Corporation* 16
8. A Setup Which Also Uses Gravity Aided Sedimentation to Filter 800 μL of Human Blood by Using a Super Hydrophobic Membrane (`**l**iu2013membrane,liu2016high). 17
9. A Characterization of the Autofluorescence of Different Types of Polymeric Membranes that Are Used in Various Parts of the Lateral Flow Assay. 21

Figure Page

10.An Example of the Hemolysis Seen in a Strip of Pall Vivid GR Plasma Separation Membrane in the Sample of Mouse Blood. This Result Was Verified by Centrifugation of the Blood Sample. 24

11.Overflow of a 50μL Mouse Blood Sample on a Whatman MF1 Membrane Mounted on a Glass Slide with Double Sided Tape. 24

12.An Example of Inconsistent Blood Deposition on the Vivid Gx Membrane that Was Done with the Finger Touch Method. The Plasma Front Is Clearly Seen, but the Wicking of the Plasma Occurs in Multiple Directions Which Introduces Extra Variability into the Assay. 25

13.A Schematic of the Experimental Setup for the Blood Weighing Experiment Where the Sample Pad Was Placed on Top of the Nitrocellulose and the Nitrocellulose Was Weighed after 180 Seconds. 26

14.The Results of the Plasma Recovery Experiment Created to Characterize in Each of the Plasma Membranes. 27

15.A Box and Whisker Plot Showing the Overall Evaporation of Each of the Millipore HF75 Membrane with Both K2 EDTA Sheep Blood Applied for One Group and Deionized Water Applied to the Other Group. Statistical Analysis Showed that There Was No Statistically Significant Difference between Both of the Treatment Groups. 29

16.The Results of the Low Humidity Evaporation Rate Experiment for the Millipore HF75 Membrane. The Evaporation Seems to Be Linear at All of the Fluid Amounts (50μL, 100μL, and 150μL), Which Means that a Correction Can Be Applied to Compensate for Fluid Losses. 31

Figure Page

17.The Results of the High Humidity Evaporation Condition Experiment on the Millipore HF75 Experiment and the Fluid Losses Can Be Seen to Be Linear at All the Initial Fluid Amounts. 32

18.The Results of the Fluid Loss Experiments for Both of the Pall Vivid GX/GR Membranes. 33

19.A Test Strip that Was Prepared for the Lateral Flow Blood Fractionation Tests. 34

20.A Test Strip with 10μL of Blood that Was Tested in This Experiment. 36

21.A Comparison of All of the Samples with Various Methods (Finger Touch, and Capillary) for Two Patient Samples (Solid, Striped Lines). 37

22.A Comparison of Finger Touch Blood and Capillary Deposited Blood for Three Samples with Measurements for Concentration of BSA, IgG, and EBNA for Sample D2. 37

23.A Comparison of the Concentrations of EBNA and IgG to Various Dilutions of the Pooled Plasma Samples. It Can Be Seen that Slide B in the 1:50 Dilution of the Pooled Sample Was Slightly Higher than the 1:10 Sample, but This Could Be due to a Number of Different Factors. Overall of the Other Slides Were Consistently Withing 10% of Each Other, Which Is a Good Point of Reference to the Other Samples. 38

24.A Comparison of Results between the Different Types of Application Methods (Finger Touch, Heparinized Capillary, and a Pooled Blood Plasma Sample for Both Donors. There Seems to Be No Significant Variance in the Results for Patient D2, but There Were Some Variations that Were Noticeable in the First Sample. 39

Figure Page

25.A Comparison of the Results for All of the Donors Which Takes into Account the Application Method as Well as the Inclusion of the Pooled Plasma Sample at the Two Dilutions. There Seems to Be No Significant Variation in the Results between Each of the Groups. 40

26.An Example Setup of the PID Controller with the Thermocouple Placed Directly on Top of the Heating Surface. 42

27.The Schematic of the First Iteration of the PID Controller Which Includes a 120V AC Input, a PID Controller, a 10A Relay, a Heating Pad, and a Separate 24V Power Supply to Heat the Silicone Heating Blanket. 43

28.The Schematic of the Second Iteration of the PID Controller Which Utilizes a Solid State Relay and an External Heating Element. 44

29.The Simulated Conditions of the PID Control with the Use of the Preset P and I Conditions for a Temperature of 120 Degrees. There Is Minimal Hysteresis in the Graph and the Simulated Controller Returns to Optimal Conditions in Minimal Time. 45

30.The Simulated Conditions of the PID Control with the Use of the Preset P and I Conditions for a Temperature of 120 Degrees. There Is Minimal Hysteresis in the Graph and the Heating Cord Reached the Operating Temperature in about 500 Seconds. The Stock Presets of the PID Controller Were K_p=3, K_i=0.8, K_d=0.7. Fine Tuning Will Be Done at a Further Time. 46

31.A CAD Model of the Wax Dipping Piece to Create Clearly Defined Channels in the Membrane. 49

Figure Page

32.A Comparison of the Initial Iteration of the Wax Dipping Apparatus (Seen on the left Side of the Image) and the Consequent Evolution of the Dipping Molds. There Are Noticeable Wax Residues on the Molds and This Was Removed with Isopropyl Alcohol and Compressed Air. 50

33.The Results of the Wax Fluorescent Emissions Experiment. It Can Be Seen that the Ozokerite Wax Had a Higher Intensity in Comparison to the Soybean Wax. 51

34.The Results of Effect Summary Analysis for the Wax Autofluorescence Experiment. Variables with a Higher Log Worth Are Deemed to Have a More Significant Effect on the Ramp Time. 52

35.Another Comparison of the Effects on the Ramp Time, Which Verifies the Results Seen in the Previous Figure. This Table Also Shows Which Effects Are Statistically Significant with the Use of an F Test. 52

36.The Results of the Prediction Profiler Which Uses the Data Compiled from the 8 Runs to Find the Optimal Conditions Which Maximize the Ramp Time and Minimize the Fluorescent Signal. 53

37.A Schematic of the Y Pattern that Was Used to Characterize the Flow Rates with Different Types of Hydrophobic Wax Treatments. 54

38.a Simplified Schematic of the Flow through the Y Membrane. 55

39.The Characterization of Flow Rates of Ozokerite and Soybean Waxes and the Comparison of Length Traveled versus Time. 56

40.The Characterization of Flow Rates of Ozokerite and Soybean Waxes and the Comparison of Length Traveled versus Time. 57

Figure Page

41.The Characterization of Flow Rates of Ozokerite and Soybean Waxes and the Comparison of Length Traveled versus Time. 59

42.A Schematic of the Experimental Setup of the Hold Time Experiment with a Reservoir of Fluid. 60

43.A Comparison of the Hold Times of Naphthalene Valves versus Ozokerite Wax Valves. It Can Be Seen that Ozokerite Wax Held for Longer than the Experimentation Time of 12 Hours and the Naphthalene Valves Held for an Average of about Nine Hours. 61

44.The Characterization of Flow Rates of Ozokerite and Soybean Waxes and the Comparison of Length Traveled versus Time. 62

45.The Setup of the ELISA Assay with the Plate Map of the Assay with the EBNA and GST(Negative Control). The Legend of the Plate Map Can Be Seen and Three Duplicates of Each Run Were Created. 64

46.The Legend of the ELISA Assay with All of the Necessary Controls with the Secondary, Plasma With/without the Addition of Naphthalene. 65

47.The Chemiluminescent Results of the ELISA Compatibility Experiment with the Addition of Naphthalene. It Can Be Seen that the Addition of Naphthalene with Plasma and Secondary Resulted in En Extremely High Signal, but It Is Also Noted that the Standard Deviation of This Group Was High. Overall It Is Noted that the Naphthalene Did Not Significantly Affect the Signal in the Other Wells. 66

48.The Image Import of the SEM Image of an Asymmetric Polysulfone Membrane on COMSOL Multiphysics. 71

Figure Page

49.The Screen Where the User Is Prompted to Insert the Patient and the Application Also Saves the Time and Date of the Test. 73

50.A System Block Diagram for the Software Interfaces Developed for the Lateral Flow Platform. 74

51.The Landing Screen of the FlexDx Application Where the Device Searches for Available BLE Devices. 75

52.The Screen Where the User Is Prompted to Insert the Patient and the Application Also Saves the Time and Date of the Test. 76

53.The Testing Screen of the Device Where the Timer Measures the Overall Time Elapsed for the Detection Test. 77

54.A Sample Email Screen Where the Application Compiles All of the Data into a .csv File and Prompts the User to Email the Data to a Health-Care Provider. 78

Chapter 1

INTRODUCTION

Microfluidic devices have recently become the golden standard for diagnostic devices particularly in the field of global health. These devices can be used to accurately transport fluids as well as the completion of other processes such as separation, purification and other fluidic reactions. These devices are usually fabricated via conventional photolithography methods to create features in a polymer such as polydimethylsiloxane (PDMS). However, there are certain limitations to these devices, mainly cost and the resources needed to fabricate these devices (clean room environments, photolithography spinners, etc.). This has made paper microfluidics more attractive in global health applications in developing countries.

1.1 The Emergence of Lateral Flow Assays

Paper has been utilized for a myriad of applications in analytical chemistry. Paper is thin, simple to package, and is cost effective. The surface of the paper can be functionalized and the specificity of a membrane can be altered based on the aims of the device. Reagents can also be selectively impregnated into the membrane and the porous structure of the paper can be used to alter the flow characteristics of the membrane. Paper is also relatively inert and are compatible with a number of chemicals. Since paper is versatile material it has recently experienced an uptick in the field or rapid diagnostics. Potential applications include bioterrorism, food safety, veterinary medicine, immunoassays, urinalysis, and environmental monitoring

(Yetisen, Akram, and Lowe 2013). Commercial rapid diagnostics have been successfully deployed for the detection of influenza, tuberculosis, and other bio-hazards. The most prominent manifestation of these paper microfluidic devices has been deployed for the detection of human chorionic gonadotropin (HCG) for pregnancy. Other systems implement lateral flow detection or electrochemical detection for a wide variety of analytes such as the widely available glucose sensor used by diabetics.

Some of these devices are built with a polyester or other hydrophobic backing, while other membranes come unprocessed and need to be mounted on a surface with the use of a spray adhesive or double sided tape (Ghaderinezhad et al. 2017). Various fabricated paper microfluidic devices can be seen in Fig. 1 (Yetisen, Akram, and Lowe 2013). Various fluidic structures have been fabricated with the use of a wax screen printing methods (Lu et al. 2009). Techniques that have been successfully used include wax dipping, printing of a hyrdophobic ink using a phaser printer, μPADs (microfluidic paper based microfluidic devices) cut with an automated cutter and a laminated structure, and other designs designed using photolithography techniques used in the semiconductor industry. Additional hybrid devices include a polydimethylsiloxane patterned nitrocellulose device for the creation of microfluidic channel for the selective filtration of RBCs. In Figure 1, (A) represents a μPAD fabricated using the wax screen printing method (Dungchai, Chailapakul, and Henry 2011) (B) represents the wax dipping method to direct fluid flow into two separate sensing membranes (Songjaroen et al. 2011; Songjaroen et al. 2012). (C) represents a wax printing technique with the use of a phaser printer Lu et al. 2009. (D) represents an AKD ink printed μPAD fabricated device. (E) represents a fluidic structure fabricated on chromatography paper (Li et al. 2010). (F) represents a μPAD structure cut with an automated cutter (Olkkonen, Lehtinen, and Erho 2010). (G) represents a μPAD cut with a

CO_2 laser cutter (Fenton et al. 2008). (H) represents a novel laser treatment for a nitrocellulose membrane (Fu et al. 2011). (I) represents and inkjet deposition of polystrene/toluene solution on paper (Abe, Suzuki, and Citterio 2008). (J) represents a photoresist patterned device created on chromatography paper (Martinez et al. 2007). (K) represents an alternative technique for the printing on chromatography paper with an inkjet printer (Martinez et al. 2008). (L) represents a Polydimethylsiloxane (PDMS) microfluidic patterned device (Bruzewicz, Reches, and Whitesides 2008).

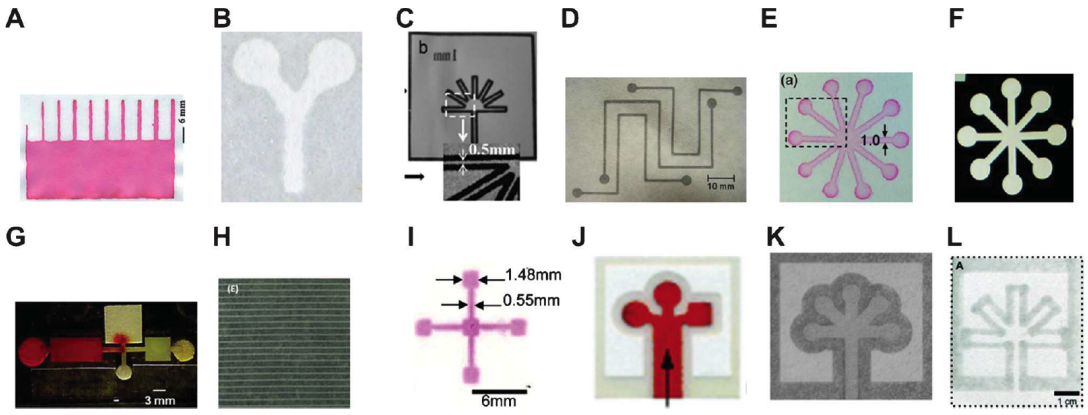

Figure 1. Various types of paper based microfluidic devices which are described in the section and the various types of functionalizations that can be applied to the surface.

The majority of these devices can be grouped into the category of point of care diagnostics, which refer to diagnostic testing at the immediate point of testing. This is appealing from a global health perspective in terms of diagnostics for developing countries which may not have the infrastructure for laboratories. In addition the detection of analytes in smaller concentrations in an appealing form factor is appealing to health-care providers. There are a number of criteria with regards to the design of a point-of-care diagnostic tool that are outlined by the World Health Organization (WHO). In general point of care devices should follow the ASSURED criteria, which

means that a potential point of care device should be Affordable, Sensitive, Specific, User Friendly, Rapid/Robust, Equipment Free, and Delivered to those needing it. This criteria has been widely adopted in the vast majority of implementations of devices for point of care or global health applications.

1.2 Blood as an Diagnostic Tool

Blood is one of the most essential biological fluids and has a number of crucial purposes from transporting nutrients and oxygen to vital organs of the body to regulating pH, essentially acting as a biological buffer. Blood also facilitates the immune response in the body by shuttling the immune cells across the vascular network to respond to potential infections and to enable the healing process(Goodman et al. 2007). Due to the presence of a plethora of cofactors, proteins, and other biomarkers, the majority of diagnostic tools have relied on the collection of a blood sample to provide information on the well-being of the patient(Bhalla et al. 2013; Castillo-León and Svendsen 2014). Health care professionals can extract a wealth of information from the collection of a blood specimen, and this is the general method of diagnosis. Blood samples are generally used for a plethora of applications, from cancer screening to general hospital diagnostics (inflammation markers, mineral concentrations in the body, etc.). Blood tests/diagnostics are generally performed in a lab setting, impacting the scope of healthcare delivery particularly in developing countries.

Blood contains both cellular and plasma components. Cellular components include platelets, leukocytes, and eryhrocytes (red blood cells) while plasma components include water, salts, enzymes, glucose, clotting factors, electrolytes, and antibodies. Plasma comprises about 55% of total blood volume and the cellular component

comprises the remaining 45% of blood volume(Cate et al. 2014). Some of the proteins contained in plasma include albumin, fibrinogen, and other globulins that may be present in blood. Blood serum refers to plasma that does not contain any clotting factors (Homsy et al. 2012). The hematocrit level of a blood sample refers to the volume percent of erythrocytes in a sample, with males having a hematocrit level of about 52% and women having a hematocrit level of about 47%. Abnormal hematocrit levels can indicate the presence of anemia, which can affect oxygen delivery across the cardiovascular system. In addition, red blood cells are geometrically larger than most components of blood and can be as large as 6μm in diameter, which allows for size exclusion filtration methods which are covered in the following section.

Red blood cells make up the majority of the cells that are present in a blood sample $> 99\%$ with the remaining $< 1\%$ of cells or formed cells being thrombocytes and leukocytes. Separating red blood cells has always been a significant issue for point-of-care diagnostic tools as standard techniques used in a laboratory such as centrifugation do not meet the criteria for point of care devices.

Other diagnostic fluids that are commonly used are urine, fecal matter, and saliva. Saliva based detection modalities are rapidly gaining widespread adoption, but blood still remains as the gold standard in terms of diagnostics.

1.3 Development of a Fluorescence-based Lateral Flow Platform for Detection of Biomarkers in Whole Blood

Our group has been developing a fluorescence-based platform for the detection of biomarkers in the form factor of a lateral flow assays. In general lateral flow assays are designed to be more qualitative, with the goal of having a yes or no reading. On the

other side of the spectrum, fluorescence platforms (Tecan scanners and other optical methods) require a trained professional to operate the equipment and can cost in the hundreds of thousands of dollars. By eliminating the expensive optics, our team has developed a device which related fluorescent intensity to the voltage-time domain.

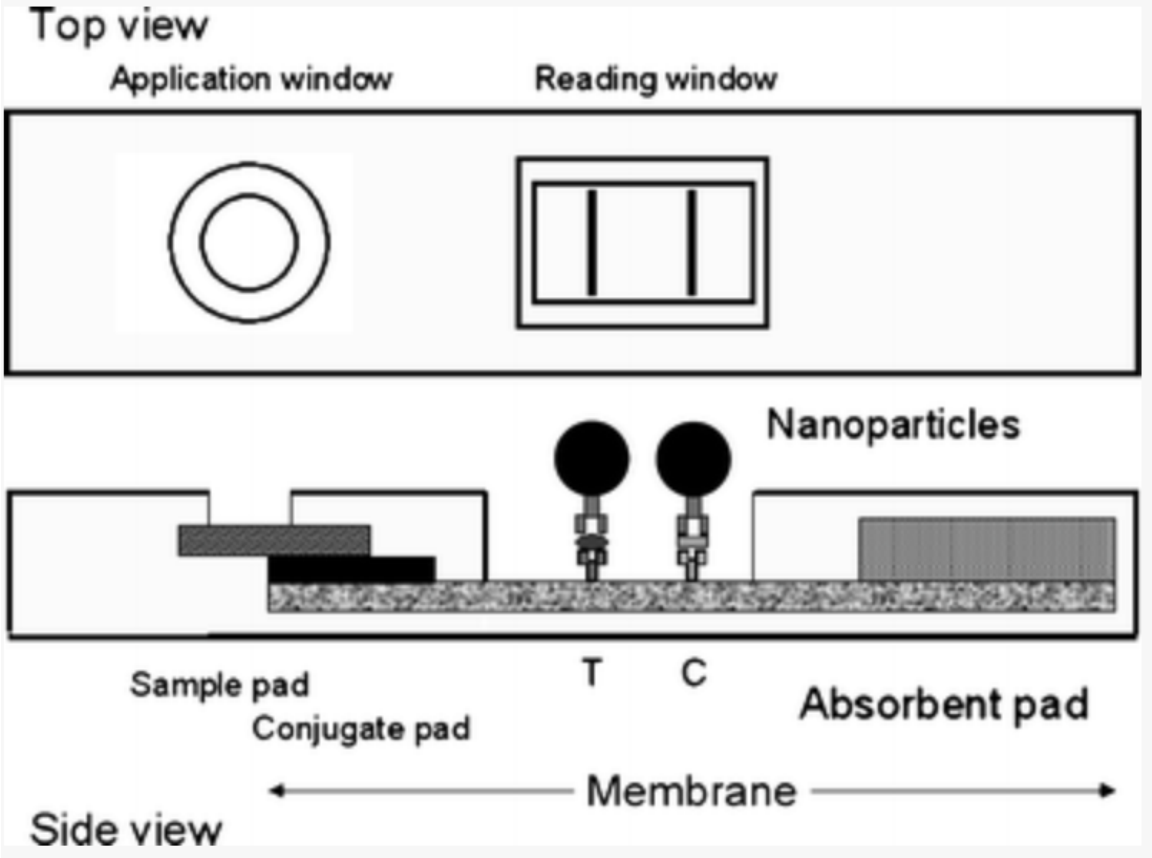

Figure 2. A sample nanoparticle based immunoassay and schematic (Posthuma-Trumpie, Korf, and Amerongen 2009).

Lateral flow assays generally use colorimetric means to measure various biomarkers with a fairly simple setup. By using varying layers of membranes, an analyte is deposited on a sample pad. The lateral flow also contains a conjugate pad (containing colorimetric markers in this situation), a testing membrane, and a wick at the end of the assay. In the test membrane, there is usually a test line and a positive control line.

This is the gold standard for qualitative measurements but in the majority of cases colorimetric methods are not sufficient. The fluorescence based assay that is designed uses an LED to emit light and a photodiode to measure the fluorescent signal emitted by the fluorophores.

The system uses a green exitation filter and an orange emission filter with a photodiode and an intergrator. In this situation, the Beer-Lambert law becomes important, with the current output of the detector being directly related to the strength of the fluorescent signal at the photodiode, which can be seen in Equation 1.

$$I_{PD} = KI_0[1 - exp(-\epsilon lc)] \tag{1}$$

where I_{PD} is the current of the photodetector, K is a variable that describes the responsitivity of the photodiode, I_0 describes the intensity of the excitation source, ϵ describes the extinction coefficient of the fluorophore, l describes the path length of the sample, and c describes the value of the capacitor (Obahiagbon et al. 2016).

$$V_{out} = \frac{1}{C}\int_0^T I_{PD}dt \tag{2}$$

Equation 2 shows the output of the charge integrator circuit, which is related to the current at the inverting terminal of the operational amplifier. C describes the feedback capacitance and t describes the integration period. Equation 3 shows the fluorophore-concentration-dependent output voltage of the integrator circuit, which directly relates the sensor voltage to the photodiode current and the integration time (Obahiagbon et al. 2016).

$$V_{out} = \frac{1}{C}\int_0^T [KI_0((1 - exp(-\epsilon lc)) + I_B]dt \tag{3}$$

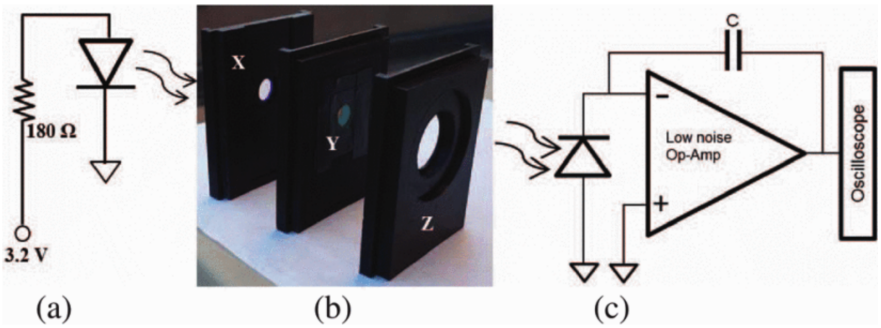

Figure 3. A schematic of the excitation and emission sources of the setup. Part (a) shows the green emission LED, (b) shows the housing of the emission and excitation filters, and (c) shows the orange excitation photodiode along with the charge integration amplifier circuit (Obahiagbon et al. 2016).

Fig. 3 displays a simplified schematic of the entire PD detection scheme. As mentioned earlier, the system uses a green excitation source and an orange emission source. There are two emission and excitation filters which are placed in a 3D printed ABS housing and a photodiode/charge integration circuit for the measurement of the intensity of the emitted signal. Fig. 4 demonstrates how the output voltage can be related to the intensity of the signal. The ramp time describes the time delta between the low and high states of the charge integrator (typically between 1V and 8V). Therefore, a sample with a faster ramp time would correlate to a higher fluorescent signal and vice versa.

1.4 Characterization of Capillary Driven Fluid Flow

The flow of fluid on a paper substrate can be essentially modelled as a flow through a porous medium. The wicking mechanism of the paper can be simplified as capillary-driven flow, which is caused by a pressure gradient along the meniscus of the fluid in a capillary. The pressure gradient is caused by the surface tension

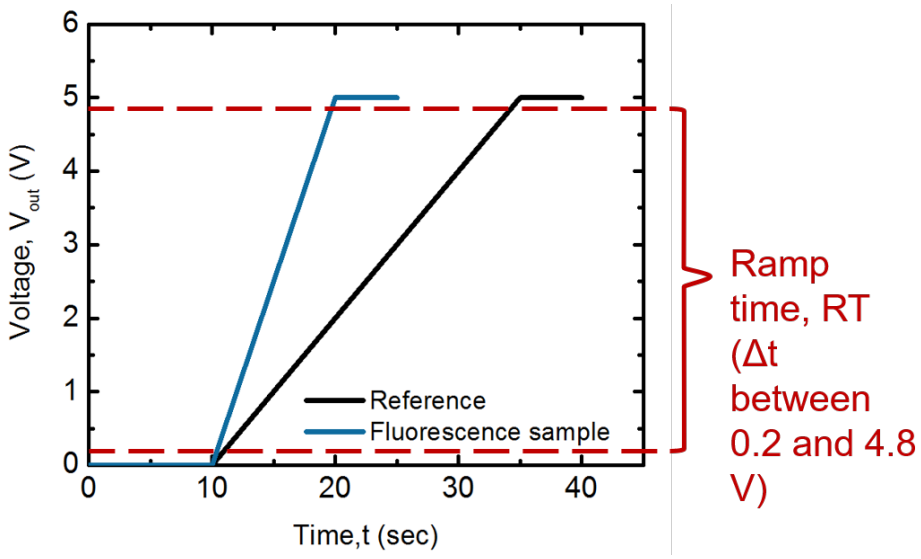

Figure 4. A relation of the output voltage of the charge integration circuit which is directly related to the intensity of the fluorescent signal (Obahiagbon et al. 2016).

induced by molecular interactions in the fluid interface.The magnitude of the cohesion of the forces can be quantified by measuring the contact angle of the liquid-to-air interface. This is measurement of surface energy provides information about the wettability of the surface, with smaller contact angles ($< 90°$) corresponding to a high wettability and larger contact angles ($> 90°$) corresponding to a lower wettability as seen in Figure 5(Yuan and Lee 2013). Higher wettability also indicates that fluid will spread and maximize its contact with the fluid interface and vice versa. Hydrophobic modifications to the paper substrate can decrease the wettability of the surface and this can be combined with lithography techniques to create fluid flow in selective areas of a substrate. This relationship between contact angle and surface tension was quantified by Thomas Young in the early 1800s:

$$\gamma_{lv} \cdot cos\theta_{\gamma} = \gamma_{sv} - \gamma_{sl} \tag{4}$$

where γ_{lv},γ_{sv}, and γ_{sl} describe the interficial tensions between the liquid-vapor, solid-

vapor, and solid-liquid interfaces respectively. This equation is commonly referred to as Young's equation. However due to contact angle hysteresis, the smoothness of the surface also plays a role in the wettability of a surface and Young's equation is only used to model the contact angle in ideal situations (no hysteresis and perfectly smooth solid surface) (Li et al. 2010). Young's equation is generally used in cases where the pore size is known as is consistent across the solid interface. However, this is unlikely in a paper or fibrous material since the contact angle and smoothness cannot be accurately quantified due to its non-uniformity. Fig 5 shows the effect of contact angle for both wetting and non-wetting fluids.

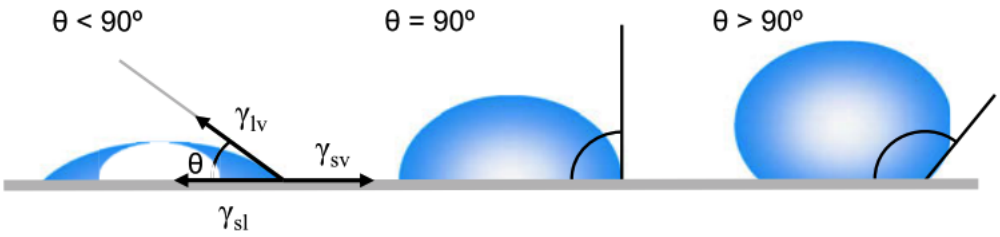

Figure 5. Contact Angle for both non-wetting and wetting fluids (Yuan and Lee 2013).

The flow of blood in the constructed microchannel as well as in the case of aggregation of erythrocytes at the site of separation can be theoretically modeled using the Casson flow model where the non-Newtonian characteristic of blood is also taken into consideration. The equation for the Casson flow model is identified as:

$$\sqrt{\tau} = \sqrt{\tau_0} + (\sqrt{\mu_c}\ \sqrt{\dot{\gamma}}) \tag{5}$$

where τ is the shear stress, μ_c is the Casson's coefficient of viscosity, τ_o is the yield stress and $\dot{\gamma}$ is the rate of shear. From experimental studies conducted on blood, it was found that the yield stress of blood is approximately 0.004 Pa. Casson's coefficient

of viscosity is given by the equation

$$\mu_c = \eta_p(1 + 0.025H + 7.35 * 10^{-4}H^2) \tag{6}$$

where η_p is the viscosity of plasma and H is the hematocrit concentration (Maria et al. 2016).

Since the aspect ration or width to height ratio of the microchannel is very high, the infinite parallel plate assumption can be made which would give a Navier-Stokes equation for a fully developed flow as

$$\frac{\partial \tau}{\partial y} = \frac{\partial P}{\partial x} \tag{7}$$

In this scenario, the driving force is the Young-Laplace pressure which is the pressure responsible for capillary flow. It is defined by the Young-Laplace equation which quantifies the capillary pressure difference across an interface between two static fluids, which in our case will be whole blood or plasma and air. The Young-Laplace pressure is given by the equation:

$$P_O = \sigma(\frac{1}{R_1} + \frac{1}{R_2}) \tag{8}$$

where σ is the surface tension of blood and R_1 and R_2 are the radii of curvature of the top and side walls of the channel respectively. These are the governing equations for capillary flow in porous media.

1.5 Characterization of Fluid Flow through Porous Media

The flow of a fluid through a fully-wetted medium can be described with Darcy's Law. This equation was used to model flow through a bed of sand. This equation is

related the relation of electrical resistance in Ohm's Law. This equation related to laminar flow when the interstices of the pores are small and do not have any turbulent flow. The pressure gradient of the flow is also directly proportional to the fluid velocity and this is given in vector form as Darcy's Law:

$$\frac{\mu U}{k} = -\nabla p \tag{9}$$

where μ represents the viscosity of the fluid, U represents the average velocity of the fluid, k represents the permeability of the fluid, and ∇p represents the pressure gradient of the fluid. The adaptation of this equation will be covered in the mathematical modeling section of this document.

1.6 Review of Blood Fractionation Methods

Blood fractionation has been generally separated into two different techniques: active methods of separation as well as passive methods. The accepted techniques for the separation of red blood cells are generally membrane based blood fractionation methods, but there has recently been significant advances in microfluidics based separation systems(Toner and Irimia 2005). Interestingly enough, there have been several paper microfluidics techniques that have been developed that combine microfluidic aspects into a nitrocellulose membrane. However, there is no widely accepted method for multiplexed detection of biomarkers from a small sample of blood. Figure 6 shows the general methods of red blood cell fractionation, which includes passive in addition to active methods.

Certain active methods seen in Fig. 6 such as magnetic activated cell sorting (MACS), fluorescent activated cell sorting (FACS), and other optical methods are too

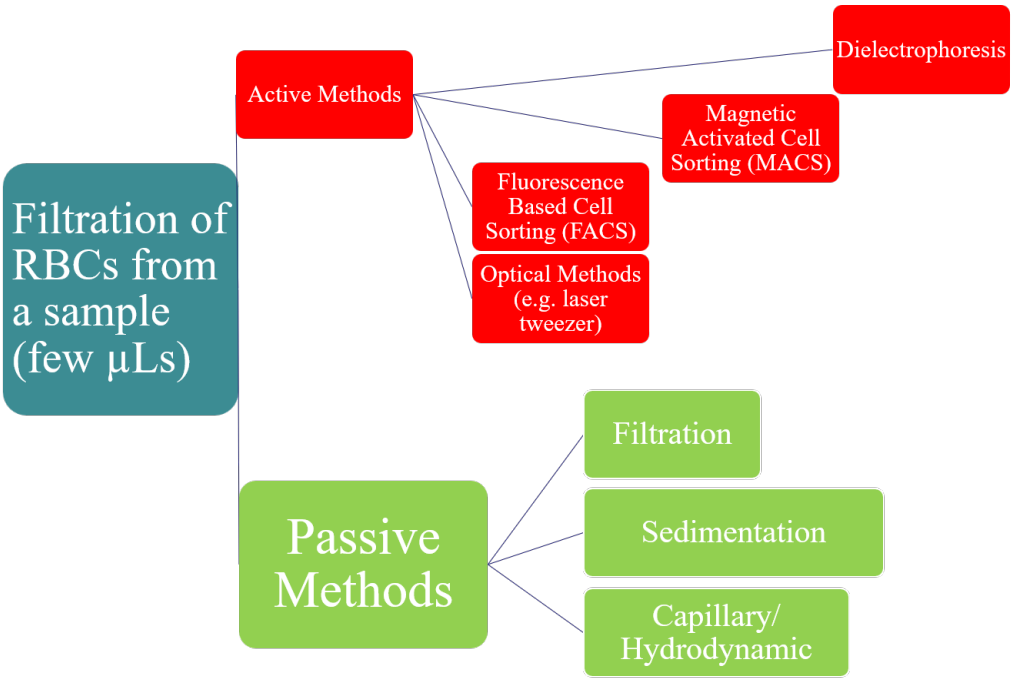

Figure 6. Various methods of blood fractionation of small samples.

expensive, require experienced users, and require significant amounts of equipment, disqualifying these methods for point of care use (Szydzik et al. 2015,Piacentini et al. 2011,Miltenyi et al. 1990, Lopez-Munoz and Mendez-Montes 2013). However, all of the passive methods are not complex by design and can be used for point of care devices in accordance to ASSURED criteria. These passive methods generally do not require any external force and depend on capillary force, hydrodynamic forces, or sedimentation forces. This section will cover recent microfluidic efforts in RBC fractionation as well as fabrication techniques and its resultant devices in the paper fluidics realm. Each method will be compared with regards to separation efficiency and purity of the separated sample.

1.6.0.1 Membrane Filtration

Membrane filtration is the most common technique for the filtration of red blood cells and relies on the size exclusion principle and capillary/hydrodynamic forces for the separation of plasma. There are some off the shelf nitrocellulose and polysulfone membranes which rely on this principle with varying degrees of success (Tageson 2013; Lam et al. 2017; VanDelinder and Groisman 2006). These membranes have a three dimensional porous structure which allows for proteins, immune cells, and other bio-markers to flow through while trapping the red blood cells in the pores of the membrane. GE Whatman, Pall, Millipore, and I.W. Tremont all create membranes which are specifically tailored for lateral flow and vertical flow assays. Some membranes are also functionalized with an agglutinating chemistry which can be used for the filtration of clotting factors in the lateral flow format. A significant factor that must be considered in these membranes is the risk of hemolysis of the red blood cells due to high pressures induced in a microfluidic system. Shear pressures must be kept to a minimum and adding more fluid to a membrane which has been saturated can increase the risk of hemolysis(Nilghaz and Shen 2015). As such, point of care assays have to be carefully designed to accommodate for fluctuations in fluid delivery. Additional factors that have to be considered include material type, thickness of the membrane, fluid capacity, and the capillary flow rate. Table 1 provides a summary of the operating specifications of the various commercial membranes which are specifically marketed for the filtration of RBCs as seen in Table 1.

The majority of the filters seen in Table 1 are rated to handle 100 μL of whole blood with minimal risk of hemolysis. Some of these filters are built with a polyester or other hydrophobic backing, while other membranes come unprocessed and need to

Table 1. A comparison of various commercial membranes marketed for the filtration of RBCs.

Brand/Model	Particle Retention (in μm)	Material Type	Thickness (in μm)	Capillary Flow Rate
GE Whatman Fusion 5	2.3	Glass Microfiber w/ Organic Binder	370	38s/4cm
GE Whatman MF1	1.5	Bound Glass Fiber	367	29.7s/4cm
I.W. Tremont Grade D-23	4	Borosilicate Glass Microfiber	500	35s/4cm
Pall Vivid 170	Asymmetric (100-2 microns)	Asymmetric polysulfone	330	150-225 sec/4cm
Millipore Durapore SLVP	5	Polyvinylidene fluoride	125	N/A

be mounted on a surface with the use of a spray adhesive or the use of double sided tape (Ghaderinezhad et al. 2017). Various fabricated paper microfluidic devices can be seen in Fig. 1 (Yetisen, Akram, and Lowe 2013). Various fluidic structures have been fabricated with the use of a wax screen printing methods (Lu et al. 2009). Techniques that have been successfully used include wax dipping, printing of a hyrdophobic ink using a phaser printer, μPADs cut with an automated cutter and a laminated structure, and other designs designed using photolithography techniques used in the semiconductor industry. Additional hybrid devices include a polydimethylsiloxane patterned nitrocellulose device for the creation of microfluidic channel for the selective filtration of RBCs.

As seen in Table 1, there are several materials that are used for the filtration of red blood cells, which include glass fiber membranes and other polymeric materials such as polysulfone. However, they all use the same premise of size exclusion but have slightly different fluid characteristics. An example of this is the Pall Vivid membrane, which employs an asymmetric membrane, which has pores which progressively decrease in size from top to bottom of the membrane. The pores at the top side of the sheet are about 100 microns and the pores gradually decrease to 2 microns on the bottom side of the sheet. A cross sectional SEM image of a Pall Vivid asymmetric polysulfone membrane can be seen in Fig. 7.

Most of these filters require a backing for proper packaging of the fluidic device. In most instances, the use of a spray adhesive or double sided tape to a non-wicking

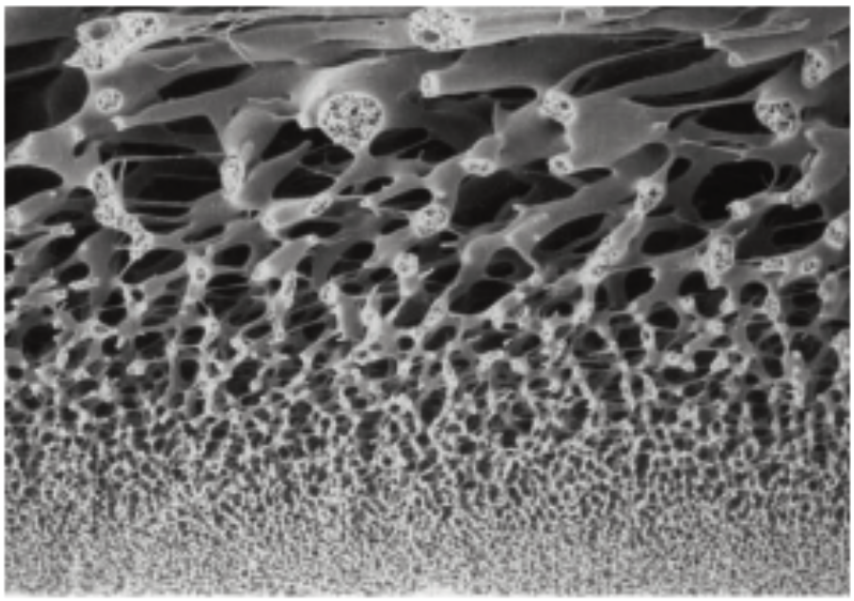

Figure 7. An SEM image of the Vivid Plasma Separation Membrane. The asymmetric nature of the polysulfone membrane can be clearly seen in this cross section.*Courtesy of Pall Corporation*

surface affects the flow characteristics of the membrane and the use of lamination to keep the strip suspended is common practice with the use of paper microfluidics. To direct fluid flow, there are a umber of surface modifications that have been attempted. The majority of these functionalizations act as passive elements and selectively add hydrophobicity to certain areas of the membrane. Membranes can also be used for sedimentation which uses the effects of gravity a blood sample can be filtered with minimal risk of biofouling.Cell sedimentation has also been used to separate red blood cells from plasma. The majority of these devices use gravity sedimentation which incorporates flow across of a porous medium (Crowley and Pizziconi 2005). By using the effects of gravity, larger amounts of samples can be filtered with minimal risk of biofouling. One particular work utilized gravity sedimentation to filter up to 1.5mL of whole blood seen in Fig. **??**(Galligana et al. 2015).

Liu et. al have proposed a superhydrophobic gravity aided blood fractionation

device which is capable of filtering up to 800μL of whole human blood (Liu et al. 2013; Liu et al. 2016). A separation membrane was mounted with double sided tape and within an hour the RBCs were seen to be fully separated from the plasma. The absorbance spectra of the extracted plasma was comparable to a sample prepared via standard centrifugation. As seen in Fig. 8, a clear interface between the separated plasma and blood is apparent after 5 minutes with the sedimentation filter.

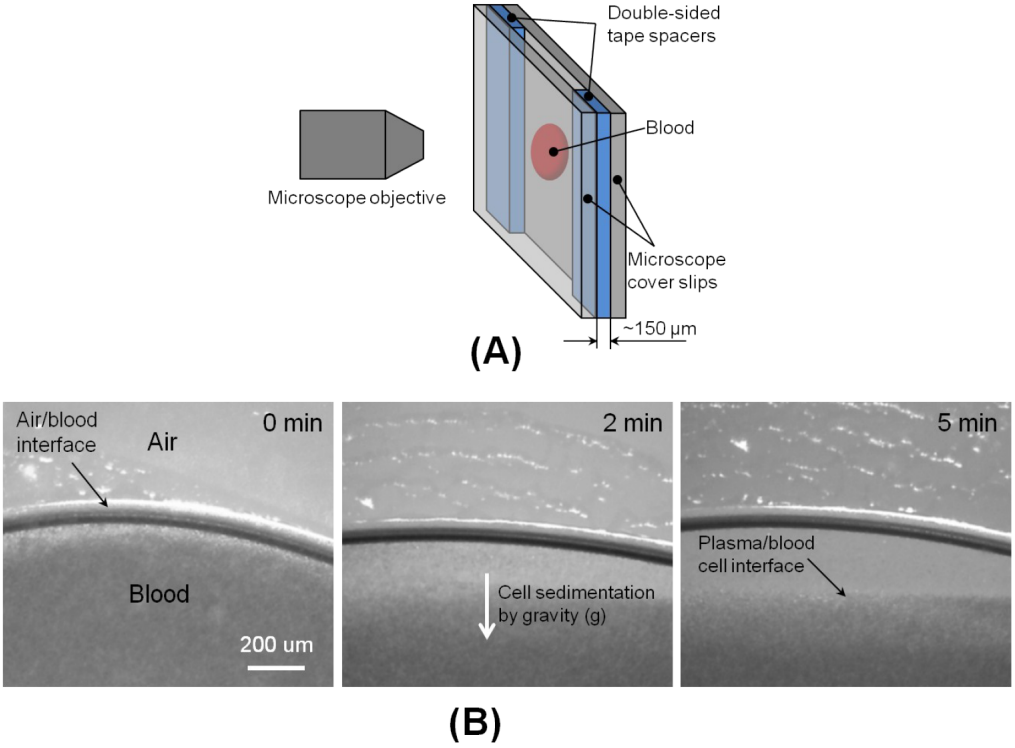

Figure 8. A setup which also uses gravity aided sedimentation to filter 800 μL of human blood by using a super hydrophobic membrane (Liu et al. 2013; Liu et al. 2016).

1.6.0.2 Capillary and Hydrodynamic Separations

As mentioned in previous sections, capillary separations involve the use of capillary forces to separate red blood cells from a sample. Capillary separations can be performed with a minimal sample size with the use of minimal auxiliary equipment. he equipment needed to carry out capillary separation is also minimal, lightweight and portable which makes it a very attractive method of plasma separation to evaluate the condition of soldiers in the midst of a war or people in places where medical services are scarce which usually makes medical help unaffordable. The difference in viscosity between red blood cells and plasma is what causes the capillary separation. Devices have been fabricated with a conjunction of hydrophilic and hydrophobic surfaces to direct fluid flow (Tripathi et al. 2016). In the majority of devices, channels are selected where a section of the channel is completely hydrophobic, and this can allow the flow of less viscous materials such as plasma while reducing the flow of red blood cells. In some situations, the accumulating red blood cells can create a barrier to eliminate the flow from other red blood cells.

For these devices the most important factor is the elimination of any additional induced shear stresses as any additional force on the red blood cells can force them to burst, which is a phenomenon known as hydrolysis. If the RBCs burst, then hemoglobin and the contents of the cells are released into the plasma and may be a confounding variable in ELISA assays and other colorimetric type diagnostic tests. Therefore it is important to eliminate any additional hydrodynamic stress in the system to ensure that the plasma/serum is pure throughout the entire detection assay process. Pre-wetting membranes with buffers or the introduction of wicking pads into a lateral flow assay may help to eliminate the incidence of this during an assay.

1.7 Experimental Overview

This thesis is split up into multiple chapters by each aspect that was developed of the lateral flow assay. Chapter 2 covers the development of a blood fractionation technique along with the characterization of the fluidic flow of each of these membranes. This chapter culminates with an implementation of the blood separation membrane in an actual lateral flow ELISA assay. Chapter 3 covers the progress made towards the creation of valve actuation on a porous membrane and the characterization of the fluidic control with the introduction of these valves. This includes the development of a heated deposition method, chemical and fluidic characterization of each of the valve materials, and the development of moulds for the development of alternative deposition methods on a porous membrane. Chapter 4 covers progress made towards modelling fluid flow in a porous media with a two pronged approach. Mathematical models in addition to computational fluid dynamics models were created and verified with experimentation. Lastly, Chapter 5 covers the development of two software interfaces created to connect the lateral flow data acquisition program to a more user friendly graphical user interface. This section covers application development for iOS devices as well as the creation of a computer application in Visual Basic.

Chapter 2

BLOOD FRACTIONATION AND ASSAY IMPLEMENTATION

This chapter covers the efforts made towards the development of the blood fractionation aspect of the lateral flow assay outlined in the first chapter. The initial set of experiments covered a means of modeling fluid losses due to evaporation and predicting these losses in various conditions. The second section covers the selection and characterization of various blood filtration membranes by testing the overall effective plasma filtration rate as well as a measurement of the baseline fluorescence of each of the membranes that were to be characterized in these experiments . The last section discusses the implementation of the optimal blood fractionation membrane in an assay as well as initial results.

The objective of these sections is to find the overall effective rate of evaporation of blood in a porous media in addition to measuring the effective rate of plasma filtration for the blood fractionation membranes. The lateral flow assay is to be deployed in India where the climate is usually humid and hot. Devices that are designed for global health applications must be somewhat stable from fluctuations from the external environment and humidity or the evaporation of the fluid measured could have a significant effect on the overall accuracy of the detection assay. In addition fluid flow characteristics are an important consideration as proper control of flow will eliminate the majority of variations in the lateral flow assay when it comes to mass transport. The initial set of experiments characterized the overall auto fluorescence of the membranes under consideration as too much background signal will decrease the overall signal to noise ratio (SNR) of the fluorescence based

reader. Afterwards the evaporation of blood was characterized in comparison to mouse blood and K2 EDTA sheep blood. Afterwards the membrane evaporation was characterized at various humidities and starting masses with the membranes which exhibited minimal autofluorescence. The final section of this chapter covers the selection of the optimal membrane and the implementation of the assay with blood samples for Epstein-Barr Nuclear Antigen (EBNA) and Immunoglobulin G (IgG) in the lateral flow configuration was performed with a whole blood sample.

2.1 Testing of Filtration Membranes

The performance of each of the membranes can be quantified with a number of metrics such as autofluorescence (addition to background signal), flow characteristics pre/post wetting, and overall capacity of the membrane. Pore size is also important for membranes that will be used for the filtration of blood as mentioned in previous sections.

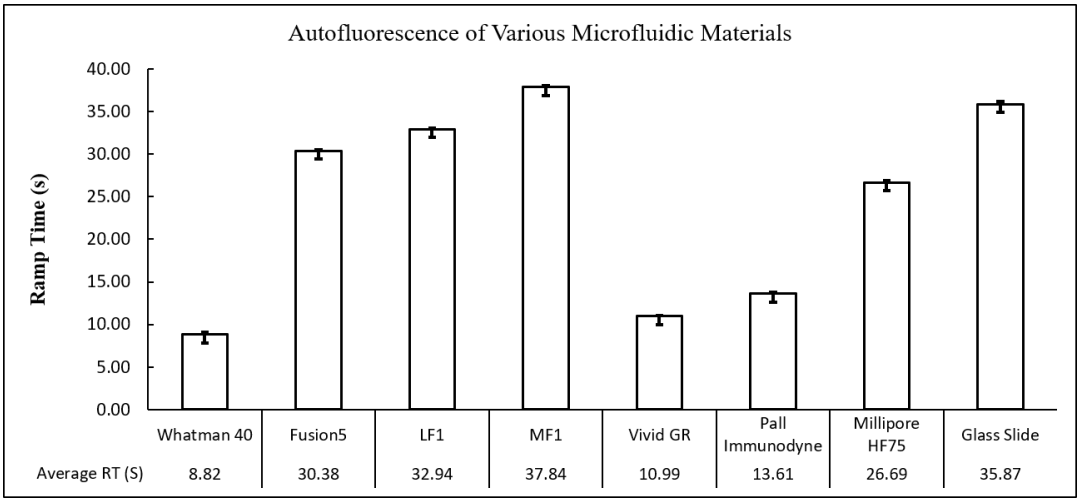

Figure 9. A characterization of the autofluorescence of different types of polymeric membranes that are used in various parts of the lateral flow assay.

Strips of (GET DIMENSIONS FROM UWA) were cut with the use of a programmable shear cutter. Three different strips were cut and the autofluorescence was measured at three different points of each of the membranes. Each strip was mounted directly on a glass slide with the use of double sided tape and was inserted into the fluorescence reader. More information about the fluorescence reader can be seen in Chapter 1. A lower ramp time indicates more overall fluorescence and vice versa. The widely used Whatman Ashless 40 Filter Paper was tested as a general basis of comparison. Blood Filters that were characterized include the Pall Vivid GR asymmetric polysulfone separator membrane, the GE Whatman LF1 glass fiber membrane, and the GE Whatman MF1 glass fiber membrane. The GE Fusion 5 multipurpose nitrocellulose membrane, Pall Immunodyne, and the Millipore HF 75 nitrocellulose are high flow membranes and were considered for selection in the testing section of the lateral flow assay.

As seen in Figure 9, The Pall Vivid GR membrane exhibited a high amount of autofluorescence, due to its asymmetric polysulfone material. On the other hand, the Whatman LF1/MF1 membranes had an autofluorescence that was comparable to the glass slide reference samples in addition to the Fusion 5 membrane. However, since the blood filters were to be placed upstream from the photodetector/LED setup, autofluorescence of the membrane should have minimal effect on the SNR from the reader.

2.1.1 Plasma Yield Experimental Setup

These lateral flow assays are meant to be run in the matter of about 10 minutes, so the effects of evaporation were tested. In these experiments, strips were weighted and

placed in a scale (Denver Instruments, Colorado, USA) to get a baseline measurement. Afterwards 50μL of mouse blood was dispensed on the strip and a tared measurement was taken of the initial weight of the sample. The humidity and temperature of the ambient environment was also recorded and the change in weight was recorded every 30 seconds for a period of 600 seconds. In this period of time, the fractionation of the sample was observed and photographs were taken of the membranes in the beginning and end of each trial.

There was significant hemolysis in the sample as seen in Fig. 10, which shows successful fractionation of the plasma from the red blood cells. However, the light red tinge in the separated plasma is indicative of hemolysis of the sample. To verify this, the sample was centrifuged to separate the blood from the plasma and the plasma layer had a slight red discoloration consistent with the samples that were tested. A 125μL sample of nonhemolyzed K2 EDTA sheep blood was ordered (BioReclamation/BioIVT, USA) and the meantime the majority of the experiments were completed with water since the majority of the blood is composed of water. After the sheep blood arrived the rate of evaporation of water was compared to that of blood to verify this result.

Another important consideration of the selection of the blood filtration membrane is proper fluid retention of the sample. The average finger prick yields anywhere from 50 μL to 150 μL of blood and membranes which cannot retain this fluid were automatically rejected from consideration. In Fig. 11, a Whatman MF1 membrane was cut to the same width as the nitrocellulose test membrane and the blood sample overflowed from the membrane. Since containment of the sample leads to the highest yield of the sample, this type of membrane was automatically rejected from consideration since it could not properly hold the minimum amount of fluid (50 μL) required for this lateral flow configuration.

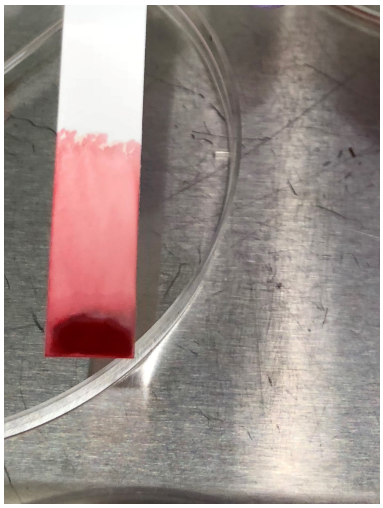

Figure 10. An example of the hemolysis seen in a strip of Pall Vivid GR plasma separation membrane in the sample of mouse blood. This result was verified by centrifugation of the blood sample.

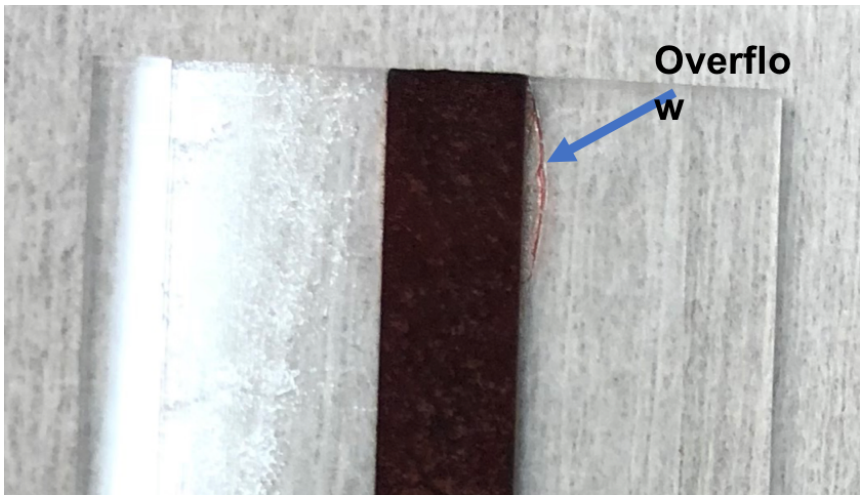

Figure 11. Overflow of a 50μL mouse blood sample on a Whatman MF1 membrane mounted on a glass slide with double sided tape.

Various techniques were attempted for the deposition of the fluid from hand pipetting the fluid to the use of a capillary to move the blood onto the membrane. In addition blood was also directly applied to the membrane by touching the finger onto the membrane during blood collection. To allow for maximum consistency, a

150μL heparin coated glass capillary was used in the remaining blood experiments. Inconsistent application of the blood with the use of the finger touch method can be seen in Fig. 12 on the Vivid GX membrane.

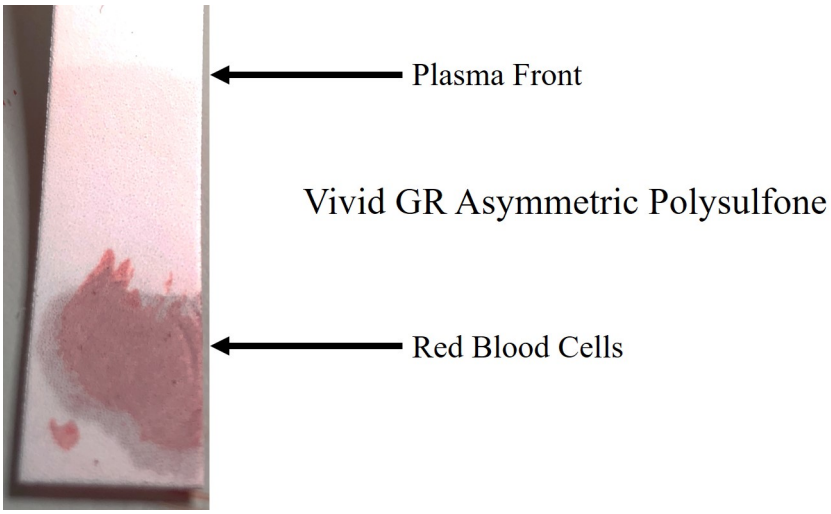

Figure 12. An example of inconsistent blood deposition on the Vivid Gx membrane that was done with the finger touch method. The plasma front is clearly seen, but the wicking of the plasma occurs in multiple directions which introduces extra variability into the assay.

There were three final membranes which visually exhibited optimal filtration characteristics in comparison to the other membranes, which were found to be the Pall Vivid GR, Pall Vivid GX, and the GE Whatman LF1 membranes. To quantify optimal percent yield of plasma a set of experiments was completed between the three polymeric membranes. 5mm by 5mm square strips were cut from each of the membranes and were placed directly on top of a 5mm by 30 mm Millipore membrane. The Millipore HF75 membrane was weighed before each experiment. Afterwards, 20 μL of K2 EDTA sheep blood was pipetted on top of the filtration membrane. The filtration membrane was allowed to filter the blood into plasma for 180 seconds and it was removed after this period. The Millipore HF75 membrane was weighed afterwards

and this change in mass was converted to an estimated plasma yield, using a general calculation of 1.025 g/ml. Three trials were completed in one sitting to eliminate any variance due to humidity or temperature fluctuations. Figure 13 shows the setup of these yield experiments.

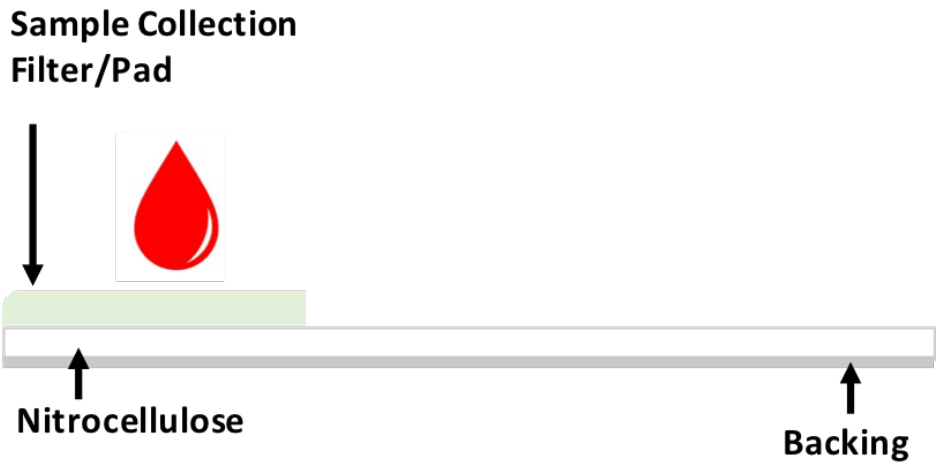

Figure 13. A schematic of the experimental setup for the blood weighing experiment where the sample pad was placed on top of the nitrocellulose and the nitrocellulose was weighed after 180 seconds.

As a point of reference, the Pall Vivid GX membrane is rated to recover at least 60% of the plasma in a sample and the Pall Vivid GR membrane is rated to recover at least 80% of the plasma in the sample. There is no published data on the plasma yield of the GE Whatman LF1 glass bound fiber membrane. It is also important to note that both the Vivid GX/GR membranes are asymmetric and they must be placed in a certain orientation for optimal results. The 'shiny' side of the membrane is the more porous side of the membrane so it must be placed face up. The GE Whatman LF1 membrane does not exhibit any asymmetry and is not orientation specific.

To find this percent recovery metric for each of the membranes, the amount of K2 EDTA blood that was pipetted (20μL) was converted to a weight with the use of a

standard density of blood (1.014 g/mL) and the weight of the plasma captured in the second membrane was used and compared to the original mass. This conversion was converted to percentage and three of each sample was completed to find out if there is any variance that is needed to be accounted for with regards to the efficiency of each membrane in addition to the calculation of the standard deviation and variance of each of the membranes. In addition all of the experiments were completed in two days with similar humidity rates (25-27% effective humidity) to equalize between the evaporation rates of the blood and plasma over time. The humidity, temperature, and barometric pressure was measured with the use of an ST Microelectronics IoT Tile and the sensor was allowed to rest for at least five minutes before any measurements were taken. In addition the scale was calibrated before every daily set of experimental runs to ensure consistency between days of experimentation. The results of this experiment can be seen in Fig. 14.

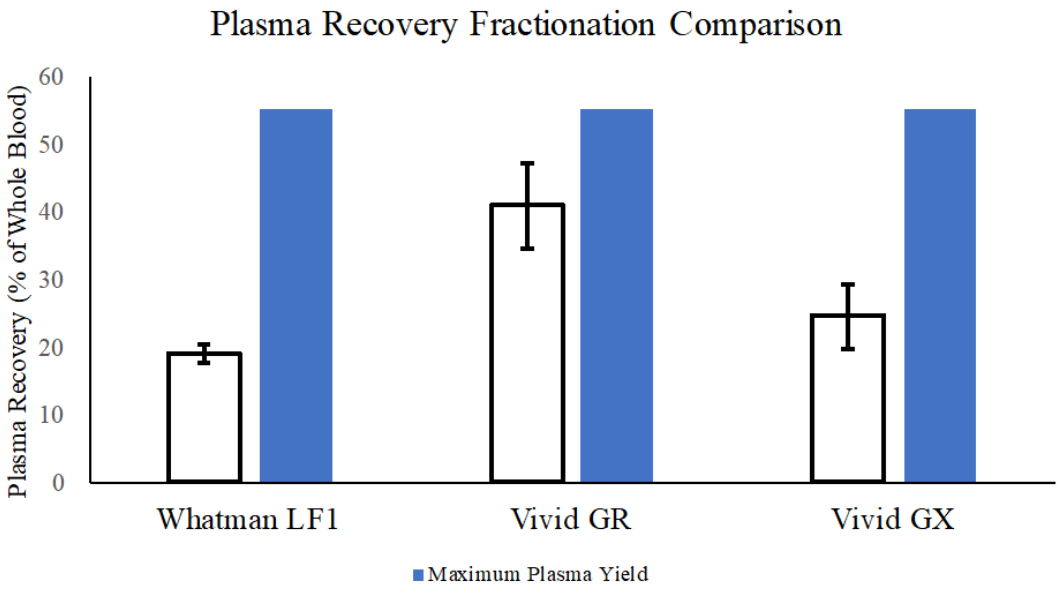

Figure 14. The results of the plasma recovery experiment created to characterize in each of the plasma membranes.

As seen in Fig. 14, the Vivid Plasma GR membrane filtered close to 40% of the plasma from the sample of whole blood. Since blood is roughly 55 percent plasma by volume, about 75% of the plasma was filtered through the membrane into the secondary capture sheet. There was significant variance in a couple of the samples, and all of the potential outliers were much lower than the other points and this is due to the fact that one or two of the samples were left out for an extended period of time, which could relate to fluid losses due to evaporation. Improvements to this experiment involve taking the measurement of the plasma instantly after the fractionation step is complete. In addition, pre-wetting the membrane and compensating for volumetric addition of the fluid would help to purge any plasma that was stuck in the pores of the membrane. In addition more runs should have been conducted to decrease the range of the error bars or the standard deviation of each of the groups. Overall the Vivid Plasma GR polysulfone membrane exhibited the best filtration characteristics and was used in the following sections in this chapter.

2.1.2 Evaporation and Fluid Retention Experiments

The Vivid GR asymmetric polysulfone membrane was selected as the blood filter since it resulted in the highest yield of plasma in comparison to the other two membranes (Pall Vivid GX and Whatman MF1). However, a noticeable issue in the field of assays in paper microfluidics is the evaporation of fluids for assays which take a longer time. The first experiment aimed to compare the evaporation rate of water to that of blood to see if there was any significant differences in their respective evaporation rates. This process was completed by measuring the change in weight of each of the membranes over a period of 600 seconds. In these series of experiments,

temperature, humidity, and barometric pressure were all measured with the use of the ST Microelectronics IoT tile and the strips were pre-weighed as well.

The first experiment compared the overall evaporation rate of deionized water to the sample of K2 EDTA Sheep blood (BioReclamation IVT, USA). Identical sized strips of Millipore HF75 were cut (5mm x 25 mm CHECK with UWA for dimensions) with the use of a programmable shear and each strip was pre-weighed before it was used in an experiment. Afterwards 50μL of either purified deionized water or K2 EDTA sheep blood were pipetted on an edge of the membrane. The humidity was noted and a weight measurement was taken every 30 seconds. Ten duplicates were completed from each group and the overall evaporation rate was compared between each of the groups with the use of a two sample t-test as seen in Figure 15.

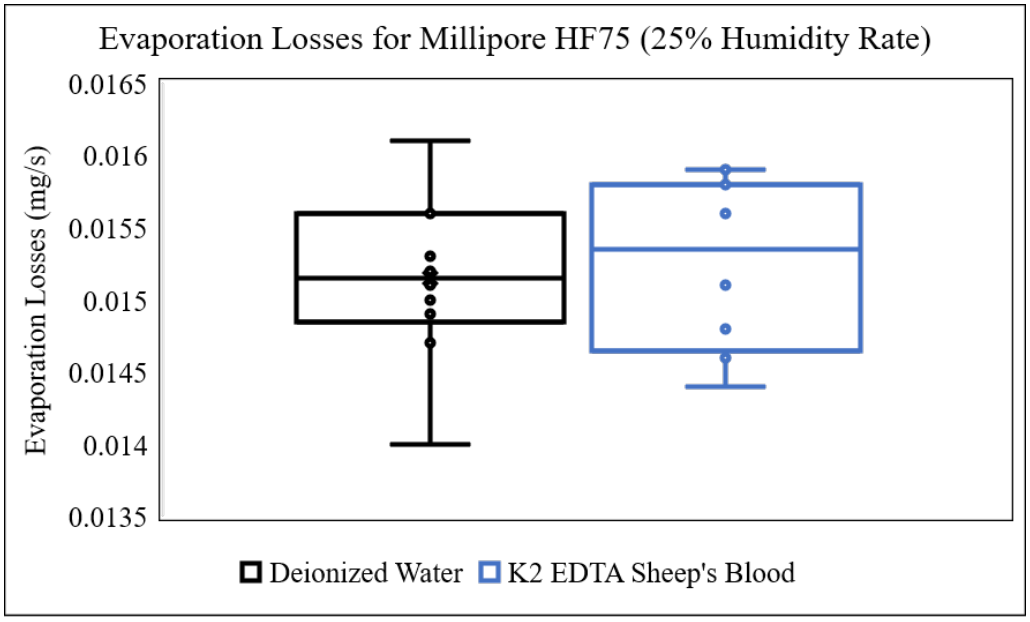

Figure 15. A box and whisker plot showing the overall evaporation of each of the Millipore HF75 membrane with both K2 EDTA sheep blood applied for one group and deionized water applied to the other group. Statistical analysis showed that there was no statistically significant difference between both of the treatment groups.

Each of the groups had roughly the same mean and variance and a two sample t-test resulted in a t statistic of 0.71 which is not significant and results in a failure to accept the null hypothesis. This means that the evaporation of water and blood is essentially similar and can be equivalent for further experimentation. This experiment was completed since there were significant hemolysis and agglutination issues with the blood samples which increased with storage time and deionized water can be used as a consistent means of measuring the evaporation rate of the fluid in porous media.

The characterization of the evaporation rate of the Millipore HF75 was done on two separate occasions, one day with a higher humidity rate and another day where the humidity day was average for Arizona standards. The same procedure was followed where the strips were preweighed and the initial ambient environmental conditions were recorded with the use of the ST Microelectronics IoT Sensor Tile. The initial weight measurement was taken and the weight was recorded every 30 seconds for a period of 600 seconds. For each of the days three different amounts of fluid (50μL, 100μL, and 150μL) were used and hand pipetted on an edge of the membrane. The fluid loss results can be seen in Fig. 16.

The fluid losses in the low humidity condition (24% relative humidity) can be seen to be fairly linear across all of the fluid amounts (50μL, 100μL, and 150μL). This allows for a correction to be applied with the use of an algorithm. The second high humidity experiment (43% relative humidity) shows similar results with a linear rate of fluid loss across all fluid amounts as seen in Fig. 17.

The last experiment of the evaporation fluid loss series of experiments covered the fluid losses of the asymmetric polysulfone membranes (Pall Vivid GX/GR). Both membranes are rated to filter blood to plasma in less than 120 seconds and

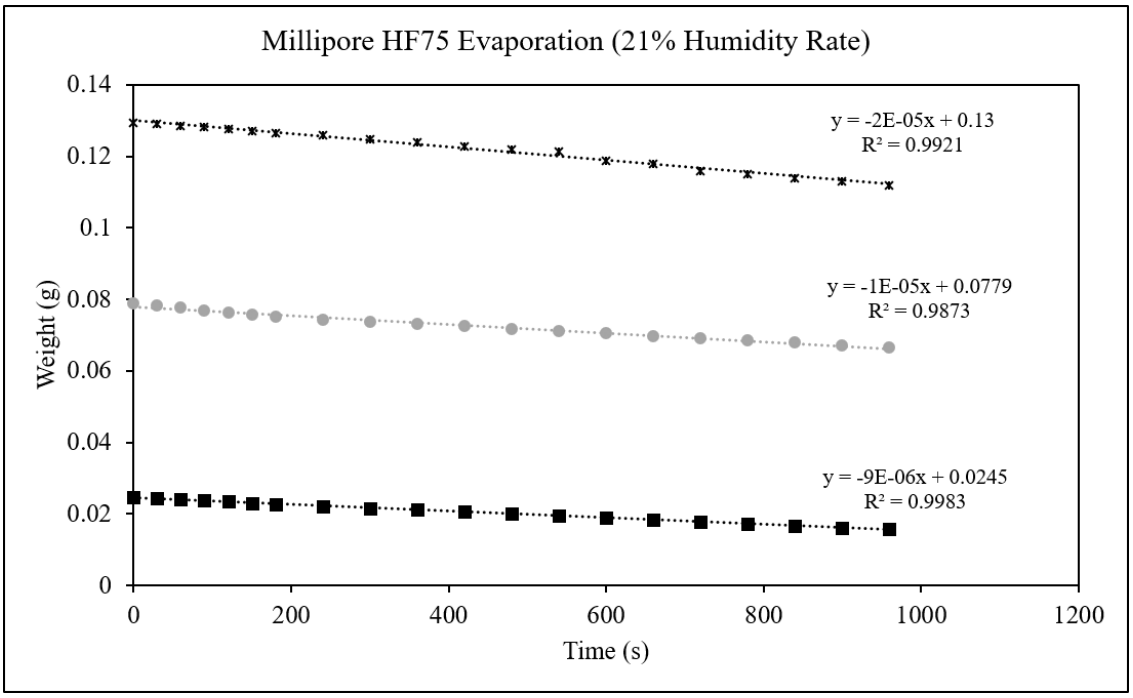

Figure 16. The results of the low humidity evaporation rate experiment for the Millipore HF75 membrane. The evaporation seems to be linear at all of the fluid amounts (50μL, 100μL, and 150μL), which means that a correction can be applied to compensate for fluid losses.

characterizing the fluid losses during this period could also help with the selection of a membrane. About 100μL of mouse blood was introduced to the Vivid GR membrane and about 50μL of mouse blood was added to the Vivid GX membrane. Both of these trials were completed in the same day to account for any fluctuations in temperature and humidity. In this setup a Millipore HF75 membrane was placed directly under the fractionation membrane. 5mm by 5mm squares of each of the membranes were cut with the use of a laser cutter (Universal Systems, Scottsdale, USA) and were mounted directly on top of one side of the Millipore HF75 membrane. As per the usual protocol, weight measurements of the strips with the blood separation membrane were taken before every run. Measurements were taken every 30 seconds for a period of 600 seconds as well. The results of this experiment are seen in Figure 18.

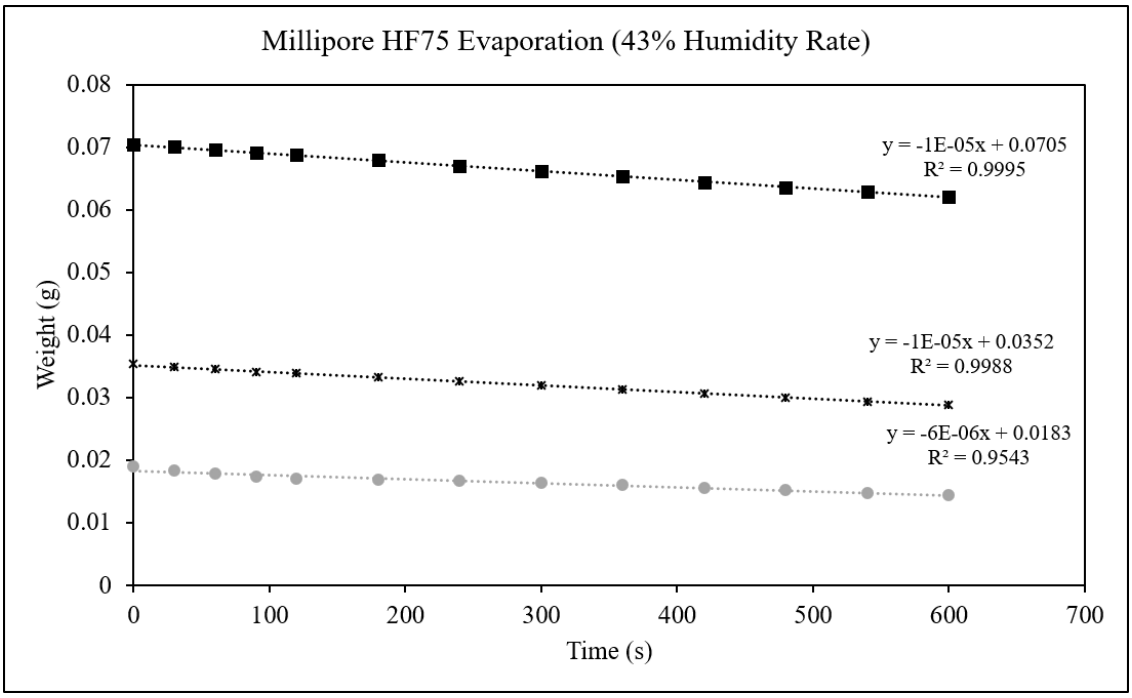

Figure 17. The results of the high humidity evaporation condition experiment on the Millipore HF75 experiment and the fluid losses can be seen to be linear at all the initial fluid amounts.

It can be seen that the fluid losses of the membranes are linear in nature which is similar to the fluid losses seen in all of the other membranes. In addition the amount of fluid added in the initial step does not seem to significantly affect the rate of fluid loss over the experimentation period. Since the plasma is separated from the red blood cells before 120 seconds, this validates the use of the asymmetric polysulfone filters as blood filters specifically for this lateral flow assay application.

2.2 Implementation in the Lateral Flow Assay

From the previous experiments it was found that the Vivid GR asymmetric polysulfone exhibited optimal filtration characteristics with the highest yield of plasma in addition to the lowest autofluorescence and normal fluid loss. A study was completed

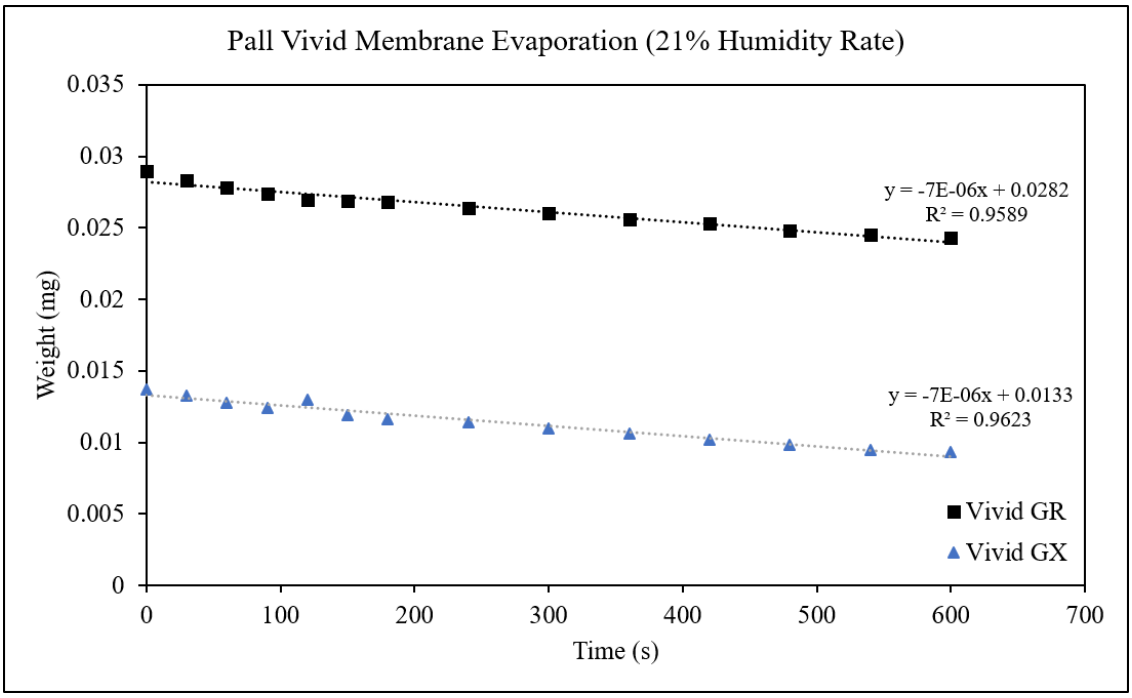

Figure 18. The results of the fluid loss experiments for both of the Pall Vivid GX/GR membranes.

to assess the efficacy of this membrane with patient samples in an EBNA IgG assay in comparison to purified plasma. This study also compared the difference between blood directly deposited onto the blood filtration membrane and a capillary as well. A Universal Systems Laser Cutter (AZ, USA) was used to cut the Vivid GX membrane into 5mm by 5 mm squares. The optimized conditions used for the laser cutter were 50% for the power, 63% for the laser speed, 500 pixels per inch (PPI), and 0.50mm for the z-axis. The filtration squares were singulated with the use of a straight razor. The standard setup for the lateral flow assay used for the lateral flow detection platform was used with the exception of the addition of the blood filter. Figure 19 shows a complete mounted strip that was used for the blood fractionation experiment, which includes the sample pad, conjugate pad, wicking pad, and Millipore HF75 test strip.

These components were mounted on a standard glass slide with the use of double-sided adhesive tape.

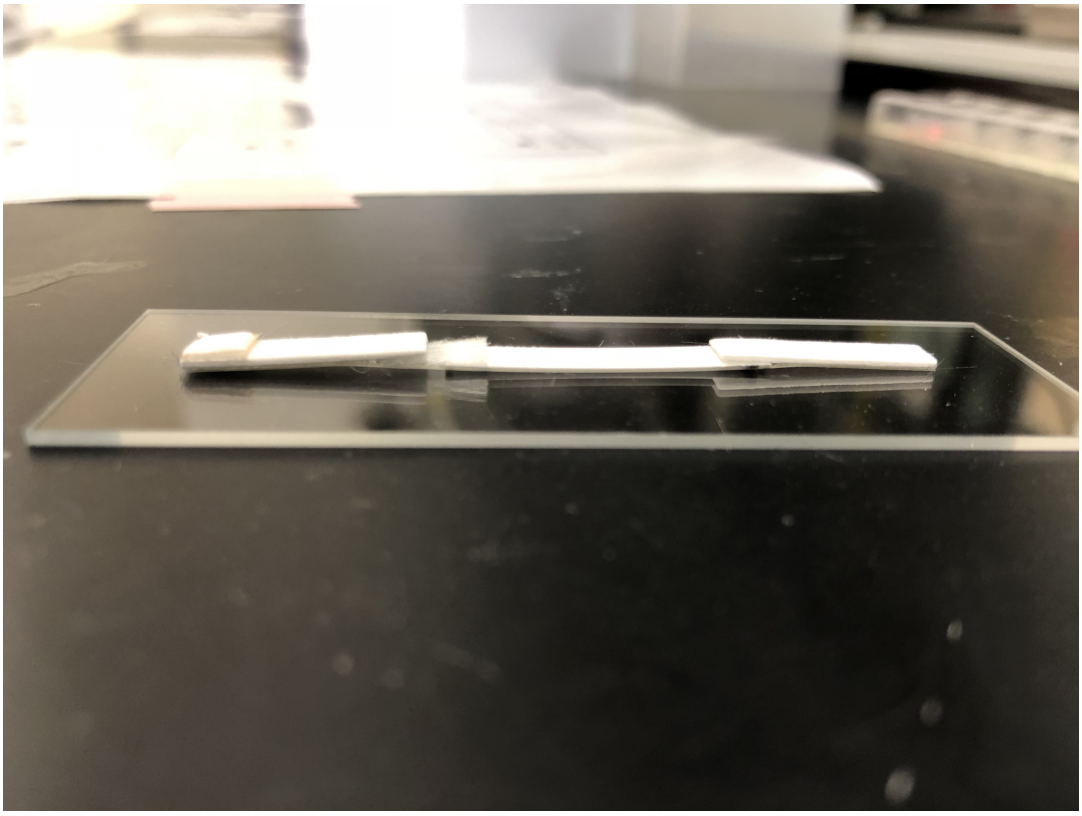

Figure 19. A test strip that was prepared for the lateral flow blood fractionation tests.

The standard protocol for the fluorescence based assay was used for IgG, BSA, and EBNA for both sets of samples that were tested. These protein concentrations were tested at 114 μg/mL, with the protein printer parameters set at 3V and 0.2 mL/min and two passes. All of the strips were mounted with the use of an adhesive backing and the dimensions of the sample pad was 23 mm by 5 mm and the dimensions of the wicking pad was 18 mm x 5 mm. All of the strips were pre-wet with 100 μL of PBST and there were three strips or duplicates tested for each of the conditions. As per usual, the test membrane (Millipore HF75) has a backing plate mounted to it to

direct fluid flow across the membrane. About 10μL of capillary blood was used and there were two conditions that were used for the blood that was spun to separate it from the red blood cells at two different concentrations (1:10 of 1:50 dilution of a 30 μL pooled plasma sample). Afterwards 50 μL of PBST was used to wash the strips. 60μL of 2:1 diluted Millipore F1-Y050 functionalized microspheres were incubated in each sample for a period of 20 minutes. Finally 50 μL of PBST was used to wash away the unconjugated microspheres from the test area.

To collect the blood a 20 gauge diabetic lancer was used to collect a sufficient amount of sample. The first drop that was collected was wiped away and light pressure was applied on the finger to allow the blood to flow out of the collection site. The methods tested included the use of an 80 μL heparinized glass capillary or the use of a manual finger touch method to see if there was any variation in results between blood application techniques. Both techniques were tested for both samples that were collected from patients D1 and D2. The fluorescent signal was recorded with the use of the lateral flow detection platform mentioned in the previous section. As per usual, a higher bar or ramp time equals a lower fluorescent signal.

Figure 20 shows a test strip with 10 μL of capillary blood that was tested in this experiment. It can be seen that there is a small amount of red blood cells that have passed through the filter into the sample pad. This could be due to a lack of a solid connection between the blood filter and the sample pad or it could also be due to the fact that the blood filter was too small for the amount of blood that was applied (the filter became over saturated and the blood was forced to flow around the filter straight into the sample pad). In the next iteration of these experiments, a larger sized blood filter will be used and techniques to immobilize the filter onto the sample pad will be researched. Figure 21 shows the difference in signal acquired by using the

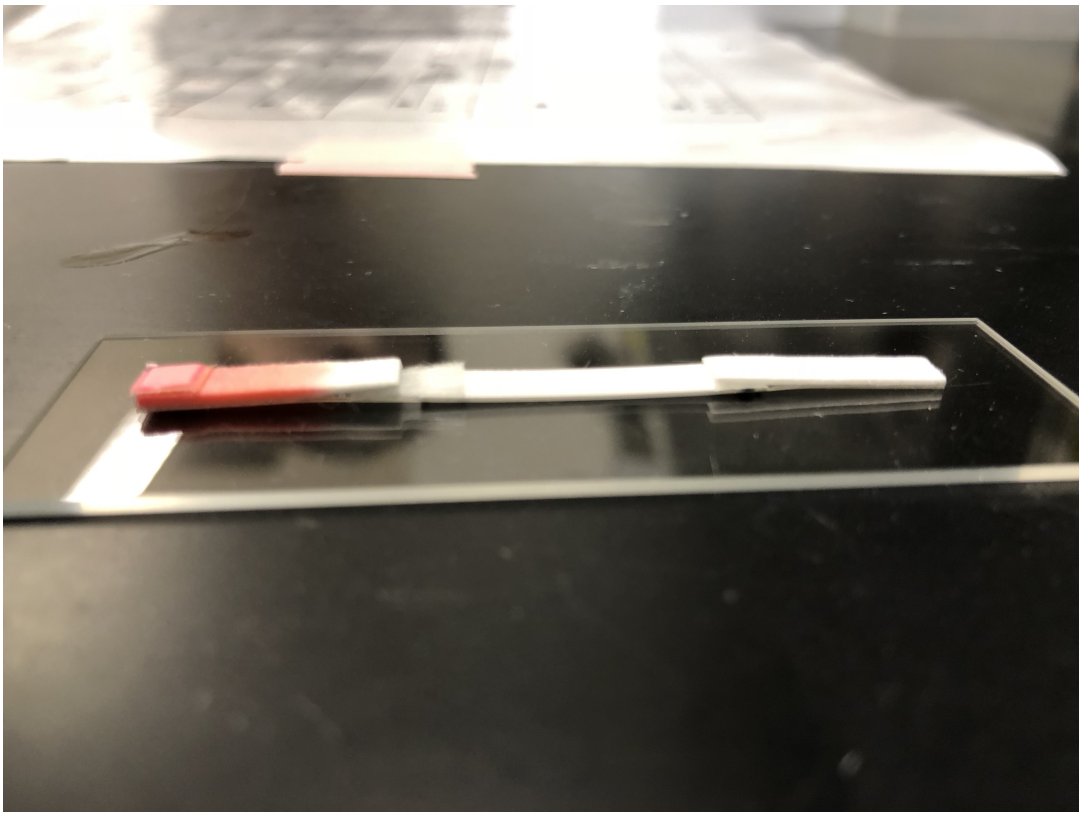

Figure 20. A test strip with 10μL of blood that was tested in this experiment.

finger touch and capillary methods in the first donor (D1). The results seemed to be fairly consistent across the capillary and finger touch methods with the exception of Slide A. The other samples were consistent across both the capillary and the finger touch method.

Figure 22 compares the results between the capillary deposition method and the finger touch method for the second donor. It can be seen that there are no significant difference between both of the methods, but Slide A seems to have a lower fluorescent signal in the capillary technique test in comparison to the finger touch method. This could be due to inconsistent application of the blood onto the membrane or due to other factors. However, there was not too much variation to warrant the testing of

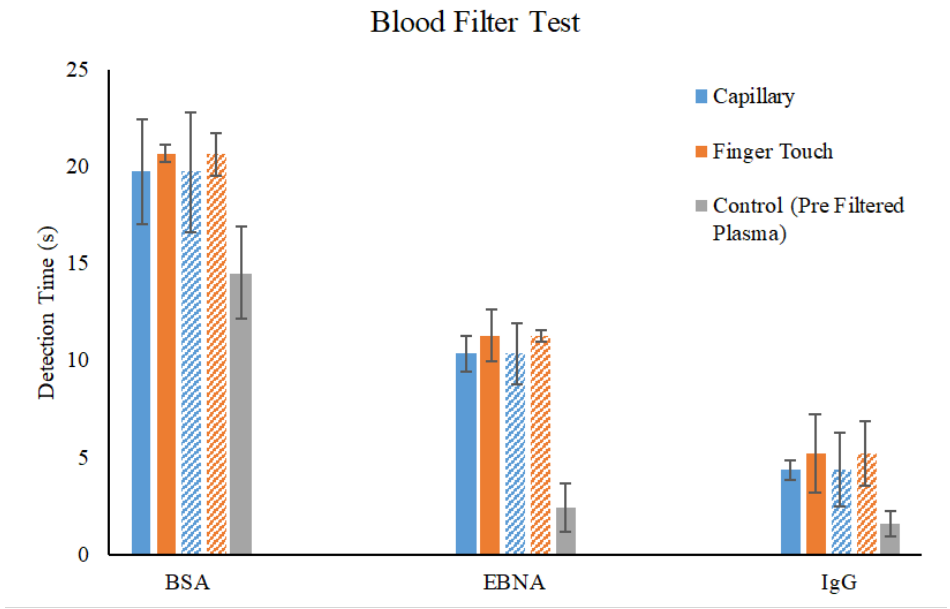

Figure 21. A comparison of all of the samples with various methods (finger touch, and capillary) for two patient samples (solid, striped lines).

more samples. However, in some of the finger touch samples, the blood filter was moved when it was touched which could add extra variance to the results of the assay.

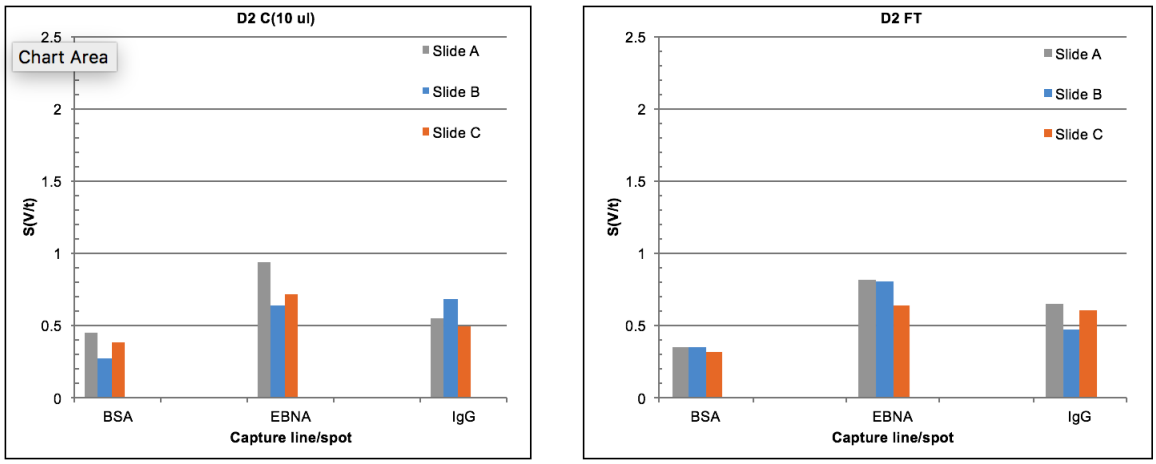

Figure 22. A comparison of finger touch blood and capillary deposited blood for three samples with measurements for concentration of BSA, IgG, and EBNA for sample D2.

Figure 23 compares concentrations of EBNA and IgG to various dilutions of the pooled sample of plasma. This served as a point of reference for the comparison of the patient samples which were applied with the different finger touch and capillary methods. It can be seen that Slide B did experience some deviations but there were no notable significant differences in the sample. This allows for this set to be used as a comparison to the other sets of data and these samples will be averaged and error bars will be added which rely on the overall standard deviation of the sample. Overall of the other slides were consistently withing 10% of each other, which is a good point of reference to the other samples since this takes into account a pooled sample of blood plasma of many individuals.

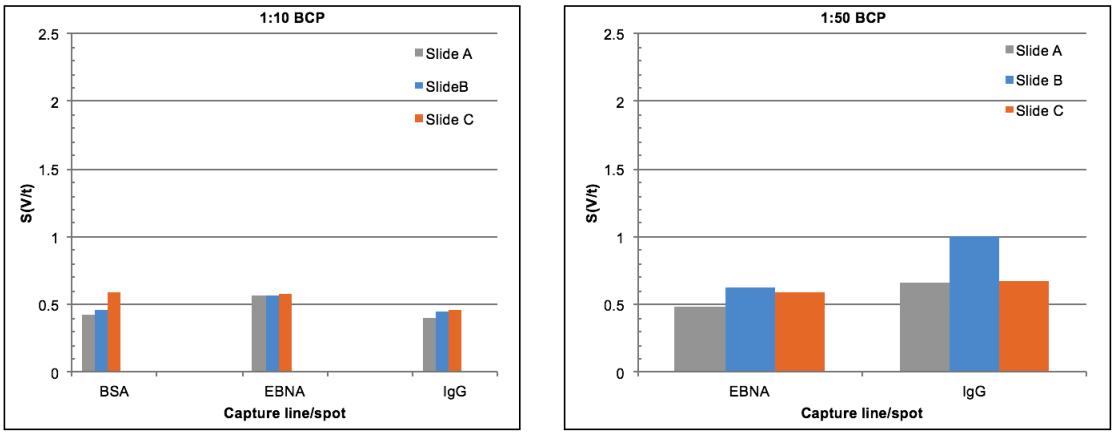

Figure 23. A comparison of the concentrations of EBNA and IgG to various dilutions of the pooled plasma samples. It can be seen that slide B in the 1:50 dilution of the pooled sample was slightly higher than the 1:10 sample, but this could be due to a number of different factors. Overall of the other slides were consistently withing 10% of each other, which is a good point of reference to the other samples.

Figures 24 and 25 show the compiled results of all three samples from each group along with an addition of error bars which include standard deviation. It is surprisingly seen that the capillary method for the first patient D1 had larger error

bars in comparison to the finger touch method, but this could be due to a number of factors which could be related to issues related to the collection of blood samples with the use of the glass capillaries or the fact that the capillaries were close to their expiration date and that the heparinization might have been affected over this period of time. On the other hand, there was minimal variance in the results from the second patient (D2) as IgG, BSA, and EBNA were similar for the finger touch method, the capillary, and the pooled blood sample. To be sure of this result and that there is no statistical significance or variations between the group, more samples have to be tested and more patients should be tested as well. As for the head to head comparison between the donors and the pooled samples, there seems to be a number of variations seen in the figure. The donor samples seem to have no correlation with the donor samples as they are different in both the EBNA and IgG results. However, the error bars were quite significant in these results so further testing has to be done to ensure that results are significant.

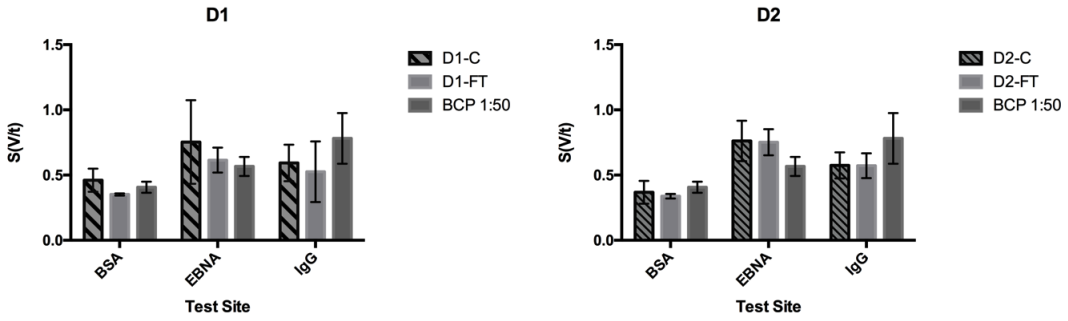

Figure 24. A comparison of results between the different types of application methods (finger touch, heparinized capillary, and a pooled blood plasma sample for both donors. There seems to be no significant variance in the results for patient D2, but there were some variations that were noticeable in the first sample.

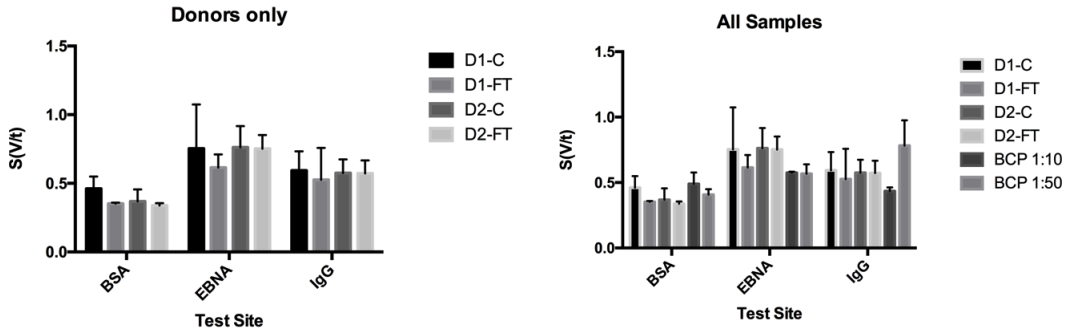

Figure 25. A comparison of the results for all of the donors which takes into account the application method as well as the inclusion of the pooled plasma sample at the two dilutions. There seems to be no significant variation in the results between each of the groups.

Overall the characterization of the membranes from a number of performance characteristics yielded the Vivid GR membrane to be the optimal membrane in terms of plasma yield and background fluorescence. This culminated in a patient study with two donors to compare levels of IgG, EBNA, and BSA with various blood application methods. From this study, the application method experiment was found to be inconclusive as there were not enough samples and duplicates to run a meaningful statistical analysis. However, the results were comparable to that of a pooled blood plasma sample, which proves that the filter performed similarly to blood that has been previously centrifuged. However, the blood filter needs to be properly mounted the dimensions of the filter need to be optimized so that the blood does not flow into the sample pad as was documented in this experiment.

Chapter 3

VALVE ACTUATION AND FLUIDIC CONTROL

3.1 Introduction

This chapter covers efforts made towards fluidic control and actuation with a paper porous substrate. The initial section covers efforts made towards the design and validation of a PID controller for controlled dispensing of valves and the requisite validation of the system with various heating elements. The second section covers efforts made in the fabrication of wax valves and actuation of these valves with regards to a diagnostic assay and the last section covers the fabrication of a novel sublimating valve that is made out of naphthalene and a demonstration of fluidic control in the system.

3.2 Design and Validation of PID Controller

Two iterations of the PID were created for the heated printing platform. The first iteration of the PID controller included a PX4 controller (Fuji Industries, Japan), a silicone heating pad (McMaster-Carr, USA), a type J stick-on thermocouple (McMaster-Carr, USA) and a 10A relay as seen in Fig 27. The entire setup was designed to plug into a 120V AC plug and inserted in a plastic box as seen in Fig. 26.

The relay was not enough to supply the heater and the initial heating pad that was purchased was rated for a 24V supply. Therefore, the system in its initial state would only work with an additional power supply to power the heating pad. Therefore

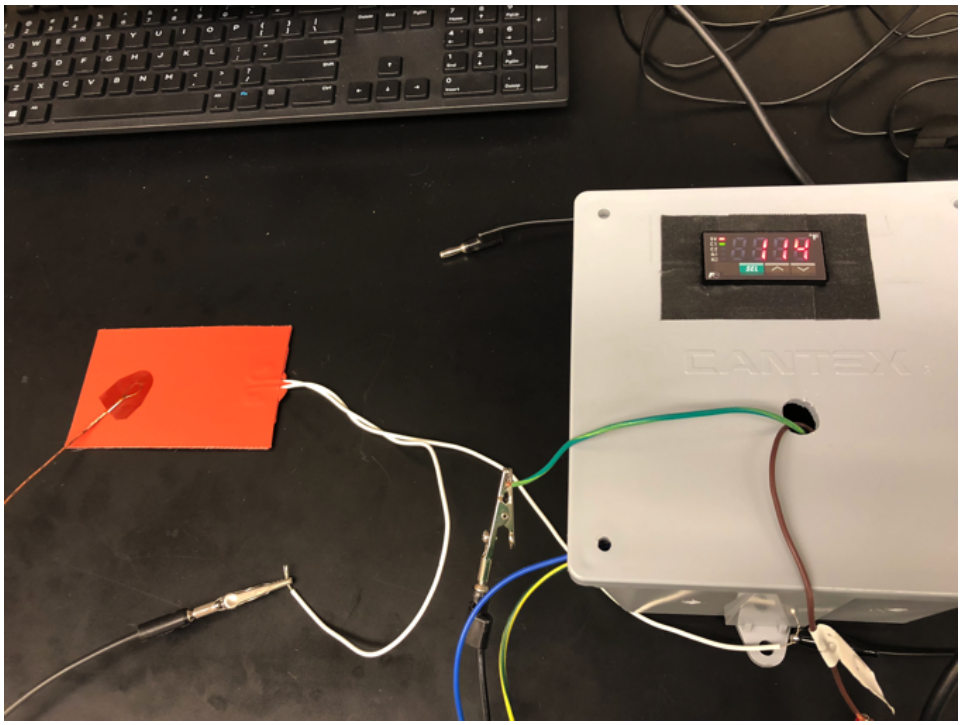

Figure 26. An example setup of the PID controller with the thermocouple placed directly on top of the heating surface.

a second iteration of the PID controller was created to accommodate a 2' heating cord (BriskHeat, USA) which allows for a 120 V supply. This second iteration included a 40A solid state relay (Inkbird, USA) and a heat sink in the same plastic enclosure. The second iteration of the PID controller was designed to be a standalone system, with all high voltage components placed inside the box. A plug on the exterior of the box would allow for the control of two heating sources if the need arises.

To calibrate the PID controller, open loop tuning was performed where the system is programmed to reach a steady state temp and power is steadily increased. This following governing equation was used to determine the operating parameters of the PID controller:

$$G(s) = \frac{K \cdot e^{-t_d s}}{\tau * s + 1} \tag{1}$$

where $G(s)$ represents the response of the PID controller, K represents the gain of the PID controller, t_d represents the dead time, or the time between the changing output and a response, and τ represents the time constant of the system $(1/1 - e)$.

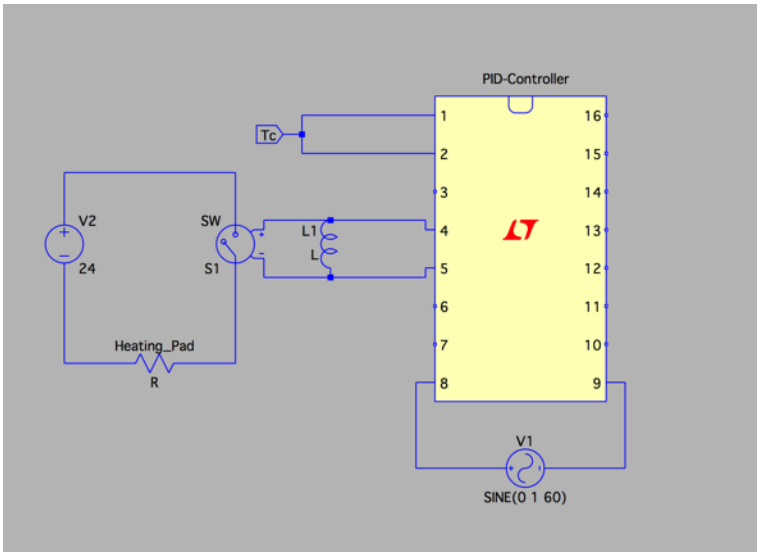

Figure 27. The schematic of the first iteration of the PID controller which includes a 120V AC input, a PID controller, a 10A relay, a heating pad, and a separate 24V power supply to heat the silicone heating blanket.

The second iteration of the PID controller schematic can be seen in 28. The PID controller was connected to a 40A solid state relay in addition to a power plug which connects to the Briskheat heating cord. Tuning of this system was burdensome since the SSR was designed to work with higher wattage heaters. The Briskheat heating cord was designed to work with lower amperage and there was no voltage reaching the input of the SSR. The light of the SSR was not operational as well in all of the situations even though the thermocouple was measuring a temperature that was lower than the set point programmed into the PID controller. Troubleshooting of this

system concluded that the output ports were not properly driving the SSR so the heating cord was not getting any power.

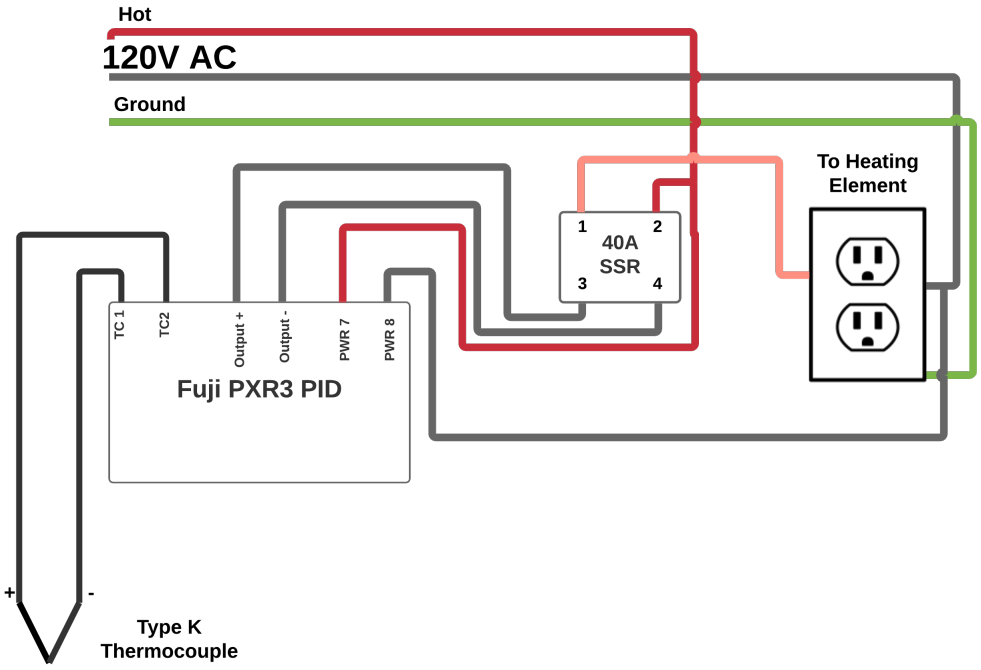

Figure 28. The schematic of the second iteration of the PID controller which utilizes a solid state relay and an external heating element.

Overall, the autotune setting was used for the PID controller and it exhibited optimal ramp temperature and hysteresis in comparison to the simulated conditions seen in Figure 29. The time for the controller to get to the starting temperature was less than 15 seconds and this is not possible if convection is taken into account on both sides of the heater. This difference can be seen in the actual measured temperature of the PID controller. To encapsulate the heating cord around the high temperature barrel high temperature Kapton tape was used to anchor the heating cord to the barrel and the entire setup was wrapped with aluminum foil to ensure that there is

minimal convection to the outside. The thermocouple was mounted to the heating cord with the us of the Kapton high temperature tape.

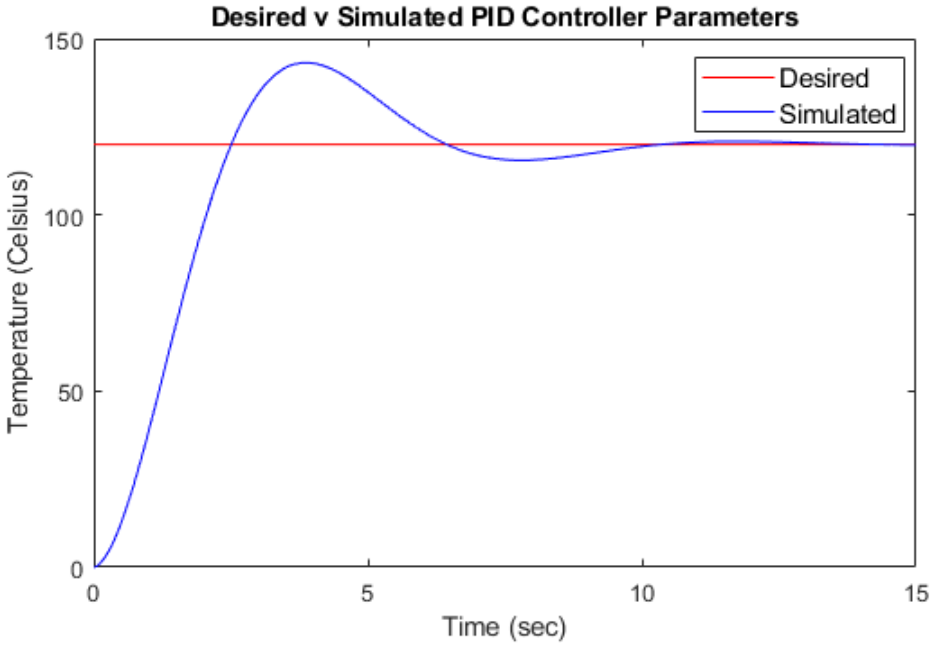

Figure 29. The simulated conditions of the PID control with the use of the preset P and I conditions for a temperature of 120 degrees. There is minimal hysteresis in the graph and the simulated controller returns to optimal conditions in minimal time.

With the presets of the PID controller (K_p=3, K_i=0.8, K_d=0.7), the PID thermocouple was used to record the temperature every 15 seconds. This was done until the controller reached a steady state. With the encapsulation of the high temperature Nordson barrel, the heating cord reached a temperature of 120 degree Celsius in about 500 seconds, which can be seen in Figure 30. It can also be seen that the hysteresis is minimal in the graph and fine tuning will be done to optimize the heating parameters at a later stage.

However there was some melting with the high temperature barrel due to improper placement of the thermocouple and further iterations of the PID controller heated

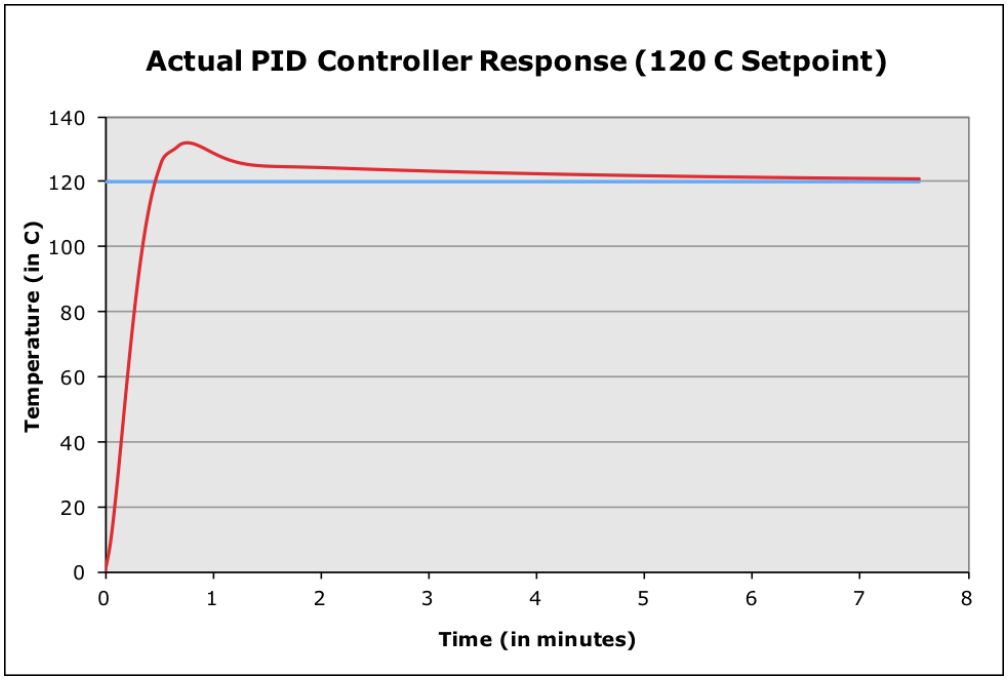

Figure 30. The simulated conditions of the PID control with the use of the preset P and I conditions for a temperature of 120 degrees. There is minimal hysteresis in the graph and the heating cord reached the operating temperature in about 500 seconds. The stock presets of the PID controller were K_p=3, K_i=0.8, K_d=0.7. Fine tuning will be done at a further time.

dispensing setup will be performed to eliminate this incidence. The PID controller was used for the precision dispensing of the wax valves and the sublimating valves in the following section and these materials were characterized in these sections as well.

3.3 Wax Valves

Wax valves have been extensively covered in the literature to direct fluid flow into certain areas of a microfluidic channel. To block the flow of the fluidic channel heat is applied onto the wax membrane to melt it and force the blockage of the flow. Wax is innately hydrophobic and can effectively prevent flow in the channel. This is usually used as a one-time actuation system and it is difficult to completely remove the wax

Table 2. The 2^3 factorial design for the set of wax experiments to test the effect of autofluorescence.

Factor	Low Factor (-1)	High Factor (+1)
A: Type of Wax Used	Ozokerite Wax	Soybean Wax
B: Temperature of Heating	125 C	155 C
C: Dipping Technique	1s (1x)	1s (2x)

from the membrane once it is immobilized into the pores of the substrate. In addition wax is an organic material and research into the fluorescent properties of wax will be completed into the following sections. In addition the inverse of the wax valves (sublimating materials) will be covered in this chapter as well.

3.3.1 Autofluorescence of Wax

Since the entire system is built to work in conjunction with a quantitative fluorescence based platform, the addition of valves would ideally not induce any additional fluorescence effects in the assay. As such, it was important to measure the background fluorescence of the various types of waxes and dipping techniques. A 2^3 factorial test was performed to find these effects and the fluorescence was measured with the reader.

A run chart was created to show the factors for each of the eight runs and this is seen in Table 3 which displays the eight runs in addition to the interactions between each of the factors, which is also known as an Analysis of Goods Table (ANOG). This includes the interactions between all possible combinations of two factors and the individual factors as well. Three duplicates were completed of each run and each duplicate was taken as an average of three points on each membrane. GE Whatman MF1 glass fiber woven membrane was used for these sets of experiments. In Table

Table 3. The 2^3 factorial run chart for the set of wax experiments to test the effects of autofluorescence which includes the interactions between each of the factors.

Run	A	B	C	A*B	A*C	B*C	A*B*C
1	-	-	-	+	+	+	-
2	+	-	-	-	-	+	+
3	-	+	-	-	+	-	+
4	+	+	-	+	-	-	-
5	-	-	+	+	-	-	+
6	+	-	+	-	+	-	-
7	-	+	+	-	-	+	-
8	+	+	+	+	+	+	+

3, a plus symbol indicates an application of the factor and vise versa for the minus symbol.

By collecting the average values generated from the ANOG table in the previous section, a Geoplot was created which compares the effect of the interaction of factors on the autofluorescent signal collected from the reader. Since there were three factors, a cubical Geoplot was created to take into account the two levels for each of the three factors in this problem. The Geoplot which contains the average values for all of the 8 runs can be seen in the figure below.

To consistently coat the surface of the membrane a dipping setup was used similar to the one seen in Chapter 1. A 3D printed mold was created for this dipping technique as seen in Figures 31 and 32 to be affixed between two magnets on either side. The membrane was mounted onto a glass slide and the entire fixture was dipped into a fixture of melted wax. the parameters of the dipping can also be seen in the factorial chart. The fixture was removed before the wax solidified and the membranes were baked for ten minutes in an oven.

There were noticeable wax residues on the molds and this was removed with

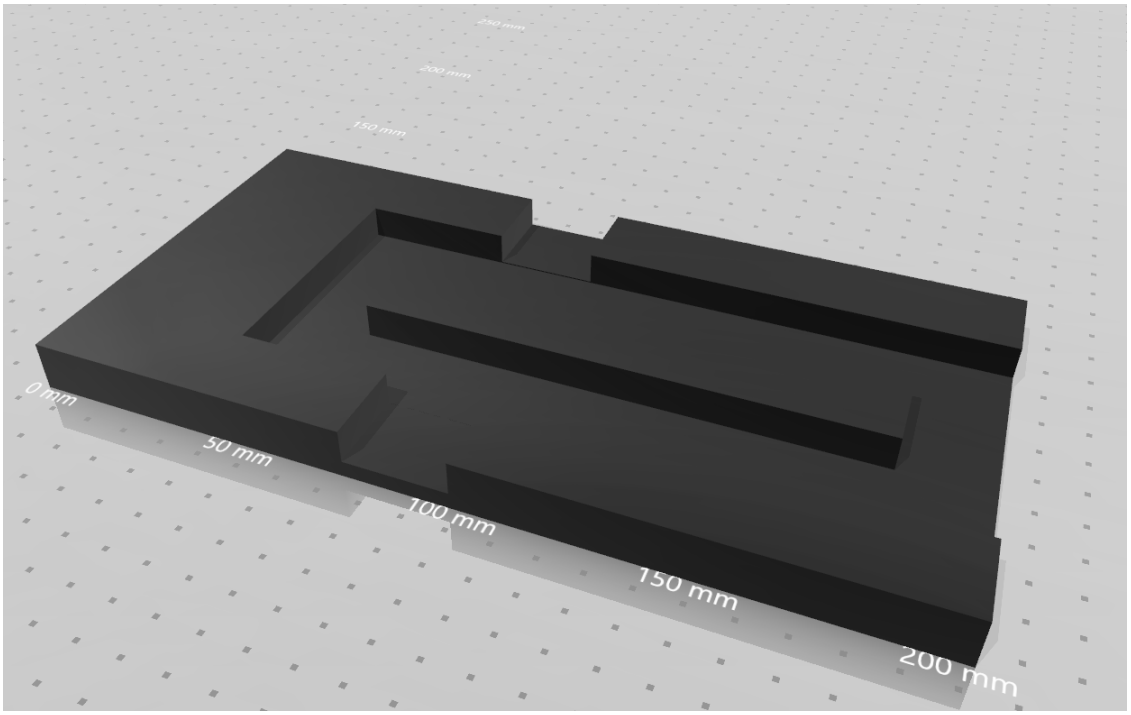

Figure 31. A CAD model of the wax dipping piece to create clearly defined channels in the membrane.

isopropyl alcohol and compressed air. In addition, the membranes were removed immediately from the fixtures as it was seen that if the wax was left to solidify for extended periods of time then the membrane was at risk of tearing and this happened in several instances. Any additional residues were also removed from the membrane with the use of a razor. To take the three measurements of the membrane, the reader was used to read the signal when it was fully in and the membrane was ejected in increments of 2 cm for the duplicate measurements for each run. This was repeated for each of the trials in similar conditions to ensure consistency across all of the runs.

The runs used a variable combination of waxes (ozokerite wax and soybean wax), different melting temperatures, and number of dipping steps to find if there was any significant difference in the fluorescent emissions of each strip. As seen in Figure 33,

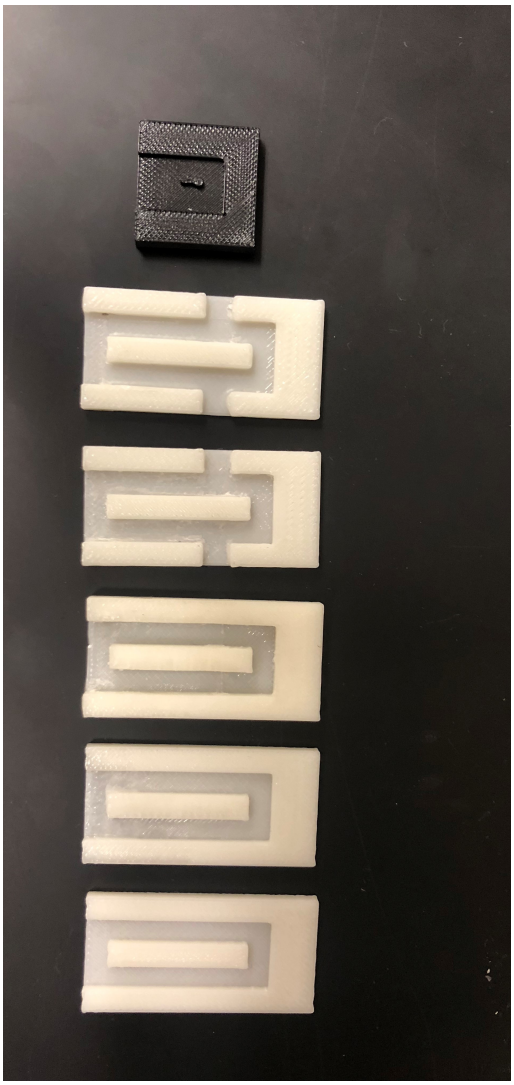

Figure 32. A comparison of the initial iteration of the wax dipping apparatus (seen on the left side of the image) and the consequent evolution of the dipping molds. There are noticeable wax residues on the molds and this was removed with isopropyl alcohol and compressed air.

the ozokerite wax had a higher fluorescent intensity in comparison to the soybean wax as seen by the smaller ramp time of the reader.

In addition, lower temperatures of the wax seemed to induce less fluorescent signal in both types of waxes. This could be due to the fact that higher temperatures can make the membrane itself more autofluorescent, as seen in previous results. This effect

was minimal, and the number of dipping steps also seemed to have a negligible effect on the fluorescent emissions of the membrane. It was also noted that additional wax on the membrane seemed to affect the structural integrity of the membrane as some of the membranes were brittle and prone to cracking when multiple dipping steps were used.

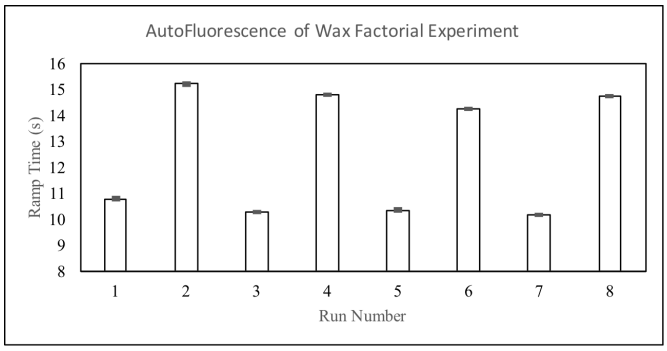

Factor	Low Factor (-1)	High Factor (+1)
A: Type of Wax Used	Ozokerite Wax	Soybean Wax
B: Temperature of Heating	125 C	155 C
C: Dipping Technique	1s (1x)	1s (2x)

Run	A	B	C	A*B	A*C	B*C	A*B*C
1	-	-	-	+	+	+	-
2	+	-	-	-	-	+	+
3	-	+	-	-	+	-	+
4	+	+	-	+	-	-	-
5	-	-	+	+	-	-	+
6	+	-	+	-	+	-	-
7	-	+	+	-	-	+	-
8	+	+	+	+	+	+	+

Figure 33. The results of the wax fluorescent emissions experiment. It can be seen that the ozokerite wax had a higher intensity in comparison to the soybean wax.

In addition, the membrane was also tested for fluorescence in an area where there is no wax and the ramp time was comparable to a blank membrane, which means that the heating and dipping processes do not affect the emission characteristics of the membrane itself. These results were promising and verifies the use of wax as a valid means of directing fluid flow. A full factorial design was completed and JMP14 was used to find the optimal interactions between each of the factors. The 8 runs were randomized and the effect of each interaction was found. The goal was to minimize the autofluorescence of the wax, which is inversely related to the ramp time outputted from the reader.

Figures 34, 35, and 36 show the results compiled from the JMP analysis of

Source	LogWorth		PValue	
Wax Type	37.565	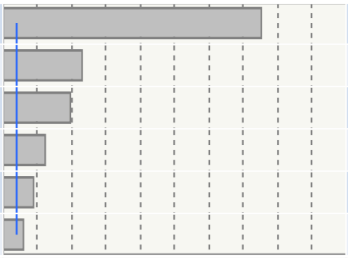	0.00000	
Dip Time (s)(1,2)	11.696		0.00000	
Temperature (Celsius)* Dip Time (s)	9.999		0.00000	
Wax Type*Temperature (Celsius)	6.100		0.00000	
Temperature (Celsius)(125,155)	4.490		0.00003	^
Wax Type* Dip Time (s)	2.970		0.00107	

Figure 34. The results of effect summary analysis for the wax autofluorescence experiment. Variables with a higher log worth are deemed to have a more significant effect on the ramp time.

Source	Nparm	DF	Sum of Squares	F Ratio	Prob > F
Wax Type	1	1	151.70643	21806.20	<.0001*
Temperature (Celsius)(125,155)	1	1	0.17776	25.5507	<.0001*
Dip Time (s)(1,2)	1	1	1.12688	161.9765	<.0001*
Wax Type*Temperature (Celsius)	1	1	0.29549	42.4733	<.0001*
Wax Type* Dip Time (s)	1	1	0.09516	13.6778	0.0011*
Temperature (Celsius)* Dip Time (s)	1	1	0.77969	112.0720	<.0001*

Figure 35. Another comparison of the effects on the ramp time, which verifies the results seen in the previous figure. This table also shows which effects are statistically significant with the use of an F test.

the wax autofluorescence experiments. The following section details in depth the characterization of flow with the addition of the hydrophobic wax treatment.

3.3.2 Characterization of Fluidic Flow with a Hydrophobic Wax Treatment

To characterize the flow of a fluid on a nitrocellulose membrane with a hydrophobic treatment, a series of experiments was created. It has been previously published that a hydrophobic wax treatment does significantly slow down the flow of a fluid in paper microfluidics, but the purpose of the experiment was to see the overall efficacy and consistency of different wax treatments on the flow rates in the membrane. The edges

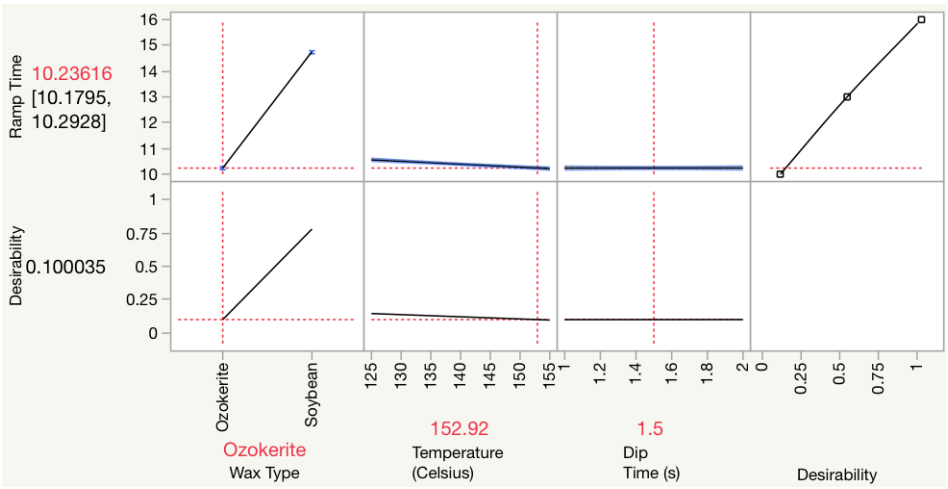

Figure 36. The results of the prediction profiler which uses the data compiled from the 8 runs to find the optimal conditions which maximize the ramp time and minimize the fluorescent signal.

of a membrane were dipped in two types of wax (ozokerite and soybean wax) and the speed of the fluidic flow was characterized. Millipore HF75 nitrocellulose was used in these experiments and was cut in a y shape seen in Figure 37 with the use of the laser cutter (Universal Systems, USA). The parameters of the laser cutter were similar to the ones chosen to cut the blood filter. The optimized conditions used for the laser cutter were 50% for the power, 80% for the laser speed, 500 pixels per inch (PPI), and 0.50mm for the z-axis. The speed was increased for these sets of experiments because the HF75 membrane is thinner than the blood fractionation membrane and the slower speed caused increased charring on the edges of the membrane, which could affect the overall flow rate of the membrane. Each y-shape was then carefully singulated with the use of a razor.

A similar mold to the one seen in Figure 31 was used to dip each side of the Y pattern with a different type of wax. Both the ozokerite and soybean wax were melted at 125 degrees Celsius and were dipped once for a period of one second in the wax.

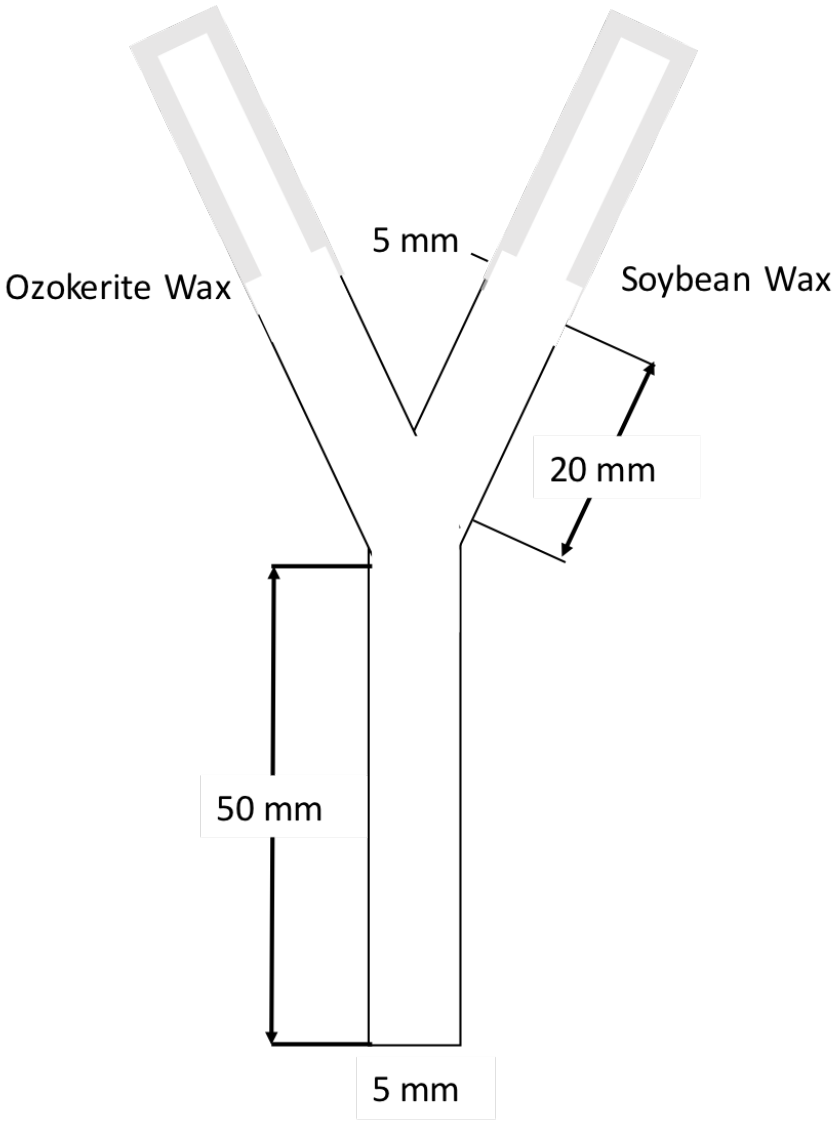

Figure 37. A schematic of the y pattern that was used to characterize the flow rates with different types of hydrophobic wax treatments.

This process was used to create a hydrophobic border on the edges of the membrane with the two different types of wax. Figure 38 shows a simplified schematic of the flow through the Y membrane. This was done with utmost care as there was some degradation of the HF75 membrane since it is thin and had to be handled with care.

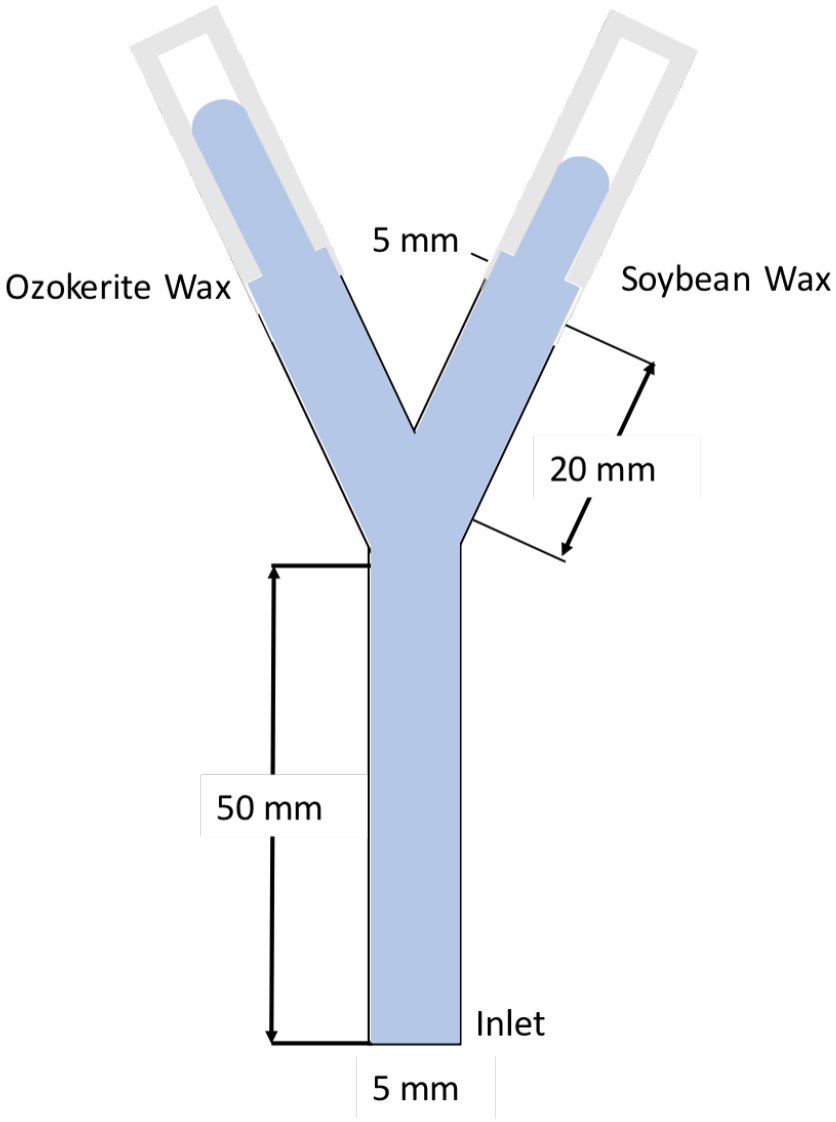

Figure 38. a simplified schematic of the flow through the Y membrane.

To characterize the speed of the fluid flow 5 milliliters of deionized water was added to the single inlet of the channel and the distance traveled over time of each of each side of the membrane (which has a different wax treatment) was measured. Three duplicates were created and the fluid was introduced with the use of a pipette at the edge of the membrane. The pattern was mounted on a flat plexiglass sheet and the length traveled of the fluid was measured every 60 seconds once the fluid traveled

past the branching point of the the y shape, which was about 50 mm plus the initial buffer distances of 20 mm seen in the diagram.

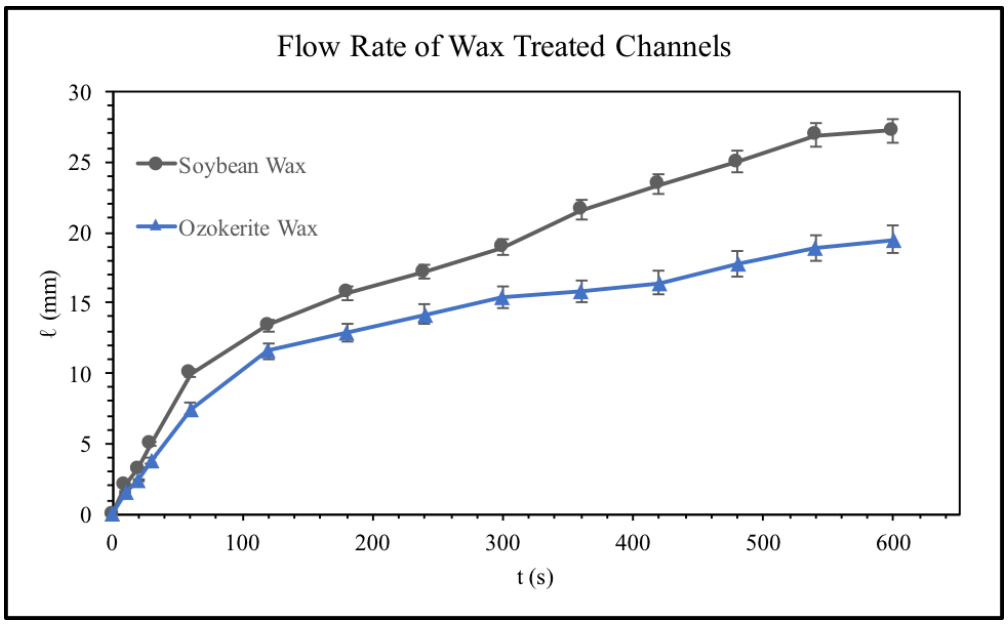

Figure 39. The characterization of flow rates of ozokerite and soybean waxes and the comparison of length traveled versus time.

As seen in Figure 39, soybean wax traveled a significantly longer distance in the y shape in comparison to the ozokerite wax. It can be seen that the soybean wax reached the edge of the membrane during the period of experimentation in almost all of the trials, while the ozokerite wax traveled about two-thirds of the way or about 20 out of the 30 millimeters until the edge of the membrane. This means that the soybean wax is overall less hydrophobic than the ozokerite wax, which comes to show that the ozokerite wax is more effective in the creation of valve since it forces the fluid to have a higher surface tension which results in a higher contact angle as well. The next steps of these experiments include the creation of a heating element to allow for the precise actuation of these valves in addition to the characterization of the pressures needed to rupture these wax valves.

3.4 Sublimating Valves

To complement the wax valves which block the porous media when heat actuation is applied, sublimating materials were researched to allow for the inverse effects (sublimation when heat actuation is applied on the membrane) and naphthalene was selected as an initial material since it has a relatively low sublimation temperature ($80 - 90^o$ C) and is cheap and easy to procure. However, studies on naphthalene have found that it is relatively carcinogenic and can potentially cause detrimental respiratory effects. In addition, naphthalene emits a foul odor and the elimination of this odor usually indicates the absence of naphthalene in this substrate. Various techniques of the deposition of naphthalene were attempted (heated dipping technique/ heated precision dispensing technique) and the flow rates were characterized of each of the substrates. The implementation of naphthalene in a lateral flow device can be seen in a simplified schematic (Figure 40). In this schematic the naphthalene valve is used as a barrier for reagents so that the blood can get to the test strip before the wash reagents. The precise control of the dispensing of the fluid is done with a heating actuator to sublimate the naphthalene at the correct time.

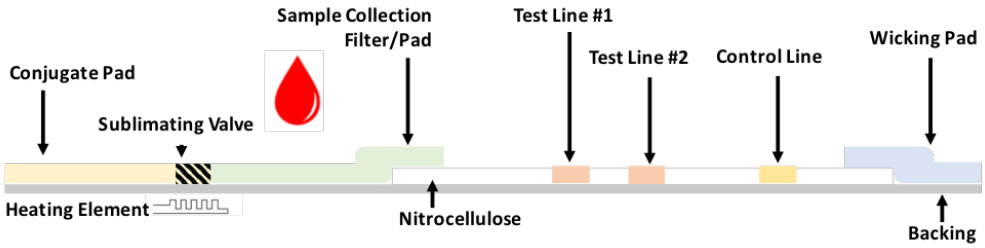

Figure 40. The characterization of flow rates of ozokerite and soybean waxes and the comparison of length traveled versus time.

In addition, a technique was developed for the quantification of the fluorescent

signal emitted from the naphthalene as well as any downstream effects that are created due to fluidic effects. The changes to fluidic flow were also studied due to any residual remains of the naphthalene as well. In addition the bio-compatibility of naphthalene was also tested with an enzyme-linked immunosorbent assay (ELISA) and was included in multiple steps of the ELISA assay as well. A complete study of the residual effects of the naphthalene in addition to its fluidic effects in a fabricated channel will be useful in future implementations of this material in lateral flow assays in the future.

3.4.1 Flow Characterization of Sublimating Valves

To characterize the fluidic properties of naphthalene in a channel, a similar form of the Y channel created in the wax experiments was created. Millipore HF75 nitrocellulose was used in these experiments and was cut in a y shape seen in Figure 41 with the use of the laser cutter (Universal Systems, USA). The parameters of the laser cutter were similar to the ones chosen to cut the blood filter. The optimized conditions used for the laser cutter were 50% for the power, 80% for the laser speed, 500 pixels per inch (PPI), and 0.50mm for the z-axis. The speed was increased for these sets of experiments because the HF75 membrane is thinner than the blood fractionation membrane and the slower speed caused increased charring on the edges of the membrane, which could affect the overall flow rate of the membrane. Each y-shape was then carefully singulated with the use of a razor.

Naphthalene was then heated to 120 degrees Celsius and a 5 mm area was added to the membrane with the use of a dipping technique with the use of a cut acrylic mold. This 'valve' was added about 20 mm from the branching point on one of the y-channels. Two experiments were performed to characterize flow with the addition of

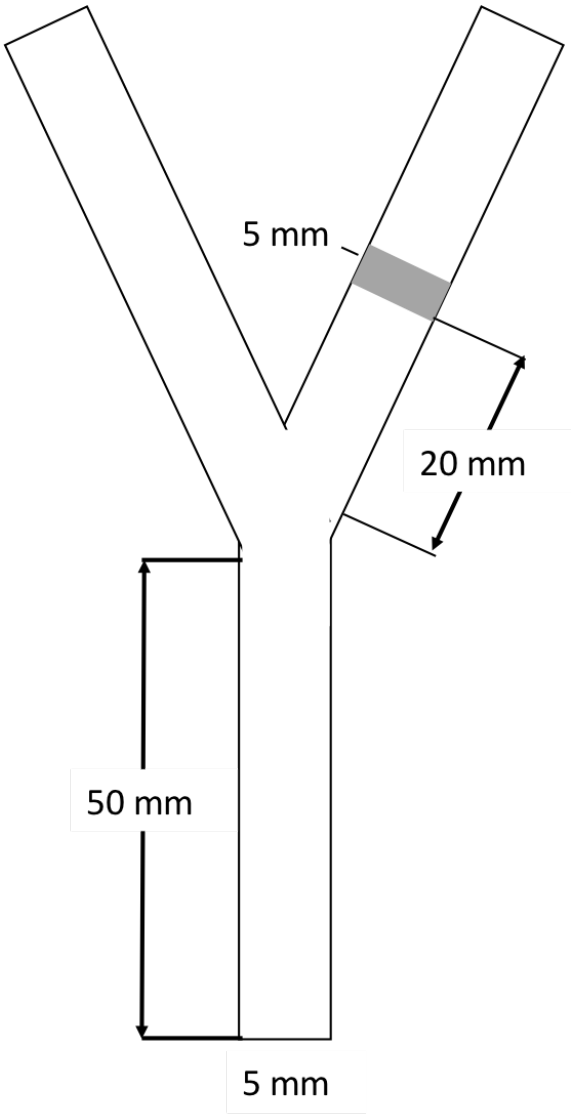

Figure 41. The characterization of flow rates of ozokerite and soybean waxes and the comparison of length traveled versus time.

naphthalene. The first experiment aimed to find the overall retention period of the naphthalene or how long a naphthalene valve can hold so that no fluid passes through the valve. This was compared to an ozokerite wax valve with a similar shape. The same y pattern was used with the recording of time starting as soon as the fluid front touched the beginning of the valve. This experiment was one with three duplicates of

the naphthalene as well as the ozokerite wax valves. To record progress of the fluid front the valve was recorded for a period of 12 hours or when the fluid passed through the entirety of the valve.

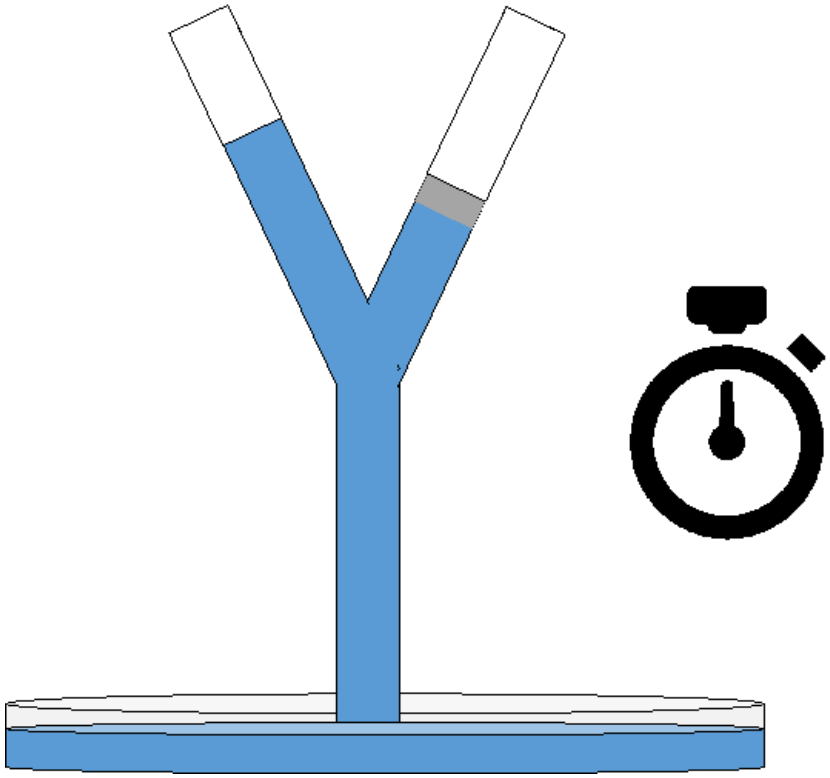

Figure 42. A schematic of the experimental setup of the hold time experiment with a reservoir of fluid.

Since this experiment was expected to take a longer time, evaporation is a significant factor and fluidic losses would significantly affect the results. To remedy this issue, a reservoir of deionized water with red food coloring was used and the y channels were mounted upright so that the edge of the y channel is submerged in about 1 centimeter of the reservoir.

As seen in Figure 43 and Fig. 42, all trials of the ozokerite wax valves were able to hold fluid back for more than the experimentation period of 12 hours. However,

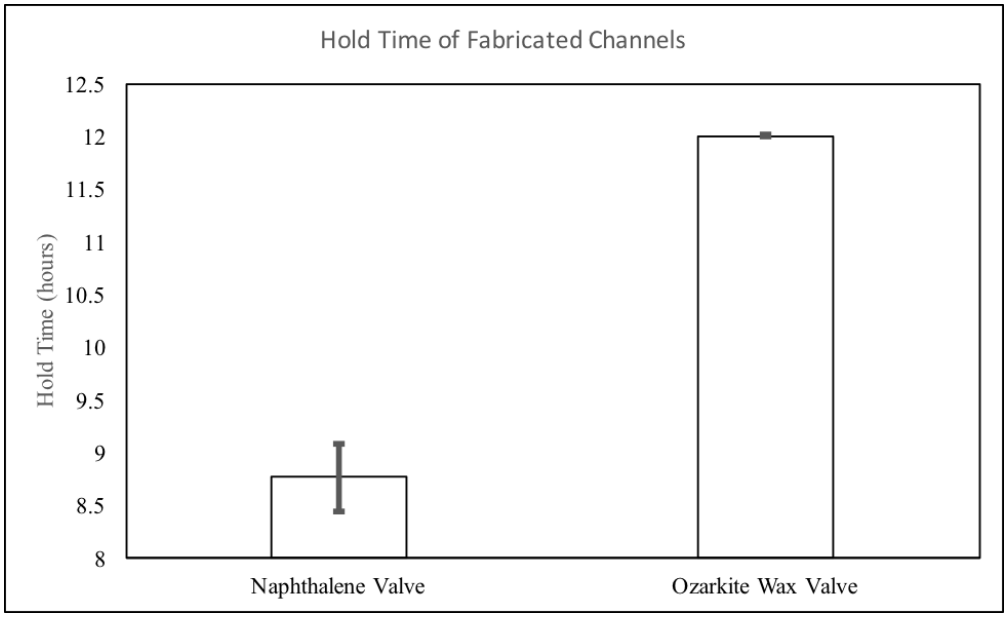

Figure 43. A comparison of the hold times of naphthalene valves versus ozokerite wax valves. It can be seen that ozokerite wax held for longer than the experimentation time of 12 hours and the naphthalene valves held for an average of about nine hours.

the naphthalene valves were able to hold the fluid back for close to nine hours on average, which is a positive result. This still means that the naphthalene valves could successfully be used to hold back washes and other reagents since the maximum expected hold time required is close to 3 or 4 hours. However, shelf life testing has to be performed for naphthalene so its longevity can be properly determined. A feasibility analysis can then be performed to see if these naphthalene valves can be consistently fabricated for implementation in field testing in a third world country.

The second experiment aimed to find the effects of surface tension in a way that was similar to the wax flow rate comparison experiment. The same pattern seen in Figure 37 was used with one of branches dipped in naphthalene which was melted in a beaker at 80 degrees Celsius. The area where naphthalene was not needed was masked with the same mold from the wax comparison section. The other branch point was

dipped in ozokerite wax to provide a comparison of hydrophobicity to a naphthalene valve. This was repeated in three separate trials.

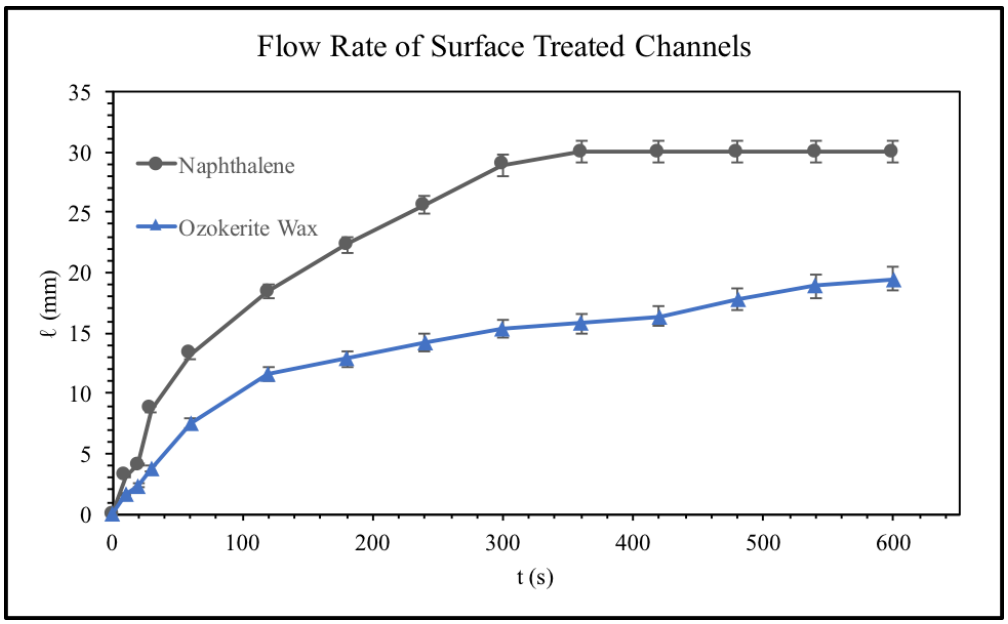

Figure 44. The characterization of flow rates of ozokerite and soybean waxes and the comparison of length traveled versus time.

3.4.2 Compatibility of Naphthalene

To find the compatibility of naphthalene when used in conjunction with an assay, it was important to find the overall compatibility of this material in an enzyme-linked immunosorbent assay (ELISA). A chemiluminescent assay was used along with a positive and negative control on a standard 96-well plate with EBNA and Gluthathione S-Transferase (GST) as the negative control. The ratios between the EBNA and the correlated GST well were compared along with the addition of naphthalene in each of the test wells. The complete protocol for this ELISA assay can be seen in Appendix B.

Each well was coated with 100 μL/well of 200 ng/mL of EBNA-1 or GST protein in 0.2M sodium bicarbonate buffer. This was left to incubate with serum overnight at 4 degrees Celsius. The next day, sodium bicarbonate was used to wash each well and afterwards 200μL/well of 5% Milk PBST was left in each well for 1.5 hours.Naphthalene was added by crushing it into a fine powder and was added into each well in accordance to the plate map. Naphthalene was added in different stages of the assay to see if there were secondary interactions to any other steps of the assay. Block serum was then added into the appropriate wells and was shaken for two hours. Another wash step was performed and sera and the primary antibodies were added to the respective wells. Another wash step was completed and 100 μL/well of secondary antibody was added with the inclusion of positive and negative controls. The plate map of the ELISA assay in addition to the labeled legend can be seen in Figures 45 and 46.

This solution was left on the shaker for a period of one hour and another wash step was performed with PBST. The chemiluminescent substrate was prepared and was added into each respective well. A luminometer (Promega Glomax) was set at a 425nm wavelength and the plate was read within a couple of minutes after the electroluminescent substrate was added. Three duplicates of each treatment were performed and it is worth noting that there was naphthalene which spread into unintended wells over the period of the assay. These wells were noted and were removed from the study. As mentioned earlier, the ratio between the EBNA and the GST wells was taken to find the overall intensity of the chemiluminescent signal in comparison to the background. Figure 47 shows the results seen from this experiment.

It is worth noting that the wash steps should have been more extensive since there

96 WELL PLATE MAP												
Well	1	2	3	4	5	6	7	8	9	10	11	12	
A	1	2	3		4	5	6	7	8		9	10	20ng EBNA
B	1	2	3		4	5	6	7	8		9	10	20ng EBNA
C	1	2	3		4	5	6	7	8		9	10	20ng EBNA
D													
E													
F	1	2	3		4	5	6	7	8		9	10	20ng GST
G	1	2	3		4	5	6	7	8		9	10	20ng GST
H	1	2	3		4	5	6	7	8		9	10	20ng GST

Figure 45. The setup of the ELISA assay with the plate map of the assay with the EBNA and GST(negative control). The legend of the plate map can be seen and three duplicates of each run were created.

were visible residues from the naphthalene powder in some wells even after five washes. In addition, some of the naphthalene powders was mistakenly placed in the wrong wells and these wells were removed from the study. It can be seen that the addition of naphthalene with plasma and secondary resulted in en extremely high signal, but it is also noted that the standard deviation of this group was high. Overall it is noted that the naphthalene did not significantly affect the signal in the other wells. It is also worth noting that Group 7 (Naphthalene and Plasma without Secondary) had minimal signal. The next step of this experiment is to perform a proper fluorescence assay to see if there are any secondary interactions between the naphthalene and the fluorescence since naphthalene in fluorescent in the green range.

Overall a complete characterization of different reagents (BSA, blocking agents,

Plate Map Legend	
Number	**Group**
1	Plasma + Secondary
2	No Plasma Control
3	No Secondary Control
4	Naph + Plasma
5	Naph + Secondary
6	Naph + Plasma + Secondary
7	Naph + Plasma w/o Secondary
8	Naph + Secondary w/o Plasma
9	Naph
10	Naph + PBST Wash

Figure 46. The legend of the ELISA assay with all of the necessary controls with the secondary, plasma with/without the addition of naphthalene.

and different nitrocellulose membranes) with the naphthalene will provide a more extensive picture of the interactions that occur with the sublimating valve material. In addition, more precise amounts of naphthalene in the ELISA wells in conjunction with a fluorescence based ELISA assay will provide a complete picture on the overall bio-compatibility of naphthalene and its feasibility in lateral flow assays.

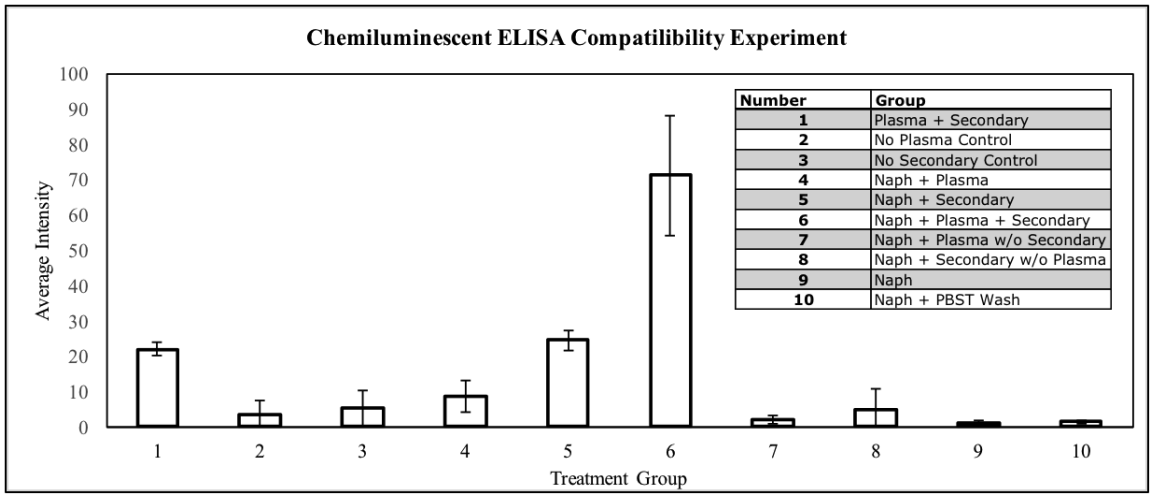

Figure 47. The chemiluminescent results of the ELISA compatibility experiment with the addition of naphthalene. It can be seen that the addition of naphthalene with plasma and secondary resulted in en extremely high signal, but it is also noted that the standard deviation of this group was high. Overall it is noted that the naphthalene did not significantly affect the signal in the other wells.

Chapter 4

MODELING OF FLUID FLOW IN A POROUS MEDIUM

This section will cover the efforts made in modeling of fluid flow in a porous medium. This was done with two methods, the development of a mathematical model in addition to a computational fluid dynamics model in COMSOL. These models were used to predict fluid flow to properly characterize the flow dynamics of the paper based microfluidic models.

4.1 Mathematical Modeling

Fluidic control in a porous medium can be simplified in terms of an electrical circuit analogy. For the sake of simplicity, fluid flow is modelled in fully wetted flow, where the membrane is already pre-wetted. Fluidic dimensions of the strip are analogous to the resistance of the electrical circuit. The current of the analogous model can be related to the volumetric flow rate and the pressure difference across the membrane is analogous to the potential difference.

4.1.1 Governing Equations and Assumptions

As mentioned in Chapter 1, the Washburn equation is used to describe capillary driven flow with the assumption that there is an 'infinite' reservoir on one side of the fluidic channel. The other side of the channel is assumed to be exposed to the ambient environment. The Washburn equation is further derived with and a number

of core assumptions are in the case of capillary flow, but cannot be assumed in the case of paper-based fluidics:

- The effects of gravity, hydrostatic pressure, and atmospheric pressure are negligible
- The walls of the capillary are no-slip and the velocity is highest at the center of the capillary
- The liquid in the capillary is incompressible and moves at a constant velocity
- The pressure gradient is constant in the x direction and is also linear
- The flow in the capillaries are laminar and constant
- The capillaries are cylindrical and have a constant diameter

These assumptions cannot all be adapted in the use of a porous medium, but it can be assumed that a porous body is composed of n number of cylindrical capillaries, which allows for the calculation of all of the volumes in a porous medium.

$$V = \pi \sum r_c^2 X = \frac{\pi}{2} \sqrt{\frac{t}{\mu}} \sum \sqrt{P_E + \frac{2\gamma}{r_c}} \cdot r_c^3 \tag{1}$$

where V is the total volume of the fluid in the porous media, r_c is the radius of the capillary, X is the length of the column of the liquid in the capillary, μ is the viscosity of the liquid, P_E is the external pressure driving the fluid, and γ is the surface tension between the liquid and air interface. In this situation, the capillary forces dominate and P_E is negligible and a similar equation can be derived with another term κ which describes the degree of penetration of the fluid. This term is similar to permeability while taking into account the interaction between the fluid and the porous medium.

$$V = \kappa \sqrt{\frac{\gamma t}{\mu}} \tag{2}$$

However, Darcy's Law can also be used to represent capillary flow through porous media. This law was originally derived to describe fluid flow through soil, but can be adapted for the purpose of paper microfluidics. The original version of this formula stated that the velocity of a fluid in a porous medium is proportional to the pressure gradient across the media. Since paper is composed of a network of fibers, the pores are essentially void spaces in the network. There are also a number of core assumptions that are applied in the case of paper-based microfluidics:

- The velocity of the fluid is proportional to the pressure gradient of the porous media
- Flow of the fluid is steady and laminar in the porous media
- The fluid has a constant viscosity and is incompressible
- The effects of gravity, hydrostatic pressure, and atmospheric pressure are negligible

By applying the Young-Laplace equation (Equation 3), it can be assumed that the pressure gradient is steady state and linear in the x direction.

$$\frac{\mu U}{k} = -\nabla p \tag{3}$$

Further derivation of this equation leads to a final form of Darcy's equation which directly relates the permeability of the porous medium to the capillary radius.

$$\kappa = \frac{r_c}{8} \tag{4}$$

To predict the behavior of the flow of the paper, this simplified form of Darcy's equation was used for the development of the mathematical model. The most significant variable that is to be selected is the approximation of the permeability variable.

4.1.2 Mathematical Model Development

The mathematical model was developed with the use of Darcy's equation since there is a permeability parameter which is quite significant in porous media. To develop a model experimental data the most important parameter was the creation of permeability constant which was found for various types of the membrane. The capillary size was empirically determines.

4.2 COMSOL Modelling

To model the flow of blood through the asymmetric polysulfone membrane, two phase porous media was utilized to model the pores for the membrane. Blood was used as a Newtonian fluid and was flown through the membrane. An SEM image of the asymmetric polysulfone membrane was acquired into COMSOL Multiphysics and its data was imported into an image for computer analysis. An image of the import can be seen in Figure 48.

A pore scale modeling technique was used which uses creeping (Stokes) flow in the interstices of a porous media. This modeling technique can be used to predict fluid velocity in a porous membrane. Extrapolating the permeability and porosity of the SEM image can be used to validate experimental results.

The future step of this model is the creation of equivalent sized particles for red blood cells so that they can be filtered through the membrane.

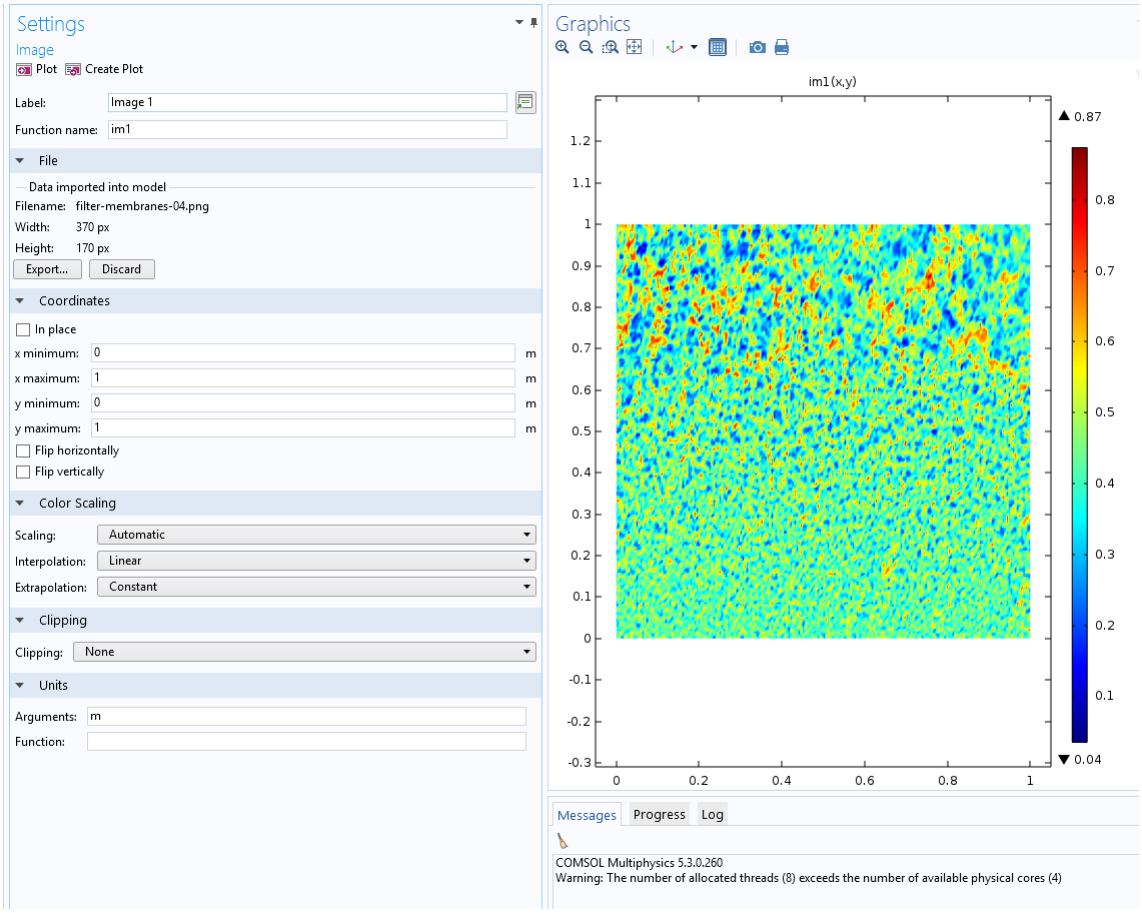

Figure 48. The image import of the SEM image of an asymmetric polysulfone membrane on COMSOL multiphysics.

Chapter 5

DEVELOPMENT OF A SOFTWARE TO INTERFACE THE DATA ACQUISITION PROGRAM FOR THE LATERAL FLOW PLATFORM

This chapter covers the efforts made towards the development of a data acquisition interface for the various iterations of the fluorescence-based lateral flow platform for the detection of biomarkers in whole blood. The entire system is based in the Arduino ecosystem, but there was a need to interface the Arduino system to an external interface such as an iPhone or a computer. The computer based system was designed for the standard Arduino platform and the iPhone application was designed to interface with the LightBlue Bean, a Bluetooth Low Energy (BLE) based Arduino system. These efforts will be outlined in the following sections.In both cases it is assumed that the Arduino script is uploaded onto the device and runs when the on button is pressed on the device.

5.1 Computer Interface Development

To interface with a standard Arduino Uno/Mega via USB a Visual Basic application was created. This Visual Basic Application was created to output data from the serial monitor of the Arduino and allowed the user to input information about the user along with the selection of the USB port. After the test is run all the data is appended into a .csv file. The user is then prompted to name and save the file along with an optional prompt to disconnect the Arduino device.

The application created in Fig. 49includes the Visual Basic Enterprise (2017

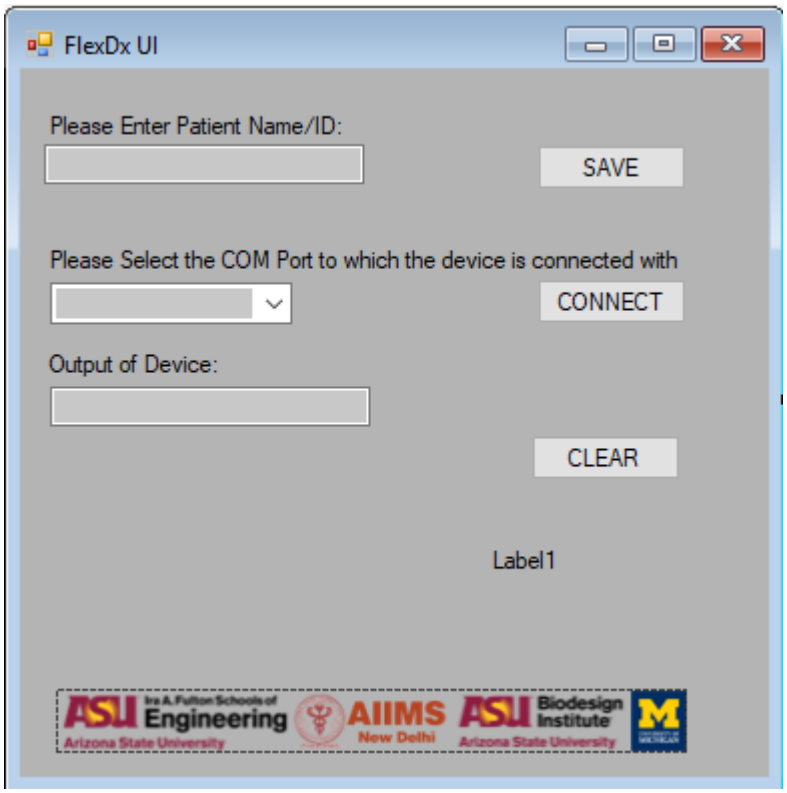

Figure 49. The screen where the user is prompted to insert the patient and the application also saves the time and date of the test.

Release) displays interface of the lateral flow reader with a computer. The application was compiled as an executable and can be loaded on any computer. In this application the user is prompted to include the patient identifier number as well as an option to selection USB port to connect to. In addition there is a box which displays the output of the serial monitor in real time as well as an option to clear that box. Once the test is running the user is given a .csv file with the time and date as well as the identifier of the patient in addition to all of the data collected from the Arduino. This application was successfully used in the 2017 BIOCAS conference as well as a site visit seen in Fig. 50.

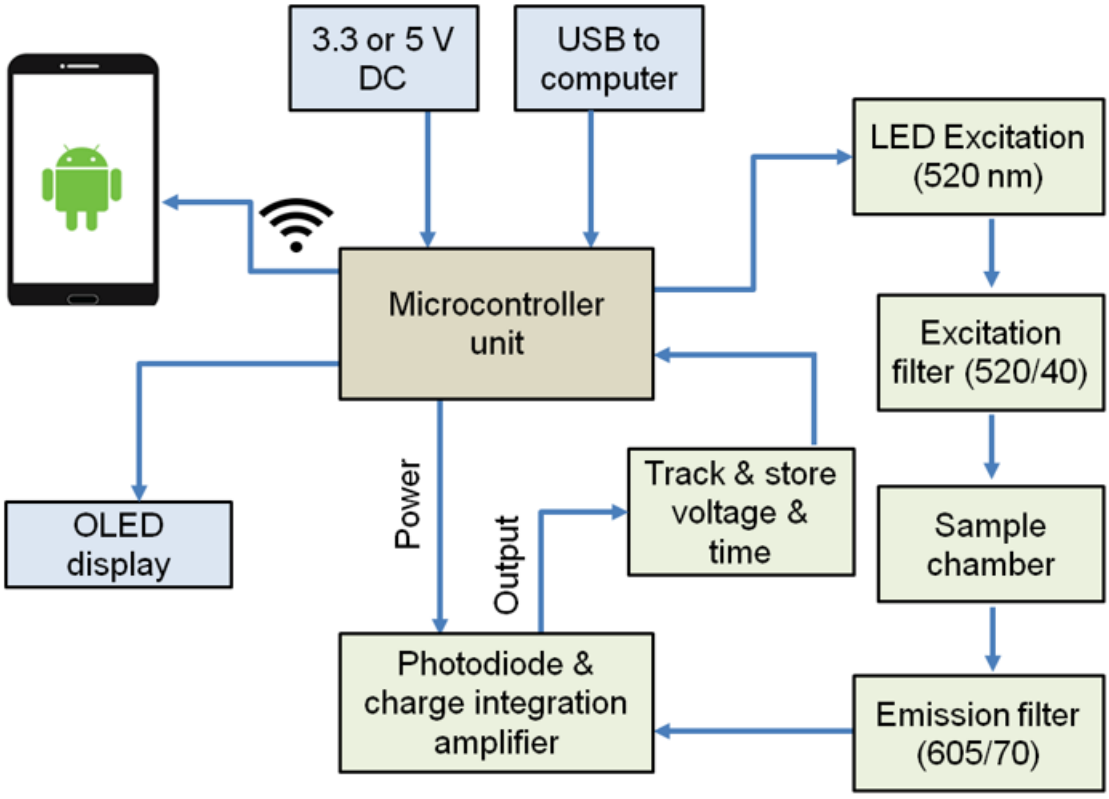

Figure 50. A system block diagram for the software interfaces developed for the lateral flow platform.

5.2 iOS Application Development

An application was created which would interface with the LightBlue Bean (designed by Punch Through Design) for field use when the lateral flow device will be deployed in rural populations in India. The application was created in Swift (Xcode) to interface with Apple devices with the use The application was created to store patient names, which appends to the data stream that is received from the LightBlue Bean. The results of the detection time are continually outputted in real time on the screen of the iPhone or Apple device. The data that is collected is stored in a .csv file and users are prompted to send the data via email in the application.

When the application is started, the application automatically searches for nearby LightBlue Beans. The user is given the option to refresh the application when it is searching for additional devices, which can be seen in Fig. 51.

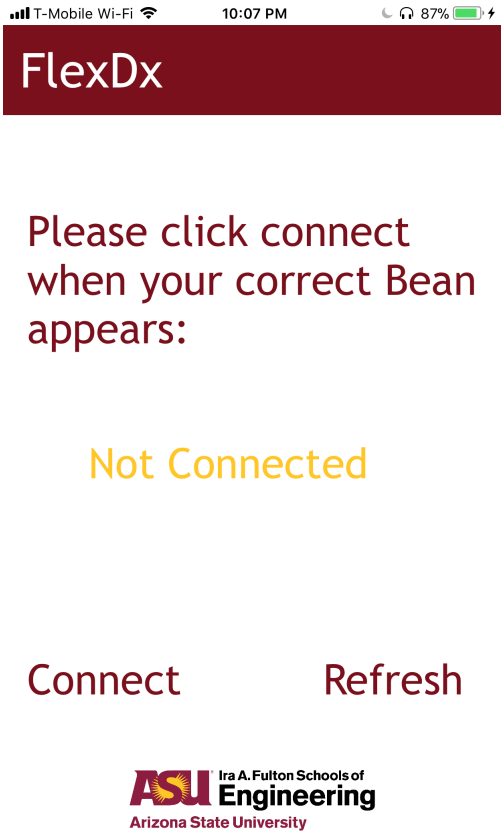

Figure 51. The landing screen of the FlexDx application where the device searches for available BLE devices.

After this is performed and the application ensures that a steady connection is created withe the LightBlue Bean, the application segues to the next screen where the user is prompted to enter the ID number of the patient. In addition, the date and time of the test is also saved at the same time and once the submit button is pressed, the LightBlue Bean is prompted to begin the test, which can be seen in Fig. 52.

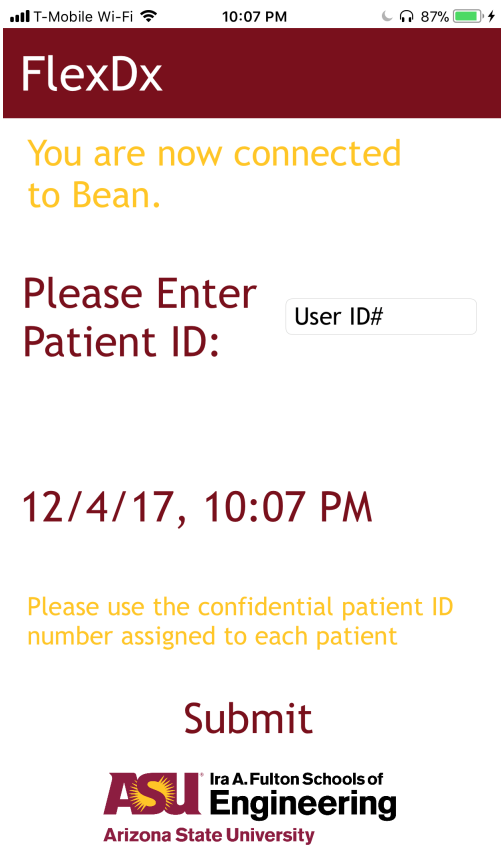

Figure 52. The screen where the user is prompted to insert the patient and the application also saves the time and date of the test.

Afterwards, the application segues to the testing screen of the device where user is prompted to start the test. Once the button is pressed, the timer begins to run and the LightBlue Bean begins to run the test. The user is also given a live readout of the progress of the test. Once the progress reaches 100%, the 'View Results" button appears where the compiled results of the test appear along with the User ID and time and date. This screen can be seen in Fig. 53.

In addition, the application also compiles the data in a .csv file, which is running in the background and only appears when the user prompts the application to send an

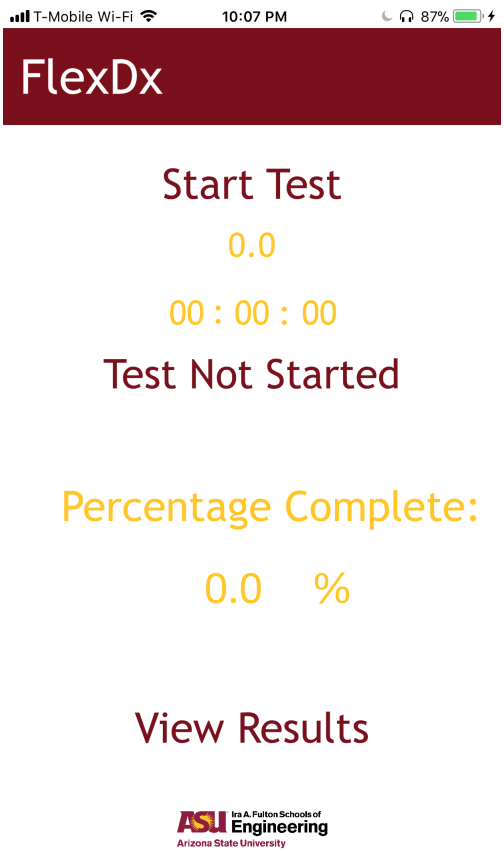

Figure 53. The testing screen of the device where the timer measures the overall time elapsed for the detection test.

email to the health-care provider with the results of the test. A sample email that can pop up can be seen in Fig. 54. The source code for this application can be seen the following Github Repository https://github.com/hmarafa/POC_iOS or in Appendix A of this document.

There were issues associated with keeping a steady connection with the application. If the connection is interrupted, the application crashes and had to be rebuilt in its initial version. In the following versions, eliminating the application in the task manager would fix the issue, but ideally, the application should segue back to the connection screen if this were to occur. Another issue that appeared was that in some

instances, the application would trigger the LightBlue Bean to run the test multiple times in quick succession. Overall, there are a number of iterations that are still required to launch the application and a significant amount of debugging is required as well. However, this application in its current state functions as an initial proof of concept and successfully demonstrates communication with a Bluetooth Low Energy Arduino device.

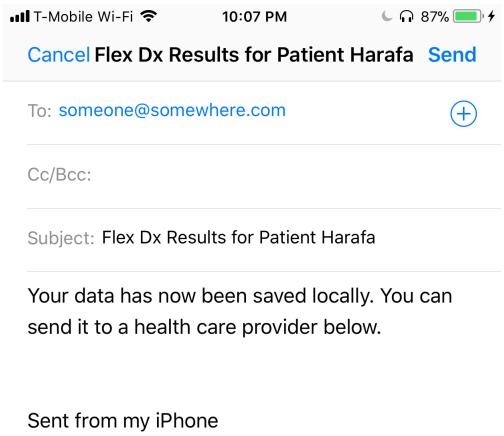

Figure 54. A sample email screen where the application compiles all of the data into a .csv file and prompts the user to email the data to a health-care provider.

Chapter 6

CONCLUSIONS & FUTURE WORK

This work describes efforts made in the development of multiple facets of the fluorescence based lateral based detection assay for global health applications. This work describes developments in the field of paper microfluidics and functionalization of porous surfaces. In addition, actuation of valves and other materials in porous membranes and paper microfluidics was researched in depth. There was significant effort made in the creation of the blood fractionation aspect of the lateral flow device by testing and characterizing various glass bound and asymmetric polysulfone membranes with blood samples. Characterization of the rate of evaporation of fluids in a porous membrane in various temperatures and humities was also completed and it was found that the rate of evaporation of blood was statistically similar to that of water. The culminating point of this chapter presented an implementation of the optimal blood fractionation filter in the lateral flow reader form factor. This experiment was favorably compared to the conventionally centrifuged pooled plasma sample. Recommendations have been made for the optimization of the blood factor in addition towards future attempts in packaging the entire lateral flow assay strips.

The third chapter of this work covered efforts made towards the development of thermally actuated valves for delayed and precise control of reagents in the lateral flow assay. The consistent and timed delivery of reagents has been shown to greatly affect the consistency of the results of the lateral flow assay and various materials were tested and characterized. A PID controller was designed and implemented in the precision printing fixture to allow for the heated deposition of these materials onto a porous

membrane. This system was validated and its operating conditions were optimized for the heated deposition of these materials. Wax valves were researched and the hydrophobicity of various waxes was tested in direct comparisons of the flow rate in the same porous materials. In addition these same tests were completed with a novel sublimating material (naphthalene) and its material characteristics were compared to conventional hydrophobic wax materials.

The fourth chapter of this work presents efforts made towards the development of mathematical and computational fluid dynamic (CFD) models for the simulation of flow in porous membranes. There needs to be significant work on the simulation front for the refinement of these models so they can compare to experimental results. The fifth chapter of this work presents efforts made towards the creation of user interfaces for the entire fluorescence based lateral flow detection platform on mobile phones and desktops. An application was created for iOS devices which successfully interfaces with an Arduino with Bluetooth compatibility (LightBlue Bean) and communicates with the device. In addition an application was created for computer use which connects to traditional Arduino Uno micro-controller boards. Both systems have been validated and tested and are close to field implementation.

Future works include the optimization of naphthalene valves in addition to the optimization of the mathematical and CFD models so they can be comparable to real world experimental results. In addition packaging of the lateral flow test strips will be researched and further optimization of the blood fractionation membrane and improved integration of the filter will be completed at a future time.

REFERENCES

Abe, Koji, Koji Suzuki, and Daniel Citterio. 2008. 'Inkjet-printed microfluidic multianalyte chemical sensing paper.' *Analytical chemistry* 80 (18): 6928–6934.

Bhalla, Nikhil, Danny Wen Yaw Chung, Yaw-Jen Chang, Kimberly Jane S Uy, Yi Ying Ye, Ting-Yu Chin, Hao Chun Yang, and Dorota G Pijanowska. 2013. 'Microfluidic platform for enzyme-linked and magnetic particle-based immunoassay.' *Micromachines* 4 (2): 257–271.

Bruzewicz, Derek A, Meital Reches, and George M Whitesides. 2008. 'Low-cost printing of poly (dimethylsiloxane) barriers to define microchannels in paper.' *Analytical chemistry* 80 (9): 3387–3392.

Castillo-León, Jaime, and Winnie E Svendsen. 2014. *Lab-on-a-Chip Devices and Micro-Total Analysis Systems: A Practical Guide.* Springer.

Cate, David M, Jaclyn A Adkins, Jaruwan Mettakoonpitak, and Charles S Henry. 2014. 'Recent developments in paper-based microfluidic devices.' *Analytical chemistry* 87 (1): 19–41.

Crowley, Timothy A, and Vincent Pizziconi. 2005. 'Isolation of plasma from whole blood using planar microfilters for lab-on-a-chip applications.' *Lab on a Chip* 5 (9): 922–929.

Dungchai, Wijitar, Orawon Chailapakul, and Charles S Henry. 2011. 'A low-cost, simple, and rapid fabrication method for paper-based microfluidics using wax screen-printing.' *Analyst* 136 (1): 77–82.

Fenton, Erin M, Monica R Mascarenas, Gabriel P López, and Scott S Sibbett. 2008. 'Multiplex lateral-flow test strips fabricated by two-dimensional shaping.' *ACS applied materials & interfaces* 1 (1): 124–129.

Fu, Elain, Stephen A Ramsey, Peter Kauffman, Barry Lutz, and Paul Yager. 2011. 'Transport in two-dimensional paper networks.' *Microfluidics and nanofluidics* 10 (1): 29–35.

Galligana, C, J Nicholsb, E Kvamc, P Spoonerc, R Gettingsb, L Zhub, and CM Puleoa. 2015. 'Mesoscale Blood Cell Sedimentation for Rapid Collection of Millilitre Samples.' *Lab on a Chip.*

Ghaderinezhad, Fariba, Reza Amin, Mikail Temirel, Bekir Yenilmez, Adam Wentworth, and Savas Tasoglu. 2017. 'High-throughput rapid-prototyping of low-cost paper-based microfluidics.' *Scientific Reports* 7 (1): 3553.

Goodman, Steven R, Karis MH Hughes, David G Kakhniashvili, and Sudha Neelam. 2007. 'The isolation of reticulocyte-free human red blood cells.' *Experimental Biology and Medicine* 232 (11): 1470–1476.

Homsy, Alexandra, Peter D van der Wal, Werner Doll, Roland Schaller, Stefan Korsatko, Maria Ratzer, Martin Ellmerer, Thomas R Pieber, Andreas Nicol, and Nico F De Rooij. 2012. 'Development and validation of a low cost blood filtration element separating plasma from undiluted whole blood.' *Biomicrofluidics* 6 (1): 012804.

Lam, Trinh, Jasmine P Devadhasan, Ryan Howse, and Jungkyu Kim. 2017. 'A Chemically Patterned Microfluidic Paper-based Analytical Device (C-μPAD) for Point-of-Care Diagnostics.' *Scientific Reports* 7 (1): 1188.

Li, Xu, Junfei Tian, Gil Garnier, and Wei Shen. 2010. 'Fabrication of paper-based microfluidic sensors by printing.' *Colloids and Surfaces B: Biointerfaces* 76 (2): 564–570.

Liu, Changchun, Shih-Chuan Liao, Jinzhao Song, Michael G Mauk, Xuanwen Li, Gaoxiang Wu, Dengteng Ge, Robert M Greenberg, Shu Yang, and Haim H Bau. 2016. 'A high-efficiency superhydrophobic plasma separator.' *Lab on a Chip* 16 (3): 553–560.

Liu, Changchun, Michael Mauk, Robert Gross, Frederic D Bushman, Paul H Edelstein, Ronald G Collman, and Haim H Bau. 2013. 'Membrane-based, sedimentation-assisted plasma separator for point-of-care applications.' *Analytical chemistry* 85 (21): 10463–10470.

Lopez-Munoz, Eunice, and Manuel Mendez-Montes. 2013. 'Markers of circulating breast cancer cells.' *Adv Clin Chem* 61:175–224.

Lu, Yao, Weiwei Shi, Lei Jiang, Jianhua Qin, and Bingcheng Lin. 2009. 'Rapid prototyping of paper-based microfluidics with wax for low-cost, portable bioassay.' *Electrophoresis* 30 (9): 1497–1500.

Maria, M Sneha, PE Rakesh, TS Chandra, and AK Sen. 2016. 'Capillary flow of blood in a microchannel with differential wetting for blood plasma separation and on-chip glucose detection.' *Biomicrofluidics* 10 (5): 054108.

Martinez, Andres W, Scott T Phillips, Manish J Butte, and George M Whitesides. 2007. 'Patterned paper as a platform for inexpensive, low-volume, portable bioassays.' *Angewandte Chemie International Edition* 46 (8): 1318–1320.

Martinez, Andres W, Scott T Phillips, Benjamin J Wiley, Malancha Gupta, and George M Whitesides. 2008. 'FLASH: a rapid method for prototyping paper-based microfluidic devices.' *Lab on a Chip* 8 (12): 2146–2150.

Miltenyi, Stefan, Werner Müller, Walter Weichel, and Andreas Radbruch. 1990. 'High gradient magnetic cell separation with MACS.' *Cytometry* 11 (2): 231–238.

Nilghaz, Azadeh, and Wei Shen. 2015. 'Low-cost blood plasma separation method using salt functionalized paper.' *Rsc Advances* 5 (66): 53172–53179.

Obahiagbon, U., D. Kullman, J. T. Smith, B. A. Katchman, H. Arafa, K. S. Anderson, and J. B. Christen. 2016. 'Characterization of a compact and highly sensitive fluorescence-based detection system for point-of-care applications.' In *2016 IEEE Healthcare Innovation Point-Of-Care Technologies Conference (HI-POCT)*, 117–120. November. doi:10.1109/HIC.2016.7797711.

Olkkonen, Juuso, Kaisa Lehtinen, and Tomi Erho. 2010. 'Flexographically printed fluidic structures in paper.' *Analytical chemistry* 82 (24): 10246–10250.

Piacentini, Niccolò, Guillaume Mernier, Raphaël Tornay, and Philippe Renaud. 2011. 'Separation of platelets from other blood cells in continuous-flow by dielectrophoresis field-flow-fractionation.' *Biomicrofluidics* 5 (3): 034122.

Posthuma-Trumpie, Geertruida A., Jakob Korf, and Aart van Amerongen. 2009. 'Lateral flow (immuno)assay: its strengths, weaknesses, opportunities and threats. A literature survey.' *Analytical and Bioanalytical Chemistry* 393, no. 2 (January): 569–582. doi:10.1007/s00216-008-2287-2.

Songjaroen, Temsiri, Wijitar Dungchai, Orawon Chailapakul, Charles S Henry, and Wanida Laiwattanapaisal. 2012. 'Blood separation on microfluidic paper-based analytical devices.' *Lab on a Chip* 12 (18): 3392–3398.

Songjaroen, Temsiri, Wijitar Dungchai, Orawon Chailapakul, and Wanida Laiwattanapaisal. 2011. 'Novel, simple and low-cost alternative method for fabrication of paper-based microfluidics by wax dipping.' *Talanta* 85 (5): 2587–2593.

Szydzik, Crispin, Khashayar Khoshmanesh, Arnan Mitchell, and Christian Karnutsch. 2015. 'Microfluidic platform for separation and extraction of plasma from whole blood using dielectrophoresis.' *Biomicrofluidics* 9 (6): 064120.

Tageson, Mackenzie Elizabeth. 2013. 'FUNCTIONAL 3-D CELLULOSE & NITRO-CELLULOSE PAPER-BASED, MULITPLEX DIAGNOSTIC PLATFORMS WITHOUT COUPLING AGENTS.'

Toner, Mehmet, and Daniel Irimia. 2005. 'Blood-on-a-chip.' *Annu. Rev. Biomed. Eng.* 7:77–103.

Tripathi, Siddhartha, YV BalaVarun Kumar, Amit Agrawal, Amit Prabhakar, and Suhas S Joshi. 2016. 'Microdevice for plasma separation from whole human blood using bio-physical and geometrical effects.' *Scientific reports* 6:26749.

VanDelinder, Virginia, and Alex Groisman. 2006. 'Separation of plasma from whole human blood in a continuous cross-flow in a molded microfluidic device.' *Analytical chemistry* 78 (11): 3765–3771.

Yetisen, Ali Kemal, Muhammad Safwan Akram, and Christopher R Lowe. 2013. 'Paper-based microfluidic point-of-care diagnostic devices.' *Lab on a Chip* 13 (12): 2210–2251.

Yuan, Yuehua, and T Randall Lee. 2013. 'Contact angle and wetting properties.' In *Surface science techniques,* 3–34. Springer.

APPENDIX A

CODE FOR PROGRAMS

A.1 Visual Basic Code for Lateral Flow Program

This section includes the Visual Basic Enterprise (2017 Release) code for the application with interfaces the lateral flow reader with a computer. The application was compiled as an executable and can be loaded on any computer.

```
Imports System
Imports System.IO.Ports
Imports System.Text

Public Class Form1
    Dim comPORT1 As String
    Dim receivedData1 As String = ""

    Private Sub flexdx_Load(ByVal sender As System.Object,
    ByVal e As System.EventArgs) Handles MyBase.Load
        Timer1.Enabled = False
        comPORT1 = ""
        For Each sp As String In My.Computer.Ports.SerialPortNames
            comPort_ComboBox.Items.Add(sp)
        Next
    End Sub


    Private Sub comPort_ComboBox_SelectedIndexChanged
    (sender As Object, e As EventArgs)
    Handles comPort_ComboBox.SelectedIndexChanged
        If (comPort_ComboBox.SelectedItem <> "") Then
            comPORT1 = comPort_ComboBox.SelectedItem
        End If
    End Sub


    Private Sub connect_BTN_Click(sender As Object,
    e As EventArgs) Handles connect_BTN.Click
        If (connect_BTN.Text = "Connect") Then
            If (comPORT1 <> "") Then
                SerialPort1.Close()
                SerialPort1.PortName = comPORT1
                SerialPort1.BaudRate = 9600
                SerialPort1.DataBits = 8
                SerialPort1.Parity = Parity.None
```

```
            SerialPort1.StopBits = StopBits.One
            SerialPort1.Handshake = Handshake.None
            SerialPort1.Encoding = System.Text.Encoding.Default
            SerialPort1.ReadTimeout = 10000

            SerialPort1.Open()
            connect_BTN.Text = "Dis-connect"
            Timer1.Enabled = True
            Timer_LBL.Text = "Timer: ON"
        Else
            MsgBox("Select a COM port first")
        End If
    Else
        SerialPort1.Close()
        connect_BTN.Text = "Connect"
        Timer1.Enabled = False
        Timer_LBL.Text = "Timer: OFF"
    End If


End Sub


Private Sub Timer1_Tick(sender As Object,
e As EventArgs) Handles Timer1.Tick
    receivedData1 = ReceiveSerialData1()
    RichTextBox1.Text &= receivedData1
End Sub


Function ReceiveSerialData1() As String
    Dim tb1Text As String
    tb1Text = tb1.Text
    Dim Incoming As String
    Dim FILE_NAME As String
    FILE_NAME = System.IO.Path.Combine(
           My.Computer.FileSystem.SpecialDirectories.MyDocuments,
           "test.txt")
    Try
        Incoming = SerialPort1.ReadExisting()

        If System.IO.File.Exists(FILE_NAME) = True Then

            Dim objWriter As New System.IO.StreamWriter(FILE_NAME,
```

```
            True)
            objWriter.WriteLine(tb1Text + "," + Incoming + ",
            " + DateTime.Now.ToString("yyyyMMddHHmm"))
            objWriter.Close()
        Else
            System.IO.File.Create(FILE_NAME).Dispose()
            Dim objWriter As New System.IO.StreamWriter(FILE_NAME,
            True)
            objWriter.WriteLine(tb1Text + "," + Incoming + ",
            " + DateTime.Now.ToString("yyyyMMddHHmm"))
            objWriter.Close()
        End If

        If Incoming Is Nothing Then
            Return "nothing" & vbCrLf
        Else
            Return Incoming
        End If
    Catch ex As TimeoutException
        Return "Error: Serial Port read timed out."
    End Try

End Function


Private Sub clear_BTN_Click(sender As Object,
e As EventArgs) Handles clear_BTN.Click
    RichTextBox1.Text = ""
End Sub

Private Sub Label2_Click(sender As Object,
e As EventArgs) Handles Label2.Click

End Sub

Private Sub TextBox1_TextChanged(sender As Object,
e As EventArgs) Handles tb1.TextChanged


End Sub

Private Sub Button1_Click(sender As Object,
e As EventArgs) Handles Button1.Click
```

```
    End Sub

    Private Sub PictureBox1_Click(sender As Object,
    e As EventArgs) Handles PictureBox1.Click

    End Sub
End Class
\end{verbatim}

\begin{figure}[h]
\centering
\includegraphics[scale=1.3]{fig/vbapp.PNG}
\caption{The screen where the user is prompted to insert the patient and the
     application also saves the time and date of the test.}
\label{fig:vbapp}
\end{figure}

\section{Swift Code for Arduino Application}

This is the compiled code for the iOS application created to interface with
    the LightBlue Bean. This code was compiled in Xcode (Version 9) using
    the Swift programming language.

\begin{lstlisting}




//
//  AppDelegate.swift
//  POC_iOS
//
//  Created by Hany Arafa on 10/30/17.
//  Copyright   2017 Hany Arafa. All rights reserved.
//

import UIKit
import CoreData


@UIApplicationMain
class AppDelegate: UIResponder, UIApplicationDelegate {

    var window: UIWindow?
```

```
func application(_ application: UIApplication,
    didFinishLaunchingWithOptions launchOptions:
[UIApplicationLaunchOptionsKey: Any]?) -> Bool {
    // Override point for customization after application launch.
    return true
}

func applicationWillResignActive(_ application: UIApplication) {
    // Sent when the application is about to move from active to inactive
        state.
    This can occur for certain types of temporary interruptions (such as
        an incoming
    phone call or SMS message) or when the user quits the application and
        it begins
    the transition to the background state.
    // Use this method to pause ongoing tasks, disable timers, a
    nd invalidate graphics rendering callbacks. Games should use this
        method to pause the game.
}

func applicationDidEnterBackground(_ application: UIApplication) {
    // Use this method to release shared resources, save user data,
        invalidate timers,
    and store enough application state information to restore your
        application to
    its current state in case it is terminated later.
    // If your application supports background execution,
    this method is called instead of applicationWillTerminate: when the
        user quits.
}

func applicationWillEnterForeground(_ application: UIApplication) {
    // Called as part of the transition from the background to the active
        state;
    here you can undo many of the changes made on entering the background.

}

func applicationDidBecomeActive(_ application: UIApplication) {
    // Restart any tasks that were paused (or not yet started) while the
        application was inactive.
```

```
    If the application was previously in the background, optionally
       refresh the user interface.
}

func applicationWillTerminate(_ application: UIApplication) {
    // Called when the application is about to terminate. Save data
    if appropriate. See also applicationDidEnterBackground:.
    // Saves changes in the application's managed object context before
       the application terminates.
    //self.saveContext()
}

// MARK: - Core Data stack

lazy var persistentContainer: NSPersistentContainer = {
    /*
     The persistent container for the application. This implementation
     creates and returns a container, having loaded the store for the
     application to it. This property is optional since there are
        legitimate
     error conditions that could cause the creation of the store to fail.
    */
    let container = NSPersistentContainer(name: "POC_iOS")
    container.loadPersistentStores(completionHandler: { (storeDescription
       , error) in
       if let error = error as NSError? {
           // Replace this implementation with code to handle the error
              appropriately.
           // fatalError() causes the application to generate a crash log
                and terminate. You should not use this
           function in a shipping application, although it may be useful
              during development.

           /*
            Typical reasons for an error here include:
            * The parent directory does not exist, cannot be created, or
                disallows writing.
            * The persistent store is not accessible, due to permissions
                or data protection
            when the device is locked.
            * The device is out of space.
            * The store could not be migrated to the current model
                version.
```

```
                Check the error message to determine what the actual problem
                    was.
                */
                fatalError("Unresolved error \(error), \(error.userInfo)")
            }
        })
        return container
    }()

    // MARK: - Core Data Saving support

    func saveContext () {
        let context = persistentContainer.viewContext
        if context.hasChanges {
            do {
                try context.save()
            } catch {
                // Replace this implementation with code to handle the error
                    appropriately.
                // fatalError() causes the application to generate a crash log
                     and terminate.
                You should not use this function in a shipping application,
                    although it may
                be useful during development.
                let nserror = error as NSError
                fatalError("Unresolved error \(nserror), \(nserror.userInfo)")
            }
        }
    }

}

//
//  ViewController.swift
//  POC_iOS
//
//  Created by Hany Arafa on 10/30/17.
//  Copyright   2017 Hany Arafa. All rights reserved.
//

import UIKit
import Bean_iOS_OSX_SDK
import CoreBluetooth
import UICircularProgressRing
```

```
class ViewController: UIViewController, UITextFieldDelegate,
   PTDBeanManagerDelegate,
PTDBeanDelegate {



    @IBOutlet weak var percentUpdate: UILabel!
    @IBOutlet weak var valueFromBean: UILabel!
    var beanManager: PTDBeanManager!
    var userID: UITextField!
    @IBOutlet weak var resetBtn: UIButton!
    var maxValue: String = " "
    var dateString: String = " "
    //@IBOutlet weak var timeTaken: UILabel!
    @IBOutlet weak var labelMinute: UILabel!
    @IBOutlet weak var labelSecond: UILabel!
    @IBOutlet weak var labelMillisecond: UILabel!
    @IBOutlet weak var testProgressLabel: UILabel!
    var myBean: PTDBean!
    var lightState: Bool = false
    var startReading: Bool = true
    var stopReading: Bool = false
    var displayTime: Bool = false
    var lastValue: Bool = false
    var newLine: String = ""
    var csvText = ""

    weak var timer: Timer?
    var startTime: Double = 0
    var time: Double = 0
    var elapsed: Double = 0
    var status: Bool = false

    override func didReceiveMemoryWarning() {
        super.didReceiveMemoryWarning()
    }

    override func viewDidLoad() {
        super.viewDidLoad()
        self.hideKeyboardWhenTappedAround()
        beanManager = PTDBeanManager()
        beanManager?.delegate = self
        lightState = false
```

```
    //Uncomment the line below if you want the tap not not interfere and
        cancel other interactions.
    //tap.cancelsTouchesInView = false

    //make the csv up here
}

//optional func textFieldDidEndEditing(_ textField: UITextField)

func textFieldShouldReturn( userID : UITextField) -> Bool {
    userID.resignFirstResponder()
    return true
}

func beanManagerDidUpdateState(_ beanManager: PTDBeanManager!)
{
    if(self.beanManager!.state == BeanManagerState.poweredOn){
        self.beanManager?.startScanning(forBeans_error: nil)

    } else if (self.beanManager!.state == BeanManagerState.poweredOff) {
        let alert = UIAlertController(title: "Error", message: "Turn on
            bluetooth to continue",
        preferredStyle: .alert)
        alert.addAction(UIAlertAction(title: NSLocalizedString("OK",
            comment: "Default action")
        , style: .`default`, handler: { _ in
            NSLog("The \"OK\" alert occured.")
        }))
        self.present(alert, animated: true, completion: nil)
        return
    }
}

func startScanning()
{
    var error: NSError?
    beanManager!.startScanning(forBeans_error: &error)
    if let e = error
    {
        print(e)
    }
    else
    {
```

```
        print("Connection is made")
    }
}

func beanManager(_ beanManager: PTDBeanManager!, didDiscover bean:
    PTDBean!, error: Error!) {
    if myBean == nil {
        if bean.state == .discovered {
            print("bean discovered")
            //      beanDiscovered = true
            viewDidAppear(true)
            myBean = bean
            beanManager!.connect(to: bean, withOptions:nil, error: nil)
            bean.delegate = self
        }
    }

    #if DEBUG
       print("DISCOVERED BEAN \nName: \(bean.name), UUID: \(bean.
          identifier) RSSI: \(bean.rssi)")
    #endif
}
func beanManager(_ beanManager: PTDBeanManager!, didConnect bean:
    PTDBean!, error: Error!) {
    if ((error) != nil) {
        let alert = UIAlertController(title: "Error", message: "This is
            an alert.",
        preferredStyle: .alert)
        alert.addAction(UIAlertAction(title: NSLocalizedString("OK",
            comment:
        "Default action"), style: .`default`, handler: { _ in
            NSLog("The \"OK\" alert occured.")}))
        self.present(alert, animated: true, completion: nil)
        return;
    }

    var theError: NSError? = nil

        self.beanManager?.stopScanning(forBeans_error: &theError)

    if ((theError) != nil) {
        let alert = UIAlertController(title: "Error", message: "This is
            an alert.", preferredStyle: .alert)
```

```
            alert.addAction(UIAlertAction(title: NSLocalizedString("OK",
                comment:
            "Default action"), style: .`default`, handler: { _ in
                NSLog("The \"OK\" alert occured.")}))
           self.present(alert, animated: true, completion: nil)
            return;
        }
            }

    func BeanManager(beanManager: PTDBeanManager!,
    didDisconnectBean bean: PTDBean!, error: NSError!) {

    }


    @IBAction func handlerefresh(_ sender: Any) {
        if(self.beanManager!.state == BeanManagerState.poweredOn){
            var theError: NSError? = nil

            self.beanManager?.startScanning(forBeans_error: &theError)

            if ((theError) != nil) {
                let alert = UIAlertController(title: "Error", message: "This
                    is an alert.", preferredStyle: .alert)
                alert.addAction(UIAlertAction(title: NSLocalizedString
                ("OK", comment: "Default action"), style: .`default`, handler:
                     { _ in
                    NSLog("The \"OK\" alert occured.")
                }))
                //let alert: UIAlertController = UIAlertAction(title: "Error",
                message: theError!.localizedDescription, delegate: nil,
                cancelButtonTitle: nil, otherButtonTitles: "Ok")
                //self.present(alert, animated: true, completion: nil)
            }
        }

        (sender as! UIRefreshControl).endRefreshing()
    }

/*   func connectionChanged(_ notification: Notification) {
        // Connection status changed. Indicate on GUI.
        let userInfo = (notification as NSNotification).userInfo as! [String:
             Bool]
```

```
    DispatchQueue.main.async(execute: {
        // Set image based on connection status
        if let isConnected: Bool = userInfo["isConnected"] {
            if isConnected {
                let alertController = UIAlertController(title: "iOScreator
                    ", message:
                    "Hello, world!", preferredStyle:
                        UIAlertControllerStyle.alert)
                alertController.addAction(UIAlertAction(title: "Dismiss",
                    style:
                UIAlertActionStyle.default,handler: nil))

            }
            else {
                let alertController = UIAlertController(title: "iOScreator
                    ", message:
                    "Bluetooth is disconnecected. Please check your
                        connection.",
                    preferredStyle: UIAlertControllerStyle.alert)
                alertController.addAction(UIAlertAction(title: "Dismiss",
                    style:
                UIAlertActionStyle.default,handler: nil))
                self.present(alertController, animated: true, completion:
                    nil)

            }
        }
    });
}

*/


/* func bean(_ bean: PTDBean!, serialDataReceived data: Data!)
 {
 if(data != nil)
 {
 var receivedMessage = NSString(data:data, encoding: String.Encoding.utf8
     .rawValue)
 print("From serial: (receivedMessage)")
 ledTextLabel.text = receivedMessage! as string
 }
 }*/
```

```
/* func connectToBean(bean: PTDBean)
 {
 var error: NSError?
 print ("hi")
 beanManager!.connect(to: bean, withOptions:nil, error: &error)
 print("Bean connected")
 bean.delegate = self


 }*/


func sendSerialData(beanState: NSData)
{
    print(myBean)
    print("bye")
    //while(lightState == true)
    //{
    myBean?.sendSerialData(beanState as Data!)
    //}
    //myBean?.sendSerialData(beanState as Data!)
    print("sent over serial data")
}


func bean(_ bean: PTDBean!, serialDataReceived data: Data!)
{
    if(data != nil)
    {
        print ("Received Data")
    }

    let stringData : String = NSString(data: data, encoding : String.
        Encoding.ascii.rawValue)! as String
    if(stringData == "The time is")
    {
        displayTime = true
        var stringData : String = NSString(data: data, encoding :
        String.Encoding.ascii.rawValue)! as String
        //timeTaken.text? = stringData
    }
    else if(stringData == "Done")
    {
        //put a new line into the csv
```

```
}
else if(stringData == "Finished Calculating Value")
{
    lastValue = true
}
else
{
    /* var onlyDigits: CharacterSet = CharacterSet.decimalDigits.
       inverted
     if stringData.rangeOfCharacter(from: onlyDigits) != nil
     {
     let newValue = (Int(stringData)! / 1000) * 100
     percentUpdate.text = String(newValue)
     }*/

    let numbers = NSCharacterSet(charactersIn: "0123456789.").
       inverted

    if stringData.rangeOfCharacter(from: numbers) == nil
    {
        let newValue = (Double(stringData)! / 100.0) * 100
        print("HIIII")
        print(newValue)
        percentUpdate.text = String(newValue)
    }

    newLine += stringData + ","
    if(lastValue == true)
    {
        maxValue = stringData
        lastValue = false
    }
    else if(lastValue == true)
    {
        testProgressLabel.text = "Test is completed."
        //timeTaken.text? = stringData
        newLine += "\n"
        csvText.append(newLine)
        //WHEN THEY CLICK SAVE WRITE THE FILE TO THE PATH WE CREATED
           then
        send data over to next view controller to export
        displayTime = false
    }
    else
```

```
    {
        valueFromBean.text? = stringData
    }


}

//var fullString : String = valueFromBean.text!

// valueFromBean.scrollRangeToVisible(NSMakeRange(count(valueFromBean.
    string!),0))
//put this in a loop (while serialDataReceived < 1000
(so led has been turned on) or stop has been pressed)
/* if(data != nil)
 {
 var stringReceived: String = ""

 let nLength: Int = data.count / MemoryLayout<UInt8>.size
 var arrData: [UInt8] = [UInt8](repeating: 0, count: nLength)
 data.copyBytes(to: &arrData, count: nLength)

 var n: Int = 0
 while(n < nLength)
 {
 let str = String(UnicodeScalar(arrData[n]))
 stringReceived += str
 n += 1
 }
 print(stringReceived)
 //   var receivedMessage = NSString(data:data, encoding: String.
     Encoding.utf8.rawValue)
 valueFromBean.text = stringReceived as String
 }*/

//    NSString *uuidSubstring = [bean.identifier.UUIDString
 substringFromIndex:bean.identifier.UUIDString.length-4];
//    serialOutput = [NSString stringWithFormat:@"%@-%@:%@",
bean.name, uuidSubstring,serialOutput];

/* if(serialOutput)
 {
 serialOutput = [self.consoleOutputTextView.string
     stringByAppendingString:serialOutput];
 self.consoleOutputTextView.string = serialOutput;
```

```
     }

     [self.consoleOutputTextView scrollRangeToVisible:
      NSMakeRange(self.consoleOutputTextView.string.length, 0)];*/
}

   /* func saveData(_ sender: Any)
{
    let fileName = "TimeData.csv"
    let path = NSURL(fileURLWithPath: NSTemporaryDirectory()).
        appendingPathComponent(fileName)

    do
    {
        try csvText.write(to: path!, atomically: true, encoding: String.
            Encoding.utf8)
        print(csvText)
    }
    catch
    {
        print("File creating failed")
        print("\(error)")
    }
}*/
func start() {

    startTime = Date().timeIntervalSinceReferenceDate - elapsed
    timer = Timer.scheduledTimer(timeInterval: 0.01, target: self,
    selector: #selector(updateCounter), userInfo: nil, repeats: true)

    // Set Start/Stop button to true
    status = true

}

func stop() {

    elapsed = Date().timeIntervalSinceReferenceDate - startTime
    timer?.invalidate()

    // Set Start/Stop button to false
    status = false
}
```

```
@objc func updateCounter() {

    // Calculate total time since timer started in seconds
    time = Date().timeIntervalSinceReferenceDate - startTime

    // Calculate minutes
    let minutes = UInt8(time / 60.0)
    time -= (TimeInterval(minutes) * 60)

    // Calculate seconds
    let seconds = UInt8(time)
    time -= TimeInterval(seconds)

    // Calculate milliseconds
    let milliseconds = UInt8(time * 100)

    // Format time vars with leading zero
    let strMinutes = String(format: "%02d", minutes)
    let strSeconds = String(format: "%02d", seconds)
    let strMilliseconds = String(format: "%02d", milliseconds)

    // Add time vars to relevant labels
    labelMinute.text = strMinutes
    labelSecond.text = strSeconds
    labelMillisecond.text = strMilliseconds

}
@IBAction func pressButtonToChangeValue(_ sender: UIButton!)
{
    if (status) {
        stop()

        //resetBtn.isEnabled = true

        // If button status is false use start function, relabel button
            and disable reset button
    } else {
        start()

        //resetBtn.isEnabled = false
        testProgressLabel.text = "Test in Progress"
        print(testProgressLabel.text)
    }
```

```
    //newLine = ""
    //print ("hi")
    //lightState = true
    //while (stopReading == false){
    //let data = NSData(bytes: &lightState, length: MemoryLayout<Bool>.
        size)
    //sendSerialData(beanState: data)
    //   updateLedStatusText(lightState: lightState)
  // }

}

/*func stopReadingBean(_ sender: Any)
{
    lightState = false
    print("debugging")
    let data = NSData(bytes: &lightState, length: MemoryLayout<Bool>.size
        )
    sendSerialData(beanState: data)
    performSegue(withIdentifier: "transfertoEmail", sender: self)

}*/

@IBAction func viewresult(_ sender: Any) {
    //lightState = false
    print("debugging")
    //let data = NSData(bytes: &lightState, length: MemoryLayout<Bool>.
        size)
   // sendSerialData(beanState: data)
    //performSegue(withIdentifier: "transfertoEmail", sender: self)
}

override func prepare(for segue: UIStoryboardSegue, sender: Any?)
{
    if segue.identifier == "transferToEmail"
    {
        //let controller = segue.destination as!EmailViewController
        //controller.csvText = csvText
        //print(userID)
        //controller.userID.text = userID.text
        //controller.mPML = maxValue
        //controller.dateString = dateAndTimeLabel.text!
        //print(emailViewController?.userID.text as Any)
    }
```

```
    }
}

//
//  ConnectionViewController.swift
//  POC_iOS
//
//  Created by Hany Arafa on 10/30/17.
//  Copyright   2017 Hany Arafa. All rights reserved.
//

import UIKit
import Bean_iOS_OSX_SDK
import CoreBluetooth


class ConnectionViewController: UIViewController, PTDBeanManagerDelegate,
    PTDBeanDelegate
{
    var beanManager: PTDBeanManager?
    var myBean: PTDBean?

    @IBOutlet weak var connectionLabel: UILabel!

    @IBOutlet weak var beanNameChanged: UILabel!


    override func didReceiveMemoryWarning()
    {
        super.didReceiveMemoryWarning()
    }

    override func viewDidLoad() {
        super.viewDidLoad()
        self.hideKeyboardWhenTappedAround()
        beanManager = PTDBeanManager()
        beanManager!.delegate = self
    }

    func textFieldShouldReturn( userID : UITextField) -> Bool {
        userID.resignFirstResponder()
        return true
    }
```

```
 override func viewDidAppear(_ animated: Bool)
 {
 if(self.myBean != nil)
 {
    beanManager?.disconnectBean(myBean, error: nil)
 self.myBean = nil
 }

 var error: NSError?
 beanManager!.startScanning(forBeans_error: &error)
 if let e = error
 {
 print(e)
 }
 else
 {
 print("Connection is made")
 }
 }

func update() {
    if (self.myBean!.state == .discovered) {
        //self.connectToBean.title = "Connect"
        self.connectionLabel.isEnabled = true

    } else if (self.myBean!.state == .connectedAndValidated ) {
        //self.connectToBean.title = "Disconnect"
        self.connectionLabel.isEnabled = true
    }

}

func beanManagerDidUpdateState(_ beanManager: PTDBeanManager!)
{
    let scanError: NSError?
    if beanManager!.state == BeanManagerState.poweredOn
    {
        print("made it here")
        startScanning()
        print("made it here part 2")
    }

}
```

```
func startScanning()
{
    var error: NSError?
    beanManager!.startScanning(forBeans_error: &error)
    if let e = error
    {
        print(e)
    }
    else
    {
        print("Connection is made")
    }
}

@IBAction func connectToBean(_ sender: Any)
{

        //self.myBean!.delegate = self
        //beanManager!.connect(to: myBean, withOptions:nil, error: nil)
        //myBean?.delegate = self
        //self.connectionLabel.isEnabled = false


  beanManager!.connect(to: myBean, withOptions:nil, error: nil)
    myBean?.delegate = self
    connectionLabel.text = "You are now connected"
}

func beanManager(_ beanManager: PTDBeanManager!, didDiscover bean:
    PTDBean!, error: Error!)
{
    if myBean == nil
    {
        if bean.state == .discovered
        {
            print("bean discovered")
            beanNameChanged.text = bean.name
            //      beanDiscovered = true
            viewDidAppear(true)
            myBean = bean
            beanManager!.connect(to: bean, withOptions:nil, error: nil)
            //    bean.delegate = self
        }
    }
```

```
    #if DEBUG
        print("DISCOVERED BEAN \nName: \(bean.name), UUID: \(bean.
            identifier) RSSI: \(bean.rssi)")
    #endif
}

func beanManager(_ beanManager: PTDBeanManager!, didConnect bean:
    PTDBean!, error: Error!) {
    if ((error) != nil) {
        let alert = UIAlertController(title: "Error", message: "This is
            an alert.", preferredStyle: .alert)
        alert.addAction(UIAlertAction(title: NSLocalizedString("OK",
            comment: "Default action"),
        style: .`default`, handler: { _ in
            NSLog("The \"OK\" alert occured.")}))
        self.present(alert, animated: true, completion: nil)
        return;
    }

    var theError: NSError? = nil

    self.beanManager?.stopScanning(forBeans_error: &theError)

    if ((theError) != nil) {
        let alert = UIAlertController(title: "Error", message: "This is
            an alert.",
        preferredStyle: .alert)
        alert.addAction(UIAlertAction(title: NSLocalizedString
        ("OK", comment: "Default action"),
        style: .`default`, handler: { _ in
            NSLog("The \"OK\" alert occured.")}))
        self.present(alert, animated: true, completion: nil)
        return;
    }
}

func BeanManager(beanManager: PTDBeanManager!, didDisconnectBean bean:
    PTDBean!, error: Error!) {
    if (myBean == self.myBean) {
        self.update()
    }
}
```

```
    @IBAction func handlerefresh(_ sender: Any)
    {
        if(self.beanManager!.state == BeanManagerState.poweredOn){
        var theError: NSError? = nil

        self.beanManager?.startScanning(forBeans_error: &theError)

        if ((theError) != nil) {
            let alert = UIAlertController(title: "Error", message: "This is
                an alert.", preferredStyle: .alert)
            alert.addAction(UIAlertAction(title: NSLocalizedString("OK",
                comment: "Default action"),
            style: .`default`, handler: { _ in
                NSLog("The \"OK\" alert occured.")
            }))
            //let alert: UIAlertController = UIAlertAction(title: "Error",
            message: theError!.localizedDescription,
            delegate: nil, cancelButtonTitle: nil, otherButtonTitles: "Ok")
            //self.present(alert, animated: true, completion: nil)
        }
        }

        (sender as! UIRefreshControl).endRefreshing()

    }







    override func prepare(for segue: UIStoryboardSegue, sender: Any?)
     {
     if segue.identifier == "transferToPatientScreen"
     {
    let controller = segue.destination as! IDViewController
    //controller.dateString = dateAndTimeLabel.text!
    //controller.myBean = myBean
     }



}
}
```

```
//
//  EmailViewController.swift
//  POC_iOS
//
//  Created by Hany Arafa on 10/30/17.
//  Copyright   2017 Hany Arafa. All rights reserved.
//

import UIKit
import MessageUI

class EmailViewController: UIViewController,
    MFMailComposeViewControllerDelegate {


    @IBOutlet weak var dateLabel : UILabel!
    @IBOutlet weak var moleculesPerMicroL: UILabel!
    var mPML: String = " "
    @IBOutlet weak var userID: UITextField!
    var userIDString: String = " "
    var csvText : String = " "
    var result : String = " "
    @IBOutlet weak var senditTapped: UIButton!
    @IBOutlet weak var sendButton: UIButton!
    override func viewDidLoad() {
        super.viewDidLoad()
        self.hideKeyboardWhenTappedAround()
        let currentDateTime = Date()

        // initialize the date formatter and set the style
        let formatter = DateFormatter()
        formatter.timeStyle = .short
        formatter.dateStyle = .short

        // get the date time String from the date object
        let result = formatter.string(from: currentDateTime) // October 8,
            2017 at 10:48:53 PM

        dateLabel.text = result
        //labelSecond.text = strSeconds
        //userID.text = userIDString
        //moleculesPerMicroL.text = mPML
        //dateTimeLabel.text = dTL
        // Do any additional setup after loading the view.
```

```
}

override func didReceiveMemoryWarning()
{
    super.didReceiveMemoryWarning()
    // Dispose of any resources that can be recreated.
}
@IBAction func testing(_ sender: Any) {
    print("touchdown")
}

/*@IBAction func exportCSV(_ sender: UIButton!)
{
    let fileName = "TimeData.csv"
    let path = NSURL(fileURLWithPath: NSTemporaryDirectory()).
        appendingPathComponent(fileName)
    do
    {
        try csvText.write(to: path!, atomically: true, encoding: String.
            Encoding.utf8)
    }
    catch
    {
        print("Failed to export file")
    }
    let emailViewController = configuredMailComposeViewController()
    if MFMailComposeViewController.canSendMail()
    {
        self.present(emailViewController, animated: true, completion: nil
            )
    }
}*/

@IBAction func sendEmailButtonTapped(_ sender: Any) {
    let mailComposeViewController = configuredMailComposeViewController()
    if MFMailComposeViewController.canSendMail() {
        self.present(mailComposeViewController, animated: true,
            completion: nil)
    } else {
        self.showSendMailErrorAlert()
    }
}
```

```
func configuredMailComposeViewController() ->
    MFMailComposeViewController {
    let mailComposerVC = MFMailComposeViewController()
    mailComposerVC.mailComposeDelegate = self // Extremely important to
        set
    the --mailComposeDelegate-- property,
    NOT the --delegate-- property

    mailComposerVC.setToRecipients(["someone@somewhere.com"])
    mailComposerVC.setSubject("Sending you an in-app e-mail...")
    mailComposerVC.setMessageBody("Sending e-mail in-app is not so bad!",
         isHTML: false)

    return mailComposerVC
}

func showSendMailErrorAlert() {
    let sendMailErrorAlert = UIAlertView(title: "Could Not Send Email",
        message: "Your device
    could not send e-mail. Please check e-mail configuration and try
        again.",
    delegate: self, cancelButtonTitle: "OK")
    sendMailErrorAlert.show()
}

// MARK: MFMailComposeViewControllerDelegate Method
func mailComposeController(_ controller: MFMailComposeViewController,
didFinishWith result: MFMailComposeResult, error: Error?) {
    controller.dismiss(animated: true, completion: nil)
}
/* func configuredMailComposeViewController() ->
   MFMailComposeViewController
{
    let emailController = MFMailComposeViewController()
    emailController.mailComposeDelegate = self
    emailController.setSubject("CSV File")
    emailController.setMessageBody("Here is the data", isHTML: false)

    let data = csvText.data(using: String.Encoding.utf8,
        allowLossyConversion: false)!

    emailController.addAttachmentData(data, mimeType: "text/csv",
        fileName: "TimeData.csv")
    return emailController
```

```
    }

    func mailComposeController(_ controller: MFMailComposeViewController,
    didFinishWith result: MFMailComposeResult, error: Error?) {
        controller.dismiss(animated: true, completion: nil)
        //pop up with notification saying "your message has been sent!"
    }
    */

    override func prepare(for segue: UIStoryboardSegue, sender: Any?)
    {
        if segue.identifier == "backToTest"
        {
            //let controller = segue.destination as! ViewController
           // controller.userID.text = userID.text!
           // print(userID.text as Any)
       //controller.dateString = dateAndTimeLabel.text!
            //controller.dateString = dateTimeLabel.text!
        }
    }
    /*
     // MARK: - Navigation
     // In a storyboard-based application, you will often want to do a little
     preparation before navigation
     override func prepare(for segue: UIStoryboardSegue, sender: Any?) {
     // Get the new view controller using segue.destinationViewController.
     // Pass the selected object to the new view controller.
     }
     */

}

//
//  IDViewController.swift
//  POC_iOS
//
//  Created by Hany Arafa on 10/30/17.
//  Copyright   2017 Hany Arafa. All rights reserved.
//
import UIKit
import Bean_iOS_OSX_SDK
import CoreBluetooth
```

```
class IDViewController: UIViewController, PTDBeanManagerDelegate,
    PTDBeanDelegate {

    @IBOutlet weak var userID: UITextField!

    var beanManager: PTDBeanManager!
    var myBean: PTDBean!

    @IBOutlet weak var dateAndTimeLabel: UILabel!
    override func viewDidLoad()
    {
        super.viewDidLoad()
        self.hideKeyboardWhenTappedAround()
        // let date = NSDate()
        //  let calendar = NSCalendar.current
        //  let components = calender.components([.Hour, .Minute], fromDate:
            date)

        let currentDateTime = Date()

        // initialize the date formatter and set the style
        let formatter = DateFormatter()
        formatter.timeStyle = .short
        formatter.dateStyle = .short

        // get the date time String from the date object
        let result = formatter.string(from: currentDateTime)
        // October 8, 2017 at 10:48:53 PM

        dateAndTimeLabel.text = result

        let border = CALayer()
        let width = CGFloat(3.0)
        border.borderWidth = width
        userID.layer.addSublayer(border)
        // Do any additional setup after loading the view.
    }

    override func didReceiveMemoryWarning() {
        super.didReceiveMemoryWarning()
        // Dispose of any resources that can be recreated.
    }
```

```
    func textFieldShouldReturn(userID: UITextField) -> Bool {
        userID.resignFirstResponder()
        return true
    }

    /**
     * Called when the user click on the view (outside the UITextField).

    override func touchesBegan(touches: Set<UITouch>, withEvent event:
        UIEvent?) {
        self.view.endEditing(true)
    }*/

    override func prepare(for segue: UIStoryboardSegue, sender: Any?)
    {
        if segue.identifier == "idSegue"
        {
            //let controller = segue.destination as! ViewController
            //controller.userID = userID.text
            //controller.dateString = dateAndTimeLabel.text!
            //controller.myBean = myBean
            //print(dateAndTimeLabel.text as Any)
        }
    }


    /*
     // MARK: - Navigation
     // In a storyboard-based application, you will often want to do a
     little preparation before navigation
     override func prepare(for segue: UIStoryboardSegue, sender: Any?) {
     // Get the new view controller using segue.destinationViewController.
     // Pass the selected object to the new view controller.
     }
     */

}

//
//  extensionkeyboard.swift
//  POC_iOS
//
//  Created by Hany Arafa on 12/3/17.
//  Copyright   2017 Hany Arafa. All rights reserved.
```

```
//

import Foundation
import Swift
import UIKit

extension UIViewController{
    func hideKeyboardWhenTappedAround() {
        let tap: UITapGestureRecognizer = UITapGestureRecognizer(target: self
            ,
        action: #selector(UIViewController.dismissKeyboard))
        view.addGestureRecognizer(tap)
    }

    @objc func dismissKeyboard() {
       view.endEditing(true)
    }
}
//
//  EmailViewController.swift
//  POC_iOS
//
//  Created by Hany Arafa on 10/30/17.
//  Copyright   2017 Hany Arafa. All rights reserved.
//

import UIKit
import MessageUI

class EmailVC: UIViewController, MFMailComposeViewControllerDelegate {


    @IBOutlet weak var dateLabel : UILabel!
    //@IBOutlet weak var moleculesPerMicroL: UILabel!
    var mPML: String = " "

    var userIDString: String = " "
    var csvText : String = " "
    var result : String = " "

    @IBOutlet weak var fff: UIButton!

    override func viewDidLoad() {
        super.viewDidLoad()
```

```
    self.hideKeyboardWhenTappedAround()
    let currentDateTime = Date()

    // initialize the date formatter and set the style
    let formatter = DateFormatter()
    formatter.timeStyle = .short
    formatter.dateStyle = .short

    // get the date time String from the date object
    //let result = formatter.string(from: currentDateTime) // October 8,
        2017 at 10:48:53 PM

    //dateLabel.text = result
    //labelSecond.text = strSeconds
    //userID.text = userIDString
    //moleculesPerMicroL.text = mPML
    //dateTimeLabel.text = dTL
    // Do any additional setup after loading the view.
}

override func didReceiveMemoryWarning()
{
    super.didReceiveMemoryWarning()
    // Dispose of any resources that can be recreated.
}
@IBAction func testing(_ sender: Any) {
    print("touchdown")
}

/*@IBAction func exportCSV(_ sender: UIButton!)
 {
 let fileName = "TimeData.csv"
 let path = NSURL(fileURLWithPath: NSTemporaryDirectory()).
     appendingPathComponent(fileName)
 do
 {
 try csvText.write(to: path!, atomically: true, encoding: String.Encoding
     .utf8)
 }
 catch
 {
 print("Failed to export file")
 }
 let emailViewController = configuredMailComposeViewController()
```

```
 if MFMailComposeViewController.canSendMail()
 {
 self.present(emailViewController, animated: true, completion: nil)
 }
 }*/

@IBAction func sendEmailButtonTapped(_ sender: Any) {
    let mailComposeViewController = configuredMailComposeViewController()
    if MFMailComposeViewController.canSendMail() {
        self.present(mailComposeViewController, animated: true,
            completion: nil)
    } else {
        self.showSendMailErrorAlert()
    }
}

func configuredMailComposeViewController() ->
    MFMailComposeViewController {
    let mailComposerVC = MFMailComposeViewController()
    mailComposerVC.mailComposeDelegate = self // Extremely important to
    set the --mailComposeDelegate-- property, NOT the --delegate--
        property

    mailComposerVC.setToRecipients(["someone@somewhere.com"])
    mailComposerVC.setSubject("Flex Dx Results for Patient Harafa")
    mailComposerVC.setMessageBody("Your data has now been saved locally.
    You can send it to a health care provider below.", isHTML: false)

    return mailComposerVC
}

func showSendMailErrorAlert() {
    let sendMailErrorAlert = UIAlertView(title: "Could Not Send Email",
        message: "Your
    device could not send e-mail. Please check e-mail configuration and
        try again.",
    delegate: self, cancelButtonTitle: "OK")
    sendMailErrorAlert.show()
}

// MARK: MFMailComposeViewControllerDelegate Method
func mailComposeController(_ controller: MFMailComposeViewController,
didFinishWith result: MFMailComposeResult, error: Error?) {
    controller.dismiss(animated: true, completion: nil)
```

```
}
/* func configuredMailComposeViewController() ->
   MFMailComposeViewController
 {
 let emailController = MFMailComposeViewController()
 emailController.mailComposeDelegate = self
 emailController.setSubject("CSV File")
 emailController.setMessageBody("Here is the data", isHTML: false)

 let data = csvText.data(using: String.Encoding.utf8,
    allowLossyConversion: false)!

 emailController.addAttachmentData(data, mimeType: "text/csv", fileName:
    "TimeData.csv")
 return emailController
 }

 func mailComposeController(_ controller: MFMailComposeViewController,
 didFinishWith result: MFMailComposeResult, error: Error?) {
 controller.dismiss(animated: true, completion: nil)
 //pop up with notification saying "your message has been sent!"
 }
 */

override func prepare(for segue: UIStoryboardSegue, sender: Any?)
{
    if segue.identifier == "backToTest"
    {
        //let controller = segue.destination as! ViewController
        // controller.userID.text = userID.text!
        // print(userID.text as Any)
        //controller.dateString = dateAndTimeLabel.text!
        //controller.dateString = dateTimeLabel.text!
    }
}
/*
 // MARK: - Navigation
 // In a storyboard-based application, you will often want to do a little
     preparation before navigation
 override func prepare(for segue: UIStoryboardSegue, sender: Any?) {
 // Get the new view controller using segue.destinationViewController.
 // Pass the selected object to the new view controller.
 }
 */
```

```
}


//
//  POC_iOSUITests.swift
//  POC_iOSUITests
//
//  Created by Hany Arafa on 10/30/17.
//  Copyright   2017 Hany Arafa. All rights reserved.
//
import UIKit
import XCTest

class POC_iOSUITests: XCTestCase {
     var app: XCUIApplication!
    override func setUp() {
        super.setUp()

        // Put setup code here. This method is called before the
         invocation of each test method in the class.
        app = XCUIApplication()
        // In UI tests it is usually best to stop immediately when a failure
            occurs.
        continueAfterFailure = false
        // UI tests must launch the application that they test. Doing this in
             setup
        will make sure it happens for each test method.
        //XCUIApplication().launch()
        app.launchArguments.append("--uitesting")
        // In UI tests  its  important to set the initial state - such as
            interface orientation -
        required for your tests before they run. The setUp method is a good
            place to do this.
    }
    func testGoingThroughOnboarding() {
        app.launch()
        app.launchArguments.append("skipEntryViewController")
        // Make sure we're displaying onboarding
        //XCTAssertTrue(app.isDisplayingOnboarding)

        // Swipe left three times to go through the pages
        //app.buttons["Connect"].tap()
        //app.swipeLeft()
```

```
        // Tap the "Done" button
        //XCUIApplication().buttons["Connect"].tap()

        // XCTAssert(app.connecttoBean.exists)
        //app.buttons["Done"].tap()

        // Onboarding should no longer be displayed
        //XCTAssertFalse(app.isDisplayingOnboarding)
    }

    override func tearDown() {
        // Put teardown code here. This method is called after the
        invocation of each test method in the class.
        super.tearDown()
    }

    func testExample() {
        // Use recording to get started writing UI tests.
        // Use XCTAssert and related functions to
        verify your tests produce the correct results.
    }

}
```

APPENDIX B

PROTOCOLS FOR ASSAYS

B.1 ELISA Assay for Naphthalene

```
RAPID ELISA

Anderson Lab
Reagents and Materials.
-Plate, EIA, Coated, White opaque, 96-Wells per strip, Flat well shape,
Max. Well Volume: 360ul, 25/cs (Pierce PI15042 \$112.89)
Supersignal ELISA Femto Chemiluminescent Substrate,
500mL (Thermo Scientific PI37074 \$452.39)
-Mouse anti GST Antibody (Cell Signaling Technology, 2624S, 0.2 mg, \$195
    .00)
- EBNA 1 and GST recombinant Protein  20ng/well
-Human Serum Samples
-HRP anti-human IgG Ab (Jackson ImmunoResearch, 109-035-098, \$120.00)
-HRP anti-mouse IgG Ab (Jackson ImmunoResearch 515-035-062, \$112.00)
-Deep well plates
- 0.2 M Sodium Bicarbonate Buffer pH = 9.4
-5\% Milk PBST 0.2\%
-PBST 0.2\%
-30 C  Incubator
-Nunc Immunowash 12
-Plate Shaker
-Promega Glomax Luminometer (or similar luminometer
with 425nm wavelength read capability)

Abbreviations:
LT    Low Throughput
HT    High Throughput

Tips and Notes:
-      Protocol is designed to use one antigen per plate.
-      Keep number of freeze thaws for serum samples low.
-      Additionally to expression, secondary, and blank controls include
    into the experiment a sample positive and negative control such as Serum
     P4 (positive on HPV) and Serum S1 (negative on HPV) on a HPV16 AG.
-      Calculate 10\%   20\% more for reagents to use from pipetting errors
    when using pipettes (single channel/multi-channel).
-      When using the Well Mate, calculate 50\% more reagents to use.
    Because of the large excess of material, use the Well Mate only for
    cheap reagents, such as 5\% milk in PBST.
```

- During IVTT preparation step, work on ice to ensure, that each AG starts expressing on the same time when put into the incubator. After expressing and adding milk to the AG, keep expression mixture on ice until ready to distribute into wells.
- Keep ECL solution covered to protect from light exposure.
- When reading the plate with the Glomax, save the data after each plate read to ensure minimal loss of data due to technical difficulties. Technical failure to read the plate occurs often when reading many plates. The most important plate is the background subtraction plate with the GST AG. Run this plate within \#1 - \#4 in a random fashion.

Day 1

1. Well Coating coat wells with 100 ul/well of 200 ng/mL of either EBNA -1 or GST recombinant protien in 0.2M sodium bicarbonate buffer overnight @ 4C.
2. Distribute serum into deep-well blocks (see complete protocol for dilution and volume). Depending on the amount of antigens to be tested and concentration of serum, this volume will vary.

Day 2

3. Make 5\% Milk PBST 0.2\% in advance (one plate will consume 50-75mL milk) and allow it to mix for at least 2 hours before using it.
4. Wash Plate remove the plate from 4C environment and dump Protein/ Sodium Bicarbonate buffer into a bucket and pat plate off on paper towels. Add 200ul/well of PBST 0.2\%. Repeat 5x. Blot Plate after fifth wash.
5. Block Plate Add 200ul/well of 5\% Milk PBST 0.2\% and let sit at room temperature for 1.5 hours.

a. LT: Use a multichannel pipet to add milk to plates.
b. HT: Use Biomek FX* to add milk to plates.

6. Prepare serum blocking buffer Add E Coli lysate to 5\% Milk PBST 0.2\% at a ratio of 1:10. See separate protocol for preparation of E Coli Lysate.
7. Block Serum block/dilute serum (1:100) with serum blocking buffer. Dilute and add positive (mouse anti-GST mAb) and negative (blank) controls to appropriate wells. Leave rotating or shaking for at least 2 hours.

a. LT Use serum blocking buffer to dilute (1:100), and concurrently block, serum samples in tubes for at least 2 hours.
b. HT after serum has thawed in deep well block, dilute serum samples 1:100 by adding appropriate amount of serum blocking buffer (

just make sure total volume equals 100ul/well). Then centrifuge plates for 1m at 1000rpm and leave on a plate shaker for at least 2 hours.

8. Wash plate Wash plate with 200ul/well with PBST 0.2\% using NUNC immunowash 12 (put 10\% bleach into waste receptacle). Repeat 5x leaving at least one minute between washes. After the last wash, wait 1 minute and blot plates on paper towels.
9. Add sera and primary antibodies add diluted human serum into appropriate wells.

a. LT and HT: Add 100ul/well of anti-GST mAB (positive control, tests for protein expression) at a 1:3000 dilution in 5\% Milk PBST 0.2\% to appropriate wells.
b. LT: add diluted sera to plate manually.
c. HT: add diluted sera using source plate on the Biomek FX.

10. Shake at 500 RPM for 1 hour at RT.
11. Wash plate - Dump sera out into a bucket with 10\% bleach and wash plate with 200ul/well with PBST 0.2\%. Repeat 5x. Leave PBST in wells for at least 1 minute between washes and after last wash. Blot plate on paper towels following last wash.
12. Add Secondary Add 100ul/well diluted secondary antibody.

a. Serum samples: HRP Goat anti-Human IgG 1:10,000 dilution in 5\% Milk PBST 0.2\%.
b. Positive Control and select negative controls: HRP Sheep anti-Mouse IgG 1:6250 dilution in 5\% Milk PBST 0.2\%.

13. Shake at 600 RPM for 1 hour at RT.
14. Prepare ECL Calculate how much ECL is required before hand (100ul total working solution per well) and combine equal volumes of both solutions shortly before use.

a. Note: ECL working solution is a combination of luminol/enhancer and stable peroxide buffer mixed together in equal volumes.

15. Wash Plate - Wash plate with 200ul/well with PBST 0.2\% using NUNC immunowash 12. Repeat 5x leaving at least one minute between washes. After the last wash, wait 1 minute and blot plates on paper towels.
16. Add ECL Add 100ul/well of the combined ECL solutions.
17. Measure luminescence using a luminometer at 425nm wavelength. Read the plate within 1-5 minutes after shaking as the signal can drop off after extended periods.

*SOP for Beckman Coulter Biomek FX Liquid Handler System

1. Turn on Biomek (Power button is on the way top. You may need a stool) and turn on computer. Username is Administrator and there is no password.
2. Tips to use are Beckman Coulter Biomek AP96 P250 Pipette Tips, #717253. Unwrap tips and remove lid, and place in tip holder underneath the robots head. Make sure the box is aligned properly!

3. Open Biomek Software
4. File Path: Methods -> ELISA_IS -> elisa-add 100ul to each well
5. Start program by selecting play.
6. A prompt up window appears. Enter the number of plates to dispense to (maximum number is 12) and select ok.
7. Instrument Set-Up window will appear with the exact layout for plates and tip box. After set up is complete hit ok.
8. There is a light curtain between the plates and edge of the robot. Disruption of this curtain will cause the robot to pause.
9. Please change tips between runs as sometimes the filter tips may get clogged if used too many times.
10. Avoid using the mouse weal, since that can of-set the settings in the program under certain circumstances.
11. When closing the program and you are asked to save. Never save over the program. Save as an alternative program with new name.
12. If an error occurs, contact Mike Gaskin (Michael.gaskin@asu.edu) or Ian Shoemaker (ishoemak@mainex1.asu.edu).

Quality Assessment

1. DNA/Plasmid Quality

a. 260/280: This ratio should be around 1.8. A ratio lower than 1.8 is an indication for contaminants absorbing at 280 nm wavelength such as protein or phenol residues. A higher ratio than 1.8 is no indication of contamination as the exact ratio is dependent on the exact composition of the nucleic acid in the plasmid.

b. 260/230: This ratio should be between 2.0 2.2. A ratio lower than 2.0 indicates presence of contaminants absorbing at the wavelength of 230 nm such as carbohydrates, residual phenol (nucleic acid extraction), residual guanidine (column based purification) or glycogen (precipitation).

2. Protein Expression Range:

RLU measurement should be above 5.0 x 108. The majority of the expression data should be at 1.0 x 109 RLU.

3. GST AG wells/plate RLU Range Background Range:

Your majority of the data for the background, between the 25 percentile to 75 percentile, ranges between 1.0 x 108 to 5.0 x 108.

4. Secondary Controls

a. a-Mouse: Values Ideally should be below 106 RLU.

b. a-Human: Values Ideally should be below 107 RLU.

APPENDIX C

IRB DOCUMENTATION FOR BLOOD COLLECTION

C.1 Bioscience IRB Form

Instructions and Notes:

Depending on the nature of what you are doing, some sections may not be applicable to your research. If so mark as NA.

When you write a protocol, keep an electronic copy. You will need to modify this copy when making changes.

1 Protocol Title

Include the full protocol title: Smart and Connected Health Study

2 Background and Objectives

Provide the scientific or scholarly background for, rationale for, and significance of the research based on the existing literature and how will it add to existing knowledge.

Describe the purpose, specific aims, or objectives.

State the hypotheses to be tested.

Describe the relevant prior experience and gaps in current knowledge.

Describe any relevant preliminary data.

Traditionally minimally-invasive biomarker screening is performed using blood, urine, or saliva. Eccrine sweat glands are heavily interwoven with capillaries beneath the epidermal surface; hence, we predict that sweat may be a resourceful bodily fluid for diagnostics. Our epidermal surfaces represent the largest organ in our body, yet relatively little is known regarding the proteins, antibodies, or nucleic acids secreted or present on its surface in healthy individuals or in response to a pathogen or disease. While we know that sweat contains electrolytes, proteins, peptides, antibodies, amino acids, and xenobiotics (drugs and ethanol), there has yet to be a comprehensive study of the proteomic content of sweat. Our goal is to investigate the proteomic composition of sweat with a focus on immune-related biomarkers. Previously, our group had discovered that there is a plethora of immunoglobulins and cytokines that have yet to be reported in human sweat samples. These findings were not concurrently confirmed in blood samples and thus, require further validation. In order to confirm any proteomic findings in sweat samples, we will also need to correlate those findings to proteins present in blood samples. Further, we will need to collect sweat, capillary blood, and venous blood samples to develop platforms for wearable and point of care biosensors.

We will use the Macroduct sweat collector (without the iontophoresis system), an absorbent pad, and/or a similar passive sweat collection device to collect sweat from adults. The Macroduct sweat collector is an FDA

approved, disposable plastic device that is strapped to the forearm to hold it in place during passive sweat collection. The sweat secreted by the sweat glands is forced from the ducts under hydraulic pressure and flows between the skin and the concave undersurface of the Macroduct collector into a microbore tubing spiral. After collection a blunt needle on a TB syringe can be inserted into the open end of the micropore tubing to withdraw the collected sample.

We will use a disposable, retractable lancet, lancing device, and/or the Hemolink blood collection device to collect capillary blood samples for a select number of participants. Venous blood samples will be collected by a trained phlebotomist at the ASU Health Service Center on Tempe campus.

3 Data Use

Describe how the data will be used. Examples include:

Dissertation, Thesis, Undergraduate honors project
Publication/journal article, conferences/presentations
Results released to agency or organization

Results released to participants/parents
Results released to employer or school
Other (describe)

The de-identified data will be used in dissertations and theses as well as publications/journal articles and conferences/presentations. The results will be presented to the National Science Foundation and National Institutes of health.

4 Inclusion and Exclusion Criteria

Describe the inclusion and the exclusion criteria for the study.
Describe how individuals will be screened for eligibility.
Indicate specifically whether you will target or exclude each of the following special populations:

Minors (individuals who are under the age of 18)
Adults who are unable to consent
Pregnant women
Prisoners
Native Americans
Undocumented individuals

We will only include adults who are able to consent. They must already be planning to participate in a physical activity as part of their normal exercise routine. We will exclude minors and adults who are unable to

consent. There will be no selection based on race, ethnicity, or immigration status. No individuals of special populations will be specifically targeted.

Inclusion Criteria

To be enrolled in the study, the patients will meet the following inclusion criteria:

1. The donor is able to give informed written consent.
2. The donor is at least 18 years old.
3. The donor is already planning to participate in a physical activity as part of their normal exercise routine.
4. Consenting adults (such as staff and students from the Biodesign Institute or ASU) who are willing to donate sweat or blood for research purposes.

Exclusion Criteria

Patients who meet any of the following criteria will be excluded from the study:

1. Subject is unable to provide a written consent.
2. The subject is a minor.
3. The subject weighs less than 110 pounds (only applies to participants donating a venous blood sample).

5 Number of Participants

Indicate the total number of participants to be recruited and enrolled

Provide a rationale for the proposed enrollment number

What percentage of screened individuals will likely qualify for the study?

We plan to recruit 300 individuals for sweat collection, another 300 individuals for sweat and blood (capillary or venous) collection, and another 300 individuals for only blood (capillary or venous) collection. We anticipate 80\% of the individuals will qualify for and complete the study. This will result in approximately 240 samples for each of the three collection groups (sweat only, sweat + blood, and blood only). We further anticipate that the sample size collected from 10\% of our participants will not provide sufficient volume of sweat or blood for our study. This will further reduce our sample size to approximately 216 samples for each of the three collection groups. Approximately 216 samples for each collection group will provide us with a sufficiently large ensemble to investigate the proteomic composition of sweat and develop platforms for wearable and point of care biosensors.

6 Recruitment Methods

Describe when, where, and how potential participants will be identified and recruited.

Describe materials that will be used to recruit participants. (Attach copies of these documents with the application.)

Does any member have a dual role with the study population?

We will recruit individuals who are already planning to participate in physical activity. This should be part of their usual exercise routine, and they should know of no health risk to conducting the exercise. The members will be recruited by word of mouth, email, and flyers. We will request e-mailing lists from local events. We will post flyers locally and via social media. The email addresses will be used for this study only and will not be linked to the samples in any way. Participants participating in the sweat only or blood (capillary or venous) only collection will receive a \$15 gift card. Participants participating in the sweat and blood collection will receive a \$20 gift card for the sweat and capillary blood collection and \$30 gift card for the sweat and venous blood collection. Participants donating capillary and venous blood will receive a \$30 gift card. Gift cards will be for Target or Starbucks, depending on the participants preference.

7 Study Timelines

Describe:

The duration of an individual participants participation in the study.

The duration anticipated to enroll all study participants.

The estimated date for the investigators to complete this study (up to and including primary analyses).

Participants, who consent to the sweat collection, will wear the sweat collection devices on either the arm or abdominal area for 12 hours per day on two days within a seven-day period, one day on which they participate in physical activity and another day with little to no physical activity. Participants, who consent to the capillary blood collection, will perform capillary blood self-collection via a disposable, retractable lancet, lancing device, or HemoLink on the same days as their sweat collection. Venous blood collections will be performed at the participants convenience at the ASU Health Services Center. No costs will be charged to the participants for a venous blood collection. We expect to start enrolling participants in the study starting April 15th, 2018 and conclude the study August 30, 2022.

8 Procedures Involved

Describe and explain the study design. Provide a description of all research procedures being performed and when they are performed. Describe procedures including:

The documents/ measures / devices/ records /sampling that will be

used to collect data about participants. (Attach all surveys, scripts, and data collection forms).

What data will be collected including long-term follow-up?

All drugs and medical devices used in the research and the purpose of their use, and their regulatory approval status.

Describe the available compensation (monetary or credit that will be provided to research participants).

Describe any costs that participants may be responsible for because of participation in the research.

The participants will sign the included consent form. There are six different consent forms as participants will be presented with six options. 1) Participant will donate only sweat samples. 2) Participants will donate sweat and capillary blood samples. 3) Participant will donate sweat and venous blood samples. 4) Participants will donate only capillary blood samples. 5) Participants will donate only venous blood samples. 6) Participants will donate capillary and venous blood samples. Participants will not be pushed to choose any specific options as the choice will be entirely voluntary.

Thus, participants, who choose option #1, will be asked to collect sweat for 12 hours on two days (one of high and one of low physical activity), record their skin hydration levels before and after each sweat collection with a commercial skin hydration measuring device, and record the types and times of physical activity on the log. Participants, who choose option #2, will be asked to collect a capillary blood sample at the same time of each skin hydration measurement in addition to the requests for option #1. Participants, who choose option #3, will be asked to schedule an appointment with ASU Health Services to receive a blood draw to donate two tubes at any time in addition to the requests for option #1. Participants, who choose option #4, will be asked to collect 4 capillary blood samples at any time. Participants, who choose option #5, will be asked to schedule an appointment with ASU Health Services to receive a blood draw to donate two tubes at any time. Participants, who choose option #6, will be asked to collect 4 capillary blood samples and schedule an appointment with ASU Health Services to receive a blood draw to donate two tubes at any time.

For participants choosing to donate sweat, we will demonstrate for them how to use the Macroduct Sweat Collector, absorbent pads, and/or similar passive sweat collection device. We will provide them with a packet containing the devices/pads and ancillary items needed for the study. They will be provided with 4 Macroduct devices (2 per day) and 4 absorbent pads (2 per day) to be used on the two days of the study. Participants may choose the area that fits most comfortably with the

device for the sweat collection. The FDA approved Macroduct Sweat Collector (a disposable plastic device) devices will be placed on the volar forearm. The forearm will be cleaned with water, rinsed, and dried prior to placement of the Macroduct. The Macroduct will be strapped to the participants arm using the Macroduct strap (Velcro). The absorbent pad or similar passive sweat collection device will be fitted to the arm or abdominal area by using medical tape. These fitting procedures will be shown to the participant who will perform the fitting procedures on themselves on the sweat collection days. Participants will also be provided a commercial noninvasive skin hydration measuring device to use on each day of sweat collection.

For participants choosing to donate capillary blood, we will also demonstrate to them how to use the disposable, retractable lancet, lancing device, or HemoLink for the capillary blood draw and provide them the appropriate materials. They will be provided with 4 capillary blood collection devices and Heparin-coated microcentrifuge tubes or Whatman protein saver cards for the blood collection (2 per day). These capillary blood samples must be dropped off at Biodesign within 12 hours of the second capillary collection for each day. Participants donating capillary blood samples without donating sweat samples may collect all four capillary blood samples at once at any time point convenient for them. For participants choosing to donate venous blood, no additional blood collection devices will be provided; however, they will schedule a time to donate two tubes (10 mL each) of venous blood at the Health Services Center on ASU Tempe campus. Participants will be allowed to schedule any time that is convenient for them, and the appointment will be at no cost to them.

When the participants are collecting sweat and/or capillary blood samples, the participants will wear the device/pad for 12 hours on a day of physical activity and a day of little to no physical activity. The capillary blood samples will also be performed on those same days. A skin hydration measurement will also be performed before and after each sweat collection. The participant will return the devices/pads to the researchers following 12 hours of use. They will also fill out a log indicating what physical activity they participated in, the times of the day they started and stopped, and the results of their skin hydration measurements.

All sweat and/or blood collections must be completed within 4 weeks of filling out the consent form. Once samples are returned, the sweat and capillary blood samples will be collected from the device/pad and stored for analysis. Participants participating in the sweat only or blood (

capillary or venous) only collection will receive a \$15 gift card. Participants participating in the sweat and blood collection will receive a \$20 gift card for the sweat and capillary blood collection and \$30 gift card for the sweat and venous blood collection. Participants will receive a \$30 gift card for capillary and venous blood collection. Gift cards will be for Target or Starbucks, depending on the participants preference. Participants will be handed the preferred gift card of choice of the appropriate dollar amount once all sweat and/or blood samples are returned to Biodesign. These gift cards will be awarded regardless of sample quality or quantity. The possible cost to the participant is transportation to and from ASU Tempe campus.

Macroduct Sweat Collection System Model 3700 SYS instruction/service manual page 16-17 describes the devices (note: the iontophoresis component of the device will not be included in this study). The instructions for use adapted from the instruction/service manual that will be provided to the participants has also been included.

9 Withdrawal of Participants

Describe anticipated circumstances under which participants will be withdrawn from the research without their consent.

Describe procedures that will be followed when participants withdraw from the research, including partial withdrawal from procedures with continued data collection.

Participation in the study by students or faculty is purely voluntary. There will not be any coercion to participate of any kind. Participants can remove themselves from the study at any time by informing the PI in writing or email. If sample quality is poor during blood processing and cannot be used for experiments, the participants samples will be destroyed. Since these are samples to be used for exploratory studies, participant withdrawal will not impact our study.

10 Risks to Participants

List the reasonably foreseeable risks, discomforts, hazards, or inconveniences to the participants related the participants participation in the research. Include as may be useful for the IRBs consideration, the probability, magnitude, duration, and reversibility of the risks. Consider physical, psychological, social, legal, and economic risks. Reference this information when appropriate.

If applicable, indicate which procedures may have risks to an embryo or fetus should the participant be or become pregnant.

If applicable, describe risks to others who are not subjects.

For the sweat collection, the possible risk to the participant is dermal

irritation from wearing the device/pad that would result from strap or collection cup of the device.

The capillary and venous blood drawing will provide minor discomfort to the participants. There is less than a 1\% risk of fainting secondary to blood drawing, and there is less than a 1\% risk of a local hematoma secondary to blood drawing. There are no other risks involved.

Data confidentiality will be a risk to the participants. All efforts will be made to ensure patient confidentiality and assurance of HIPAA compliance. Samples will be exclusively used for biomarker discovery and biosensor platform development. No other information will be obtained from the patient or normal samples. The names of the patients will not be released to any outside organizations or to persons not involved with the study. No efforts will be taken to identify the participant, or be revealed in written reports or publications detailing the research findings. Subjects will be referred to by subject number, not name or initials in any manuscripts.

11 Potential Benefits to Participants

Realistically describe the potential benefits that individual subjects may experience from taking part in the research. Include the probability, magnitude, and duration of the potential benefits. Indicate if there is no direct benefit. Do not include compensation or benefits to society or others.

There is no direct benefit to the participant from the study. However, the study will benefit society by determining the proteomic content of sweat. Knowledge of the content will allow for the development of non-invasive assays eliminating the need for blood draws.

12 Setting

Describe the sites or locations where your research team will conduct the research.

Identify where research procedures will be performed.

For research conducted outside of the ASU describe:

o Site-specific regulations or customs affecting the research.

o Local scientific and ethical review structures in place.

The participants will meet with the PI, co-PI, or approved research assistant to sign the paper work and go over the instructions for the proper use of the sweat collection devices and capillary blood collection devices for this study. The self-collection of the sweat and capillary blood samples will be performed at the participants location of choice. The venous blood collection will be performed at ASU Health Services on Tempe campus. They will also schedule a time to return the devices. The research using the obtained samples will occur at the ASU

Tempe Campus in the Biodesign Institute, Engineering Research Center, and Goldwater Center.

13 Multi-Site Research

If this is a multi-site study where you are the lead investigator, describe the processes you will use to ensure communication among sites, such as:

Each site has the most current version of the protocol, consent document, and HIPAA authorization.

Required approvals have been obtained at each site (including approval by the sites IRB of record).

Describe processes you will use to communicate with participating sites.

Participating sites will safeguard data as required by local information security policies.

Local site investigators conduct the study appropriately.

Not applicable.

14 Resources Available

Describe the qualifications (e.g., training, experience, oversight) of you and your staff as required to perform your roles. When applicable describe knowledge of the local study sites, culture, and society. Provide enough information to convince the IRB that you have qualified staff for the proposed research.

Describe other resources available to conduct the research: For example, as appropriate:

Describe your facilities.

Describe the availability of medical or psychological resources that participants might need as a result of any anticipated consequences of the human research.

Describe your process to ensure that all persons assisting with the research are adequately informed about the protocol, the research procedures, and their duties and functions.

The administration of the sweat and capillary blood collection devices requires minimal training that will be provided by research staff, PI or Co-PI. The training can take place in an office. All researchers or assistant interacting with the participants or samples will undergo CITI training. Since the study involves minimal risk to the participants, medical or psychological resources are not necessary. The PI will ensure that any personnel interacting with the participants will be trained to adequately inform them about the protocol, research procedures, and their duties and functions.

Venous blood draws will be performed at the ASU Health Services Center on Tempe campus by a trained phlebotomist. Physicians, nurses, and other health professionals will also be available during the sample collection.

Lab facilities

Our lab space is located on the second floor with enough lab space for 12 researchers and lab equipment. We have incubators, two -20 degree freezers, one -80 degree freezer a 4-degree refrigerator and a walk-in cooler. There are four computers (two PCs and 2 Macintosh) for lab use, all equipped with relevant software (Graphpad prism, MS office, DNA sequencherTM etc). There is also one MVE 800 Series 190 Liquid Nitrogen Cell Storage System, to maintain and stockpile all cell lines and study samples obtained for this study. Our lab is also right next to the Biodesign flow cytometry core facility housing the BD FACSaria flow sorter which we will use CTL studies.

The 500 sq foot BSL2+ cell culture room is access only and is equipped with four Baker sterile Biosafety cabinets (with UV lights). The room is locked at all times with negative air flow and is card accessible only, requiring OSHA and biohazard trainings. It also has two water baths and four 37-degree CO2 incubators. The cell culture room also has its own 4-degree refrigerator, two Beckman Allegra tabletop centrifuges, three Thermo HeraCell 240i CO2 incubators and an inverted microscope (Nikon) with GFP capability.

Office space

We also have office space for 3 researchers in the office area opposite to the lab with computers. All office computers (PCs) are equipped with relevant software (Attune v2.5 for flow cytometry, Graphpad prism, DNA sequencherTM etc) to be used for research purposes. The computers are connected to the internet at all times and have all appropriate firewall and anti-virus security systems. CPD also has its own server and shared drive on which research data can be stored for back up.

Equipments

The Anderson lab has an automated Biotek ELX405 magnetic plate washer, many manual and electronic single and multichannel pipettes, high and low-voltage gel electrophoresis units, and a Biorad image analyzer. The lab also has one plate/tube shaker, 2 37C shakers, one nanodrop, microcentrifuges, two ABI PCR Thermocycling machines, one automated Biotek ELX405 magnetic plate washer and a new Millipore Magpix Luminex machine. In addition to general lab equipment mentioned above, we also have the 4D Lonza Amaxa Nucleofector with two single-cuvette, 16-well microcuvette and 96-well capability. The 4D Nucleofector is highly efficient in transfections of different cell lines with optimized programs for each of them. Also, its 96 well microcuvette system gives

us high throughput transfection capability without compromising on transfection efficiency and time.

We have an Attune flow cytometer (Life Technologies) with single tube and 96-well capability to be used for our high throughput studies. Our Attune has a Blue/Violet laser configuration and works on principle of acoustic focusing. This helps rapid high throughput analysis without compromising on sensitivity. Our researchers are certified trained to handle the Attune cytometer for T-cell epitope screening studies. The Attune is also robot-compatible which we could make use of in the future.

Since we only seek English-understanding consenting adult volunteers, we will describe in brief what the research is about, and what it will be used for. The subjects will have the opportunity to review the consent form prior to donating sweat and/or blood. They will also have the opportunity to decline from donating sweat and/or blood at any time when they want to.

15 Prior Approvals

Describe any approvals that will be obtained prior to commencing the research. (E.g., school, external site, funding agency, laboratory, radiation safety, or biosafety approval.)

N/A

16 Data Management and Confidentiality

Describe the data analysis plan, including procedures for statistical analysis.

Describe the steps that will be taken to secure the data during storage, use, and transmission.

Training, authorization of access, password protection, encryption, physical controls, certificates of confidentiality, and separation of identifiers and data

Describe how data and any specimens will be handled:

What personal identifiers will be included in that data or associated with the specimens?

Where and how data or specimens will be stored?

How long the data or specimens will be stored?

Who will have access to the data or specimens?

Who is responsible for receipt or transmission of the data or specimens?

How will data and specimens be transported?

If data or specimens will be banked for future use, describe where the specimens will be stored, how long they will be stored, how the specimens will be accessed, and who will have access to the specimens.

Describe the procedures to release data or specimens, including: the

process to request a release, approvals required for release, who can obtain data or specimens, and the data to be provided with specimens.

The collected devices and samples will be de-identified upon receipt with only a male/female identifier, physical activity log, and a random code that cannot be linked back to the participant and will allow us to match only the sweat and/or blood samples to the activity logs but not back to the participant. The specimens will be transferred to a microcentrifuge tube and stored in a -80oC freezer. The specimens will be kept for the entire length of the study and at least 3 years following its conclusion, if any sample remains. The specimens will not be transported from the building, and electronic access to the laboratory is required. The data will be maintained on a secure network drive with access given only to those researchers directly involved with the project who have completed the CITI training. The data will only be published in de-identified and/or aggregate form. The data will be maintained on the servers for a period of no less than 3 years following the conclusion of the study. The consent forms will be secured in a secure, separate location (locked container in the PIs office) from the rest of the study data for a period of three years and then will be destroyed. Researchers will sign a confidentiality statement.

Again, subjects will not be identified by any personal identifiers in any oral or written reports related to the study. No personal identifiers will be kept on file. Since we are only analyzing proteomic content, no information will be exchanged with the donors. Participation is purely voluntary and no other information will be obtained from the participant.

17 Safety Monitoring

This is required when research involves more than Minimal Risk to participants. The plan might include establishing a data monitoring committee and a plan for reporting data monitoring committee findings to the IRB and the sponsor. Describe:

The plan to periodically evaluate the data collected regarding both harms and benefits to determine whether participants remain safe.

What data are reviewed, including safety data, untoward events, and efficacy data?

How the safety information will be collected (e.g., with case report forms, at study visits, by telephone calls with participants).

Who will review the data?

Since the protocol involves only sweat and blood collection, it poses minimal risk to the participants. Therefore, no follow-up visits or additional monitoring is essential for the donors. Furthermore, as stated earlier, the participation is purely voluntary and participants may withdraw at any time.

18 Consent Process

Describe the process and procedures process you will use to obtain consent. Include a description of:

Who will be responsible for consenting participants?

Where will the consent process take place?

How will consent be obtained?

If participants who do not speak English will be enrolled, describe the process to ensure that the oral and/or written information provided to those participants will be in that language. Indicate the language that will be used by those obtaining consent. Translated consent forms should be submitted after the English is approved.

C.2 Capillary Blood Consent Form

A. INTRODUCTION

We are inviting you to take part in a research study titled Smart and Connected Health Study funded by the National Science Foundation. This is a study to develop platforms for wearable and point-of-care diagnostic devices, which can detect health and disease (biomarkers). It is expected that about 300 people will take part in this research study at Arizona State University. You must be 18 years or older to participate, and you must already be planning to participate in physical activities as part of your normal exercise routine. You must know of no risks to your health by participating in this activity.

This form was created to help explain to you the nature of this study and if you choose to participate, it will be used to document your agreement to be part of this study.

Included in this form is a description of why this study is being done, what is involved in participating in the research study, the possible risks, inconveniences or discomforts you may experience, alternatives to participation, and your rights as a research subject. The decision to participate is yours. If you decide to participate, please sign and date at the end of this form. We will give you a copy so that you can refer to it while you are involved in this research study.

B. WHY IS THIS RESEARCH STUDY BEING DONE?

We are researchers at Arizona State University, and we are conducting research to develop wearable and point of care diagnostic platforms. We are doing this study to collect capillary and venous blood from men and women to measure proteins, electrolytes, and biomarkers using point of

care devices, which we are working to optimize. We plan to use this information to make diagnostics more accessible and cheaper.

C. WHAT IS INVOLVED IN THE RESEARCH STUDY?

Participation in this research is entirely voluntary. If you agree to participate in this study:

You will spend about 15 minutes filling out this consent form.

You do not have to answer any questions that make you uneasy. Whether or not you answer any question will not affect your medical care. We will keep the paper copies of the questionnaire in a locked file to protect your privacy. You can choose to not donate blood at any point during this study and we will not coerce you.

You will be asked to schedule an appointment with ASU Health Services to donate 2 tubes (10 mL/tube) of venous blood drawn by a trained health professional. A venous blood draw includes a health professional inserting a syringe needle into a vein, usually on the forearm, to draw up blood. There will be no costs to you for this appointment with ASU Health Services.

You will be asked to self-collect four small volume blood samples that either from a finger or arm prick. This self-collection would be performed using the provided retractable lancet, lancing device, or HemoLink. These devices have a small metal blade that will push out at the press of a button and then immediately retract. Retractable lancets may be disposed in any landfill waste container. When held to a fingertip or a part of the arm, the device will draw a few drops of blood. Samples will be collected into a provided heparin-coated microcentrifuge tube or Whatman protein saver card. The capillary blood samples must be returned within 12 hours of the collection.

Once you return the capillary blood collection devices, they will be marked with only as male or female and a random number to protect your privacy and ensure that the results of testing cannot be associated with you in any way. Your participation will be confidential. The results of this study may be used in reports, presentations, or publications but your name will not be used. The results will only be shared in the aggregate form only.

All sweat and/or blood collections must be completed within 4 weeks of filling out this consent form.

In addition, you can stop participating in the research study at any time. However, before you decide to stop participating in this study, we encourage you to reach out to the research team first.

E. HOW LONG WILL I BE IN THIS RESEARCH STUDY?

This project is designed to gather capillary and venous blood from participants. Your participation is expected to take about 2 hours of your time. After consenting to participate in this study, you do not have to do anything active to continue to participate. You may, of course, withdraw at any time. Because we cannot predict when new biomarkers may become available for study, we are asking you to permit us to store this information and share it with other investigators in a form that could not be identified as yours for an indefinite period of time. We are asking you to give us permission to use your capillary and venous blood, which will be stored in a way that cannot be linked back to you for future research studies. All efforts will be made to protect your privacy at all times.

The research team may decide to take you off the research study for many reasons, including:

It is considered to be in your best interest
There is any problem with following study treatments and procedures
There are any problems with research funding
Or other unforeseen reasons

If you are removed from the research study, we will explain to you why you were removed.

F. WHAT ARE THE RISKS AND CONFIDENTIALITY OF THE RESEARCH STUDY?

Physical Risks:

The capillary venous blood collection will provide minor discomfort to the participants. There is less than a 1\% risk of fainting secondary to blood drawing, and there is less than a 1\% risk of a local hematoma secondary to blood drawing. There are no other risks involved. Occasionally, there are technical problems with the laboratory analysis. If this happens, we would discard your samples. This has no significance in terms of results, and should not alarm you in anyway.

Non-Physical Risks:

We will collect information from you on your physical activity and your gender. This information will be coded with a unique number.

G. WHAT ARE THE BENEFITS OF THE RESEARCH STUDY?

You will be provided a \$30 gift card to Target or Starbucks (your choice) for participating in this study. It will be provided after you complete

the capillary and venous blood collection and return the materials as indicated in the instruction packet.

H. CAN I STOP BEING IN THE RESEARCH STUDY AND WHAT ARE MY RIGHTS?

You have the right to choose not to sign this form. If you decide not to sign this form, you cannot participate in this research study. You may also stop being in the research study at any time. If you choose to not participate, or if you are not eligible to participate, or if you withdraw from this research study, this will not cause any penalty to you.

WHAT ARE THE COSTS?

No charges will be billed to you for this study. There will be no costs to you for your appointment with ASU Health Services.

What happens if I am injured or sick because I took part in this research study?

We do not anticipate you becoming physically sick or injured from taking part in this study. If you think you have been injured as a result of taking part in this research study, tell the person in charge of this study as soon as possible and seek standard medical care. You may have to pay for this treatment. The research teams name and phone number are listed in this consent form.

I. WHOM DO I CONTACT IF I HAVE QUESTIONS ABOUT THE RESEARCH STUDY?

If you have questions about the study, please contact the research study staff as listed below:

Jennifer Blain Christen PhD 480-965-9859

Karen Anderson, MD, PhD 480-965-6982

For questions about your rights as a research participant, please contact a representative of the Office for the Protection of Research Subjects at Arizona State University. This can include questions about your participation in the study, concerns about the study, a research related injury, or if you feel/felt under pressure to enroll in this research study or to continue to participate in this research study.

J. PRIVACY OF PROTECTED HEALTH INFORMATION

Federal law requires research teams to protect the privacy of information that identifies you and relates to your past, present, and future physical and mental health conditions (protected health information). If you enroll in this research study, we will only collect information on your age, gender, and physical activity. This information will be coded

and linked to your capillary and venous blood samples, but no personal information will be retained (i.e. your name).

K. DOCUMENTATION OF CONSENT

PLEASE READ THE FOLLOWING QUESTIONS AND INSTRUCTIONS VERY CAREFULLY. For your own safety, you CANNOT participate in this study if you have a medical condition for which capillary and venous blood donation is not advised. You should also NOT participate in this study if you are incapable of understanding the consent process, or cannot understand English.

To be enrolled in the study, you must meet the following inclusion criteria:

1. Are you able to give informed written consent?
   a) Yes b) No
2. Are you at least 18 years old?
a) Yes b) No
3. Do you weigh over 110 pounds?
   a) Yes b) No

My signature below indicates my willingness to participate in this research study and my understanding that I can withdraw at any time. I also confirm my understanding that I will receive a \$30 gift card to Target or Starbucks (of my choice) upon returning all collected samples for participating in this study.

Signature of Subject Date
or Legally Authorized Representative

To be completed by person obtaining consent:

The consent discussion was initiated on (date) at (time.)

0 A copy of this signed consent form will be given to the subject.

For Adult Subjects

0 The subject is an adult and provided consent to participate.

Signature of Individual obtaining consent:

Printed name of above:

Date:

BIOGRAPHICAL SKETCH

Hany Arafa graduated with his Bachelor's degree in Biomedical Engineering from ASU in the Spring of 2017 and is currently completing his MS in Biomedical Engineering. As a member of the BioElectrical Systems and Technologies Lab, he specializes in biosensors and point-of-care diagnostics. His previous work was primarily focused on the development of an integrated system for the ex vivo continuous assessment of tumor cell proliferation, resulting in several publications. He has also worked on the development of a wearable, crowd-sourced air quality monitoring device for respiratory disease. His thesis project focused on various aspects of fluorescence-based bio recognition system architecture for multiplexed point-of-care molecular diagnostics such as the optimization of the fluidic systems in addition to the development of thermally actuated systems. He has industry experience in the development of DNA and protein microarrays for diagnostics with Applied Microarrays and is currently working part time at Medtronic as a test engineer. After graduating, Hany will be pursuing a doctoral degree in biomedical engineering at Northwestern University.